

Study of $\gamma p \rightarrow \eta \pi^0 p \rightarrow 4 \gamma p$ reaction at GlueX

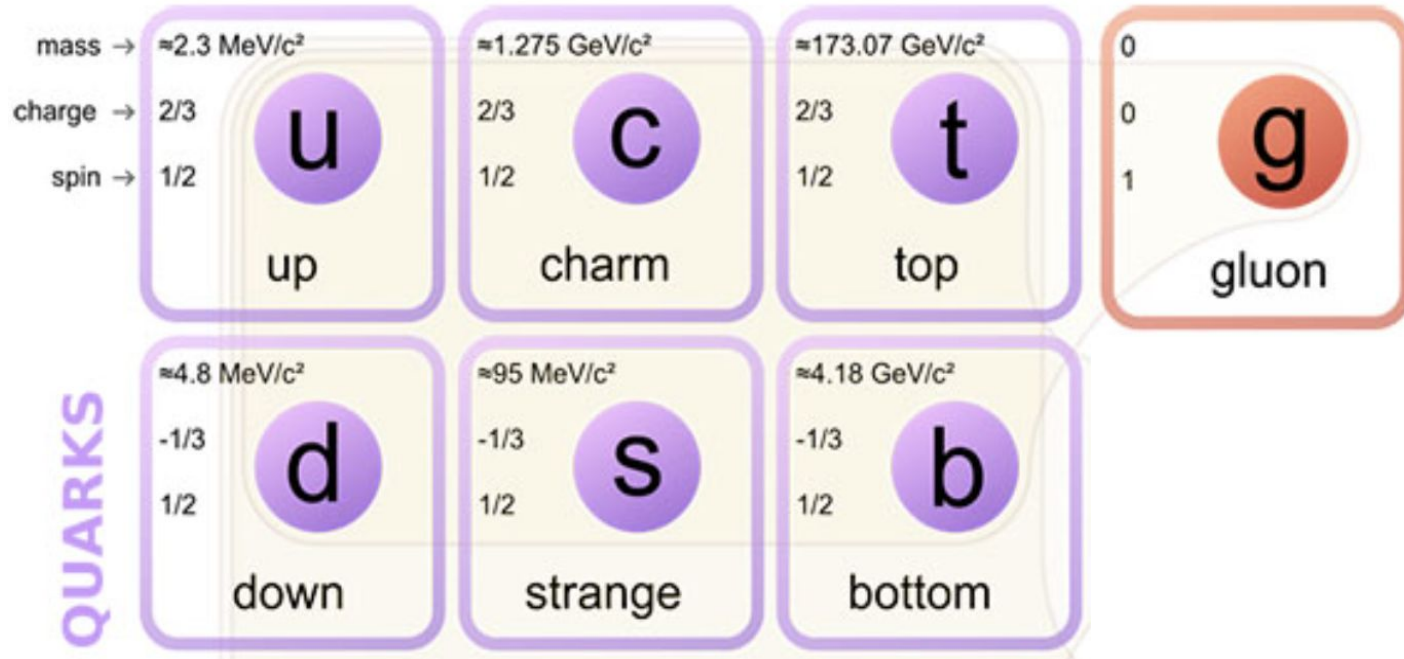


Lawrence Ng
Florida State University



Quantum Chromodynamics

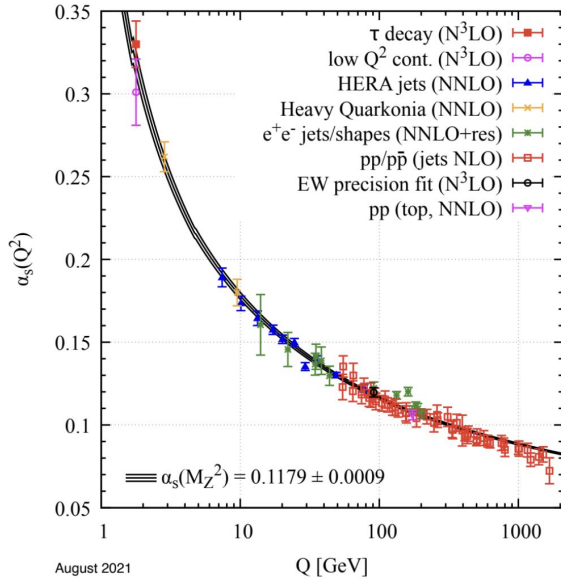
https://en.wikipedia.org/wiki/Standard_Model



“Three **quarks** for Muster Mark!” - Finnegans Wake

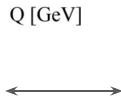
Quantum Chromodynamics

Particle Data Group, *Review of Particle Physics*,
Volume 2022, Issue 8, August 2022, 083C01,



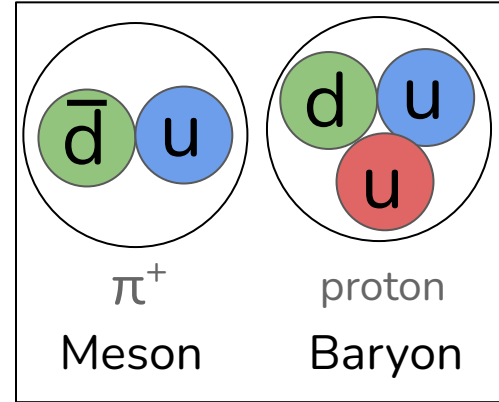
August 2021

Low energy
Large distance
Non-perturbative



High energy
Small distance
Perturbative

Non-perturbative Regime



Hadrons

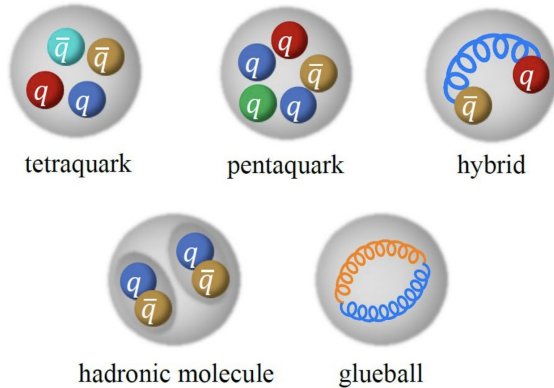
Asymptotic Freedom

Confinement - How does it arise?

Perturbative ~ Allows for high precision calculations
Non-perturbative ~ higher order terms to achieve same level of precision and may not converge at all!

Exotic Hadrons

- Existence predicted by Gell-mann and Zweig in 1964
- Systems of quark and gluons beyond the conventional meson ($q\bar{q}$) and baryon (qqq) states



https://indico.bnl.gov/event/11669/contributions/50918/attachments/36102/59226/PSQ%40EIC_FKGuo.pdf

- What color singlet states exist in nature?
- What is the role of gluons?

Study hybrid mesons to understand gluonic excitations

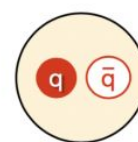
Hybrid Mesons

- ❖ Meson system has two spin $\frac{1}{2}$ quarks in relative orbital motion
 - J^{PC} where $J=L+S$, $P=(-1)^{L+1}$, $C=(-1)^{L+S}$

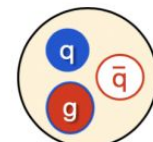
- ❖ Hybrid mesons contain gluonic excitations that directly contribute to the wavefunction
 - **Exotic hybrid mesons** have J^{PC} not accessible as $q\bar{q}$
 - $0^{+-}, 1^{-+}, 2^{+-}, \dots$
 - Easier to search for since they do not mix with conventional states

L	S	J^{PC}	L	S	J^{PC}	L	S	J^{PC}
0	0	0^{-+}	1	0	1^{+-}	2	0	2^{-+}
0	1	1^{--}	1	1	0^{++}	2	1	1^{--}
			1	1	1^{++}	2	1	2^{--}
			1	1	2^{++}	2	1	3^{--}

TABLE I. The allowed J^{PC} quantum numbers for $q\bar{q}$ systems.



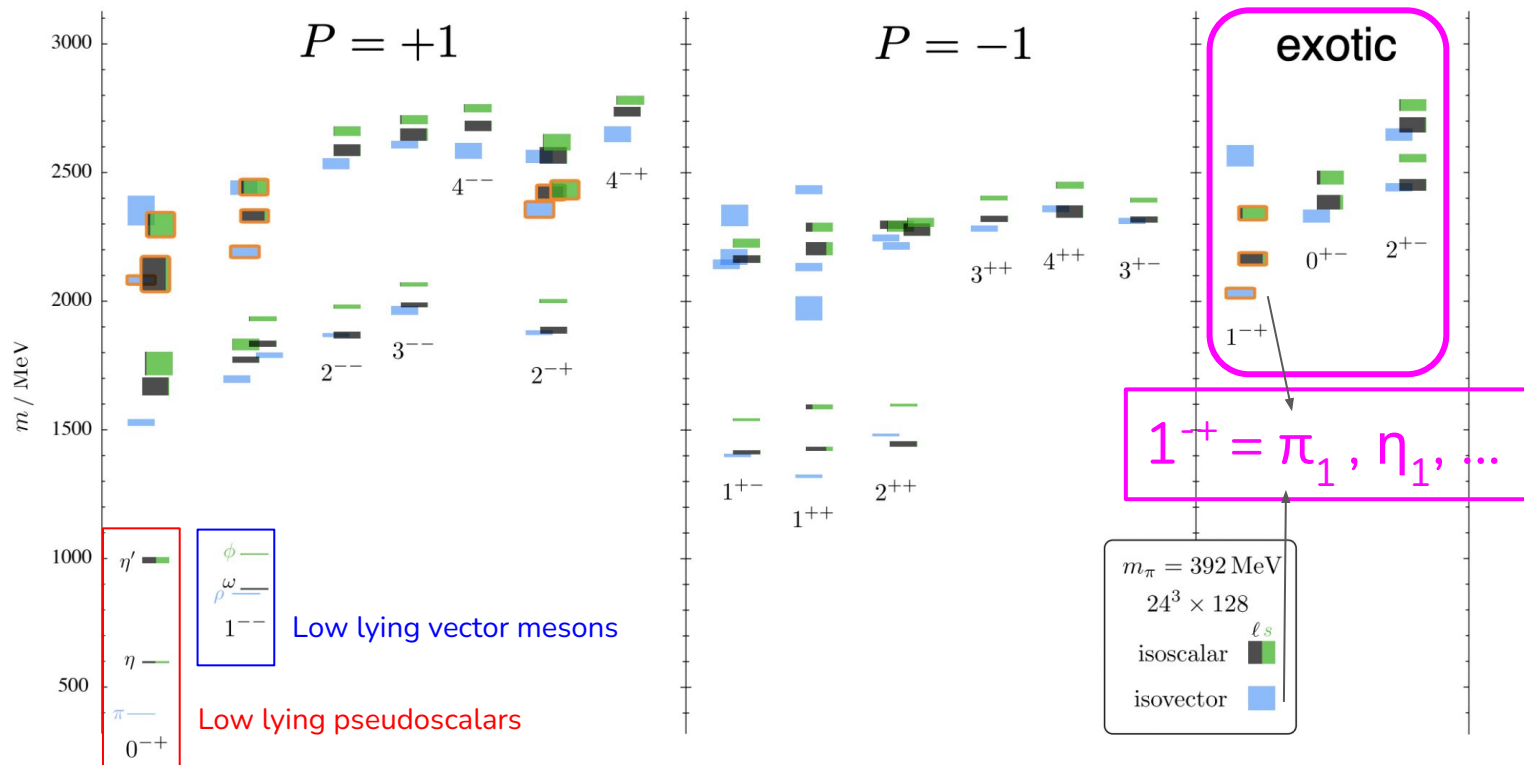
mesons



“hybrid” meson

So... where to search?
 ➡ Theory Spectrum

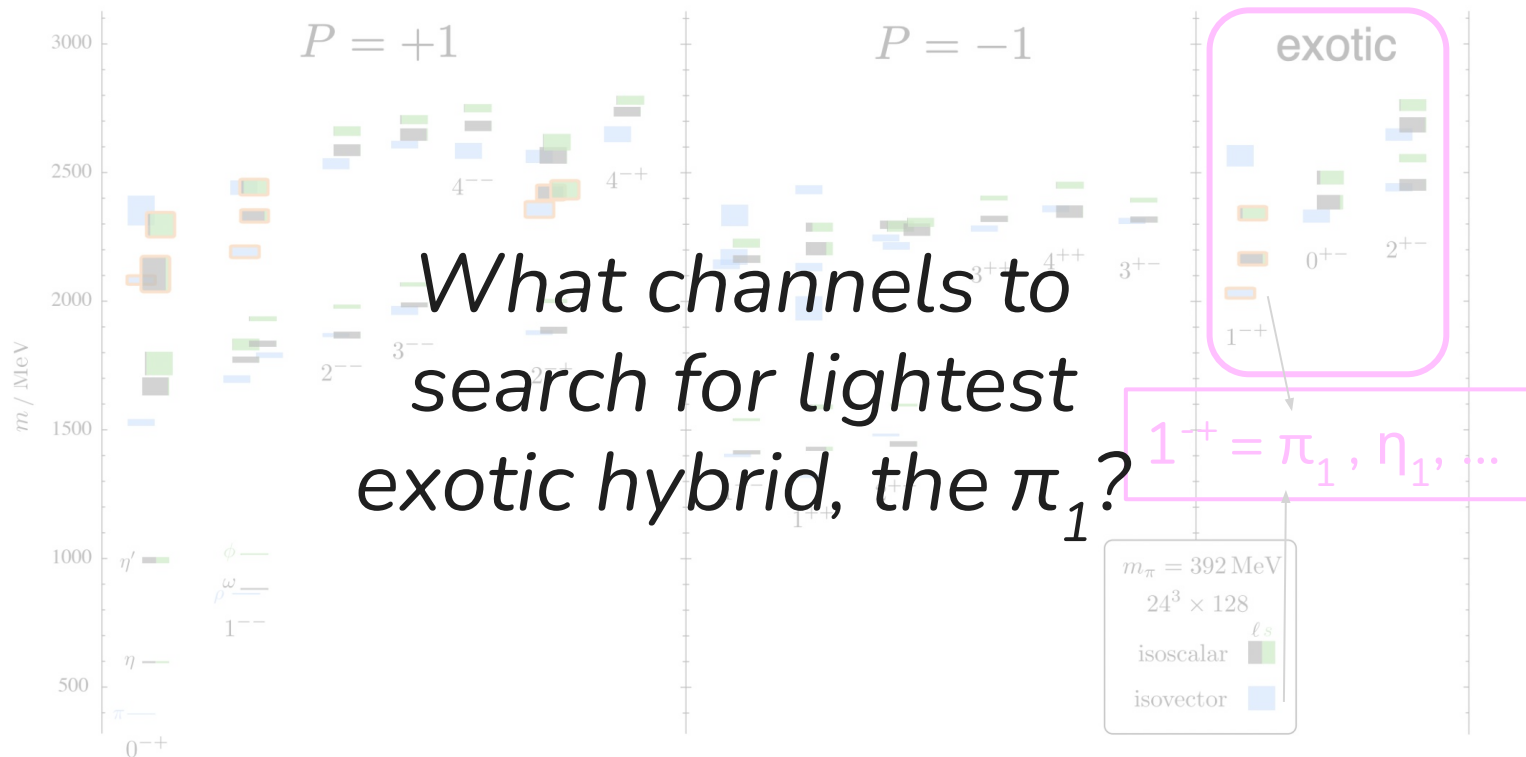
Lattice QCD: Light Meson Spectrum



[Dudek, Edwards, Guo, Thomas, PRD **88** 094505(2013)]

- Lightest spin-exotic state: $J^{PC} = 1^{-+}$, $M \approx 2 \text{ GeV}/c^2$

Lattice QCD: Light Meson Spectrum

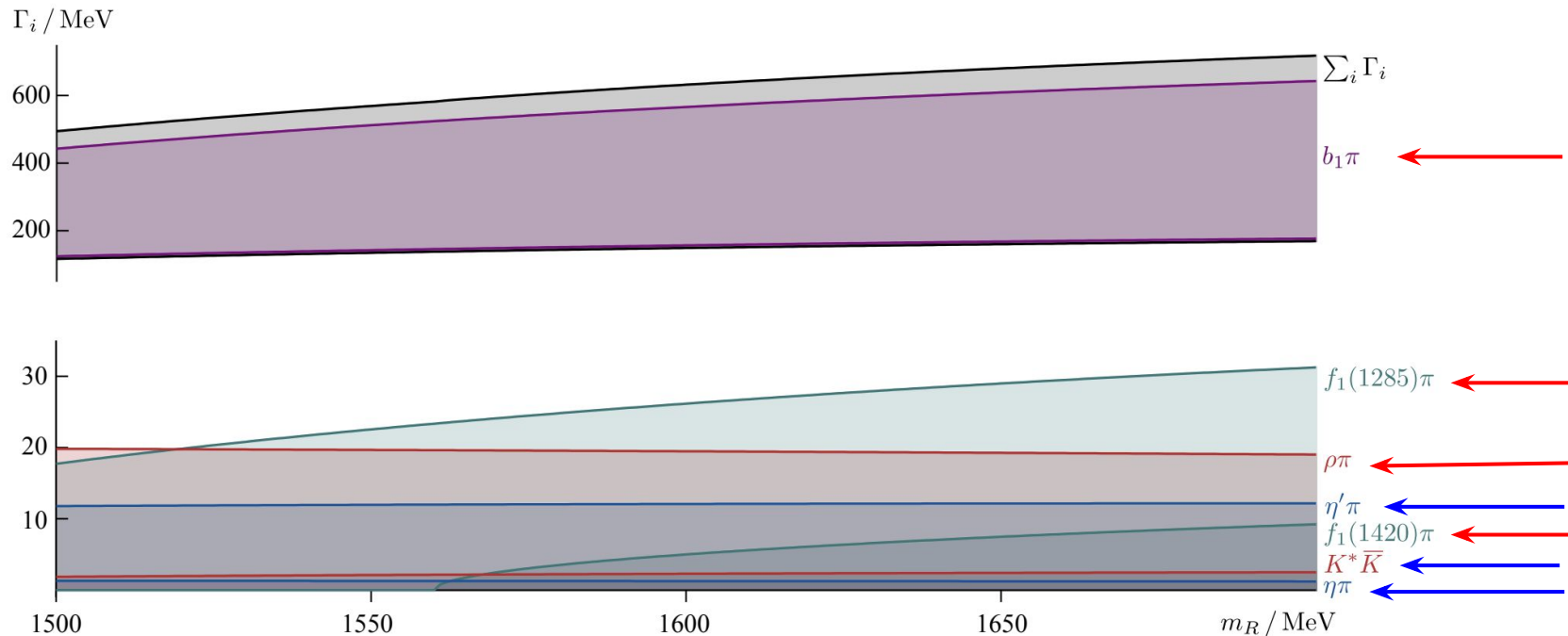


What channels to search for lightest exotic hybrid, the π_1 ?

[Dudek, Edwards, Guo, Thomas, PRD **88** 094505(2013)]

- Lightest spin-exotic state: $J^{PC} = 1^{+-}$, $M \approx 2 \text{ GeV}/c^2$

Lattice QCD: π_1 Branching Fractions

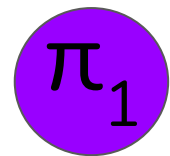


π_1 decay to **vector-pseudoscalar** \gg **two pseudoscalar** final states

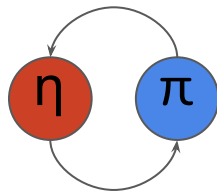
Tradeoff: vector-pseudoscalar states are more complicated to reconstruct

Why Search for the π_1 in $\eta\pi$?

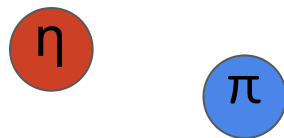
- J^{PC} of π and $\eta \sim 0^{-+}$
 - $S=0, J=L, P=(-1)^L, C=+$
 - Examples: $J^{PC} = 0^{++}, 1^{-+}, 2^{++}, 3^{-+} \dots$
 - Odd-L impossible as a conventional meson
- Simpler reconstruction + η/π are narrow states



$J^{PC}=1^{-+}$



$L=J=1$



Decay as a “P-wave”

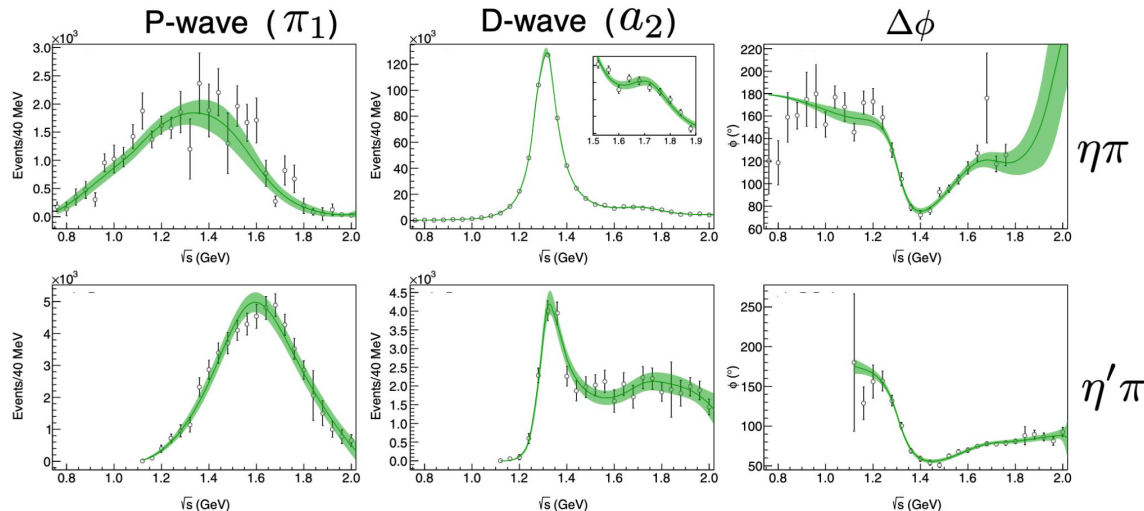
Borrow from spectroscopy
 $L=0$: S-wave
 $L=1$: P-wave
 $L=2$: D-wave
....

Recent Observations: COMPASS/JPAC

Long history of previous searches...

COMPASS (pion beam) published results on the $\eta'\pi$ and $\eta\pi$ system

Joint Physics Analysis Center (JPAC) described 1^{-+} wave with 1 pole, 2-channel K-Matrix



~155k Events in total

PRL 112 042002 (2019)

Poles	Mass (MeV)	Width (MeV)
π_1	$1564 \pm 24 \pm 86$	$492 \pm 54 \pm 102$

Crystal Barrel

- Coupled channel analysis of: $p\bar{p} \rightarrow K^+K^-\pi^0, \pi^0\pi^0\eta, \pi^0\eta\eta$ + 11 $\pi\pi$ scattering datasets + COMPASS $\eta'\pi$ and $\eta\pi$ data

Confirms JPAC results

Eur. Phys. J. C (2020) 81:1056

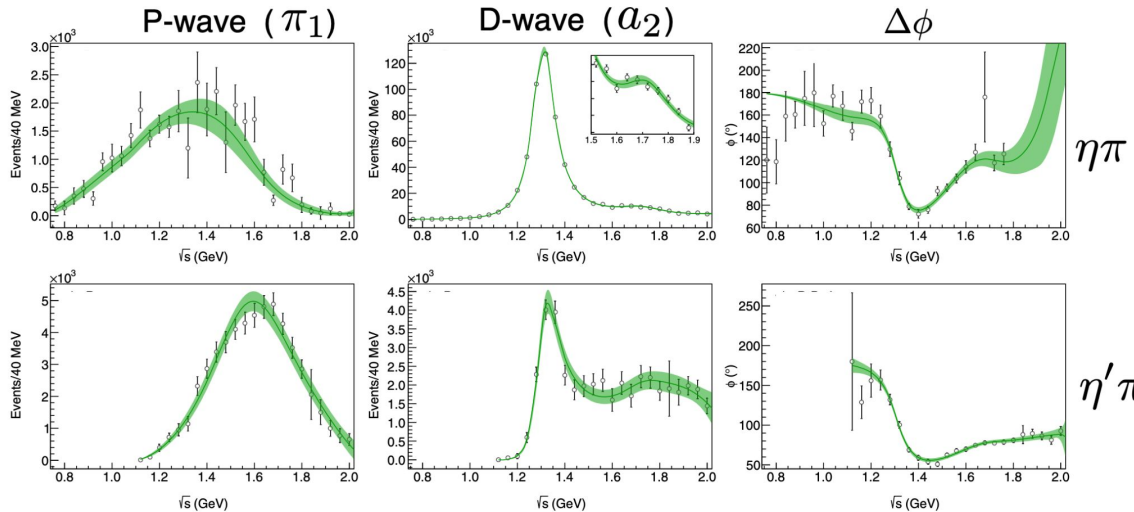
Recent Observations: COMPASS/JPAC

Long history of previous searches...

COMPASS (pion beam) published results on the $\eta'\pi$ and $\eta\pi$ system

Joint Physics Analysis Center (JPAC) described 1^{+-} wave with 1 pole, 2-channel K-Matrix

reaction that I study!



~155k Events in total

PRL 112 042002 (2019)

Poles	Mass (MeV)	Width (MeV)
π_1	$1564 \pm 24 \pm 86$	$492 \pm 54 \pm 102$

Crystal Barrel

- Coupled channel analysis of: $p\bar{p} \rightarrow K^+K^-\pi^0, \pi^0\pi^0\eta, \pi^0\eta\eta$ + 11 $\pi\pi$ scattering datasets + COMPASS $\eta'\pi$ and $\eta\pi$ data

Confirms JPAC results

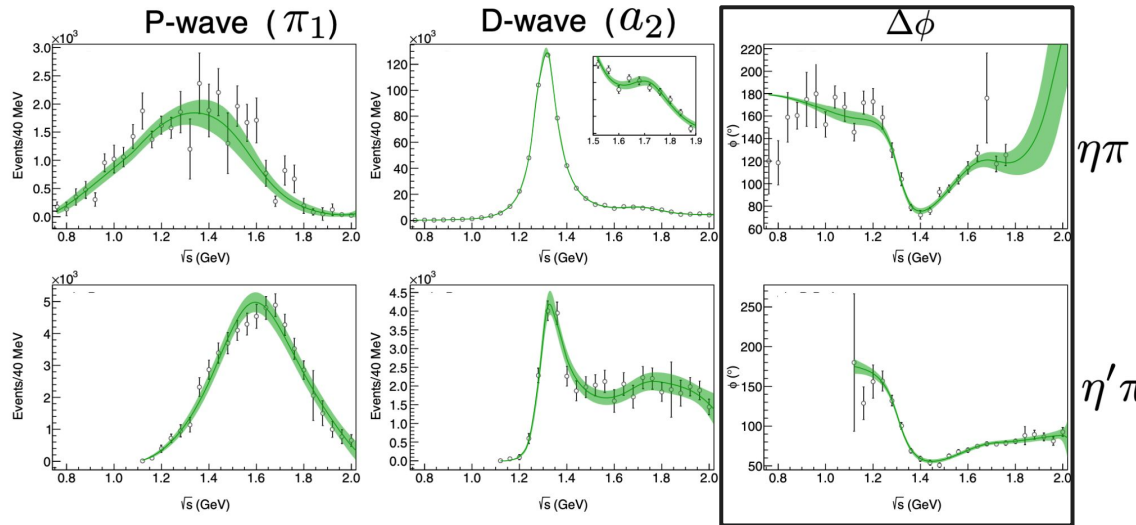
Eur. Phys. J. C (2020) 81:1056

Recent Observations: COMPASS/JPAC

Long history of previous searches...

COMPASS (pion beam) published results on the $\eta'\pi$ and $\eta\pi$ system

Joint Physics Analysis Center (JPAC) described 1^{-+} wave with 1 pole, 2-channel K-Matrix



~155k Events in total

PRL 112 042002 (2019)

Poles	Mass (MeV)	Width (MeV)
π_1	$1564 \pm 24 \pm 86$	$492 \pm 54 \pm 102$

*Strong phase motion
indicates
Resonant P-wave*

Crystal Barrel

- Coupled channel analysis of: $p\bar{p} \rightarrow K^+K^-\pi^0, \pi^0\pi^0\eta, \pi^0\eta\eta$ + 11 $\pi\pi$ scattering datasets + COMPASS $\eta'\pi$ and $\eta\pi$ data

Confirms JPAC results

Eur. Phys. J. C (2020) 81:1056

Good experimental evidence for the π_1 in hadroproduction

What about other production mechanism?

Different mechanisms different ways to generate a signal

And, What about other hybrids?



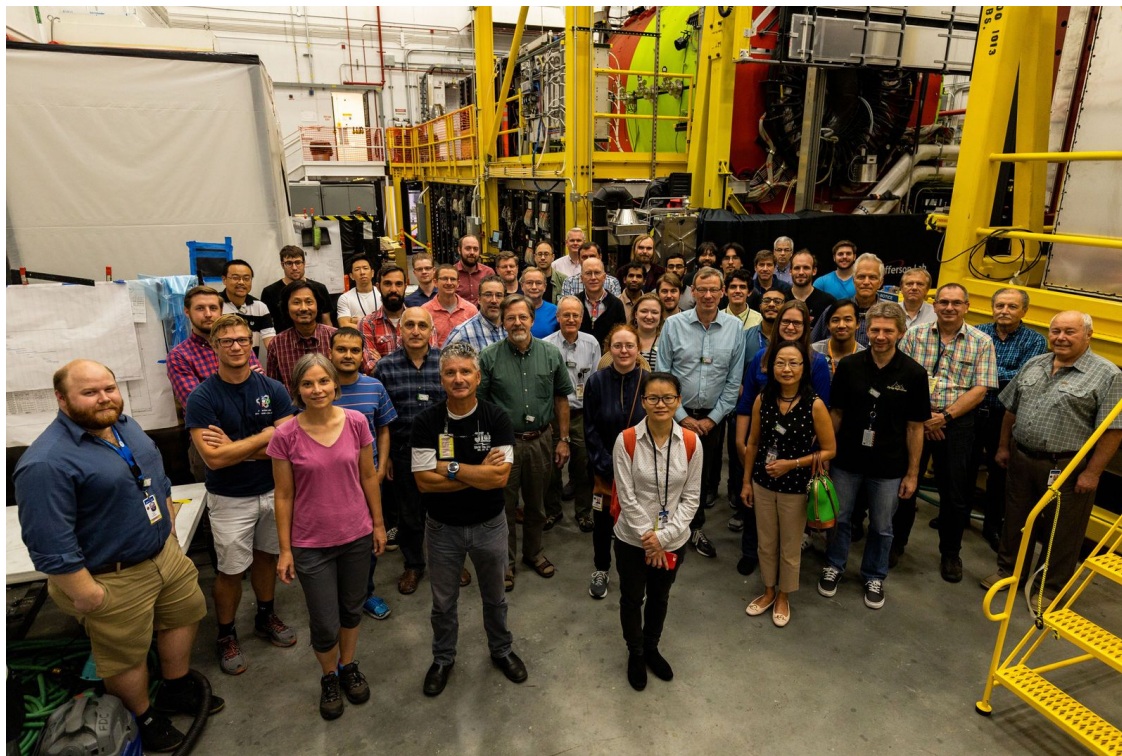
GlueX

Primary Purpose

- ❖ Understand confinement by mapping the light meson spectrum for hybrid and exotic mesons

Features

- ❖ Linearly Polarized Photon Beam
- ❖ High statistics



GlueX

Primary Purpose

- ❖ Understand confinement by mapping the light meson spectrum for hybrid and exotic mesons

Features

- ❖ Linearly Polarized Photon Beam
- ❖ High statistics



14 FSU Members ~10% of GlueX member list

Chandra S Akondi	Florida State University
Jason Barlow	Florida State University
Edmundo Barriga	Florida State University
Volker Crede	Florida State University
Sean Dobbs	Florida State University
Donavan Ebersole	Florida State University
Paul Eugenio	Florida State University
Jesse Hernandez	Florida State University
Daniel I Lersch	Florida State University
Lawrence Ng	Florida State University
Alexander I Ostrovidov	Florida State University
Saheli Rakshit	Florida State University
Alicia Remington	Florida State University
Gabriel Rodriguez	Florida State University

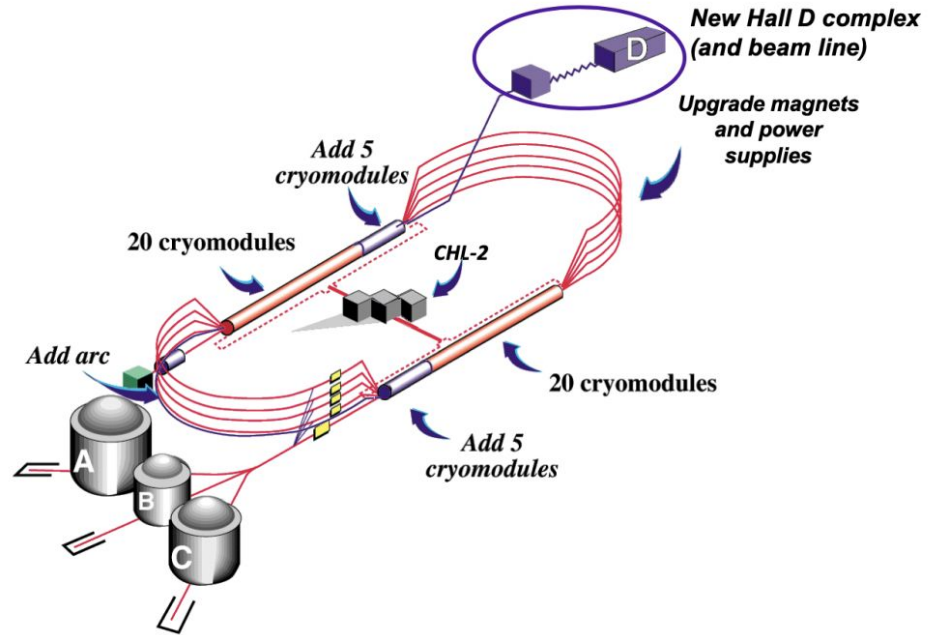


Jefferson Lab

Located in Newport News, VA
Contains 4 halls: A,B,C,D
GlueX at Hall D

Continuous Electron Beam Accelerator Facility (CEBAF)

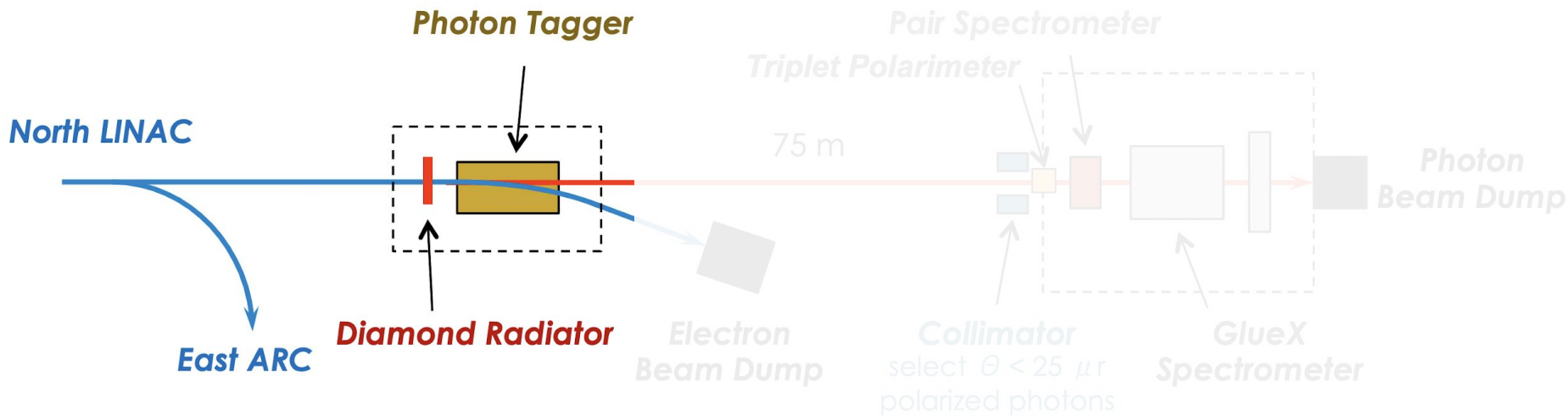
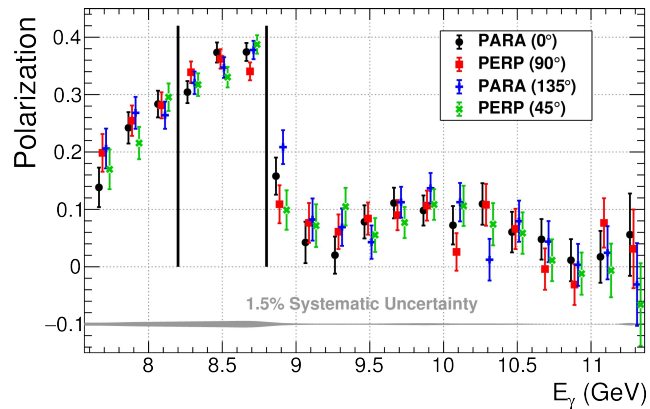
- 12 GeV polarized electron
source



Hall D Photon Beamline

**Linearly polarized
photon beam!**
Data taken in 2 pairs of
orthogonal orientations

**Coherent Peak $\sim 35\%$
Polarization**



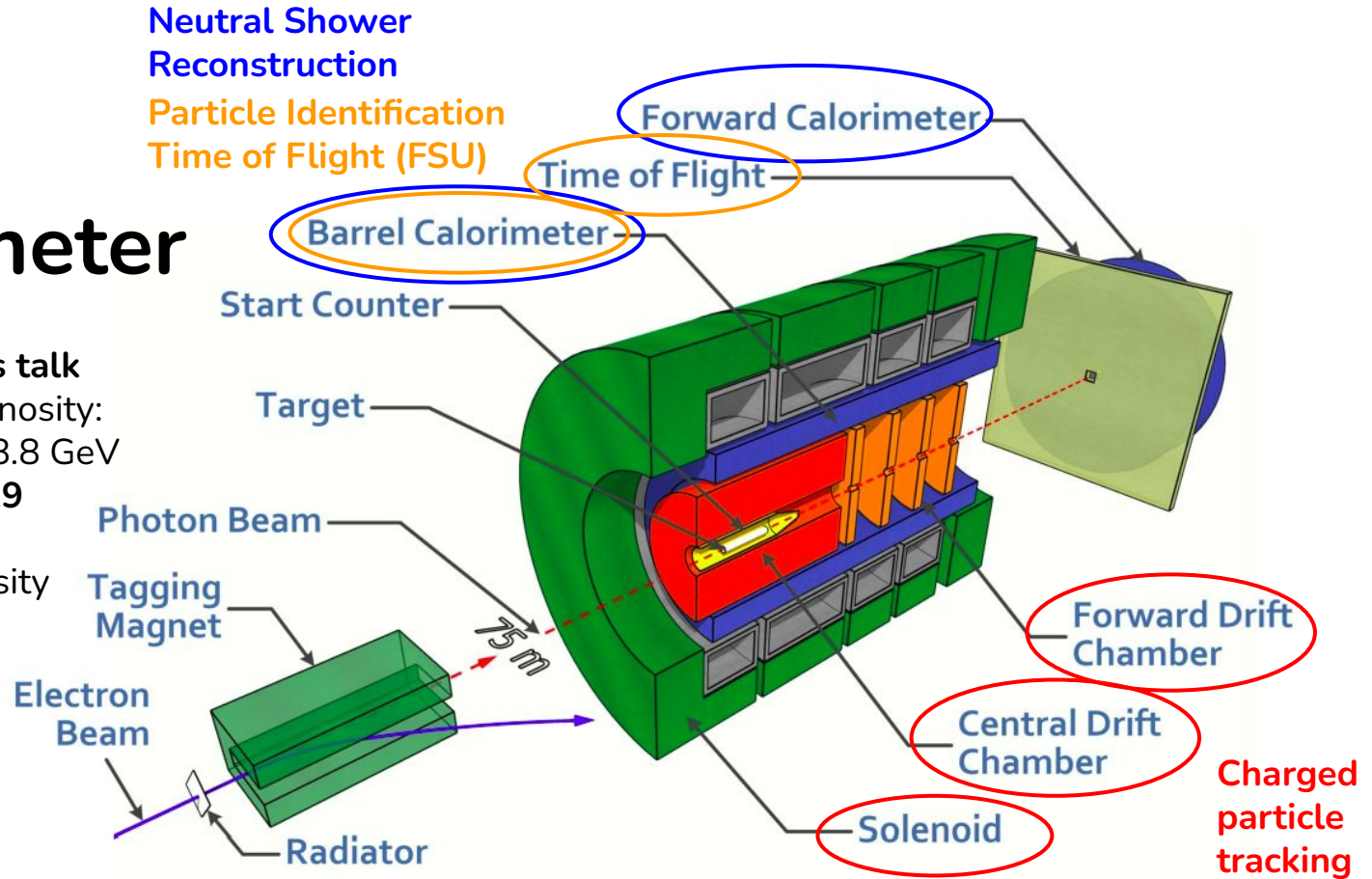
GlueX Spectrometer

Phase 1: 2017-2018

- Analyses in this talk
- Integrated Luminosity: 118.2 pb^{-1} 8.2-8.8 GeV

Phase 2: Started 2019

- Ends ~2025
- +(3-4)x Luminosity



Neutral Shower
Reconstruction

Particle Identification
Time of Flight (FSU)

Forward Calorimeter

Time of Flight

Barrel Calorimeter

Start Counter

Target

Photon Beam

Tagging
Magnet

Electron
Beam

Radiator

75 m

Forward Drift
Chamber

Central Drift
Chamber

Solenoid

Charged
particle
tracking

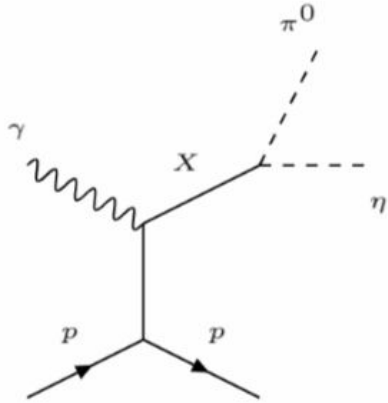
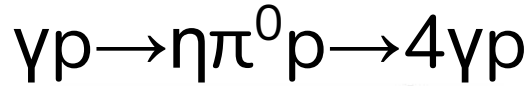
Characterizing the

$\gamma p \rightarrow \eta \pi^0 p \rightarrow 4 \gamma p$

Spectrum at



Reaction of Interest



SIGNAL REACTION

$$t = (p_{\text{recoil}} - p_{\text{target}})^2$$

Select exclusive

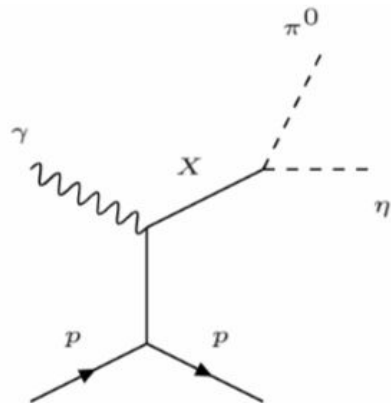
$\gamma p \rightarrow 4\gamma p$ events

Select coherent peak
(high polarization)

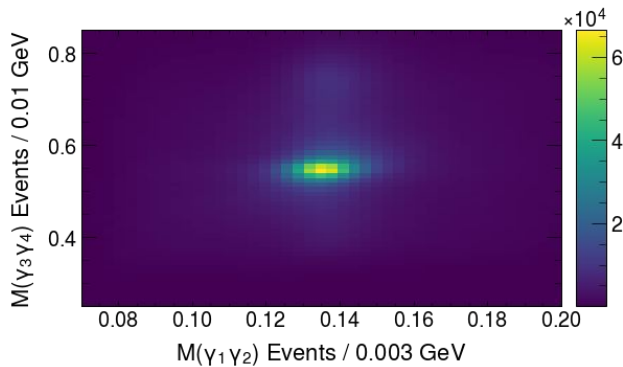
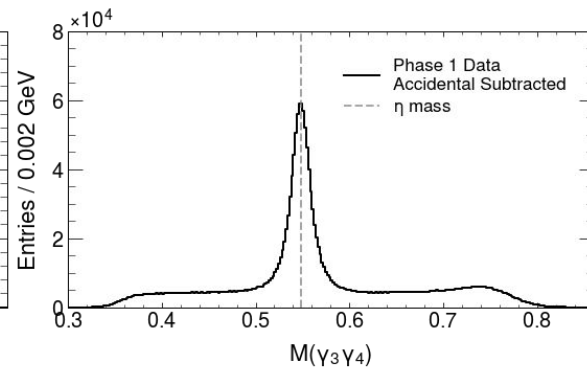
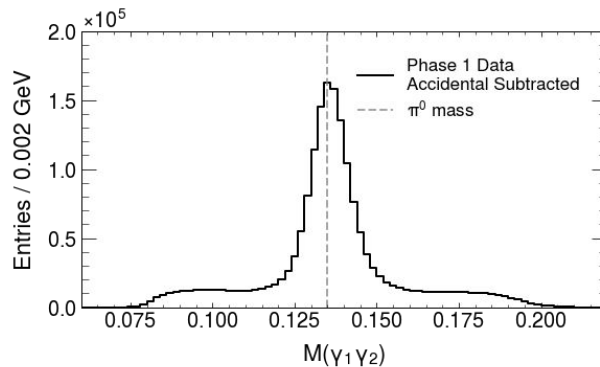
$$8.2 < E_{\text{Beam}} < 8.8 \text{ GeV}$$

Reaction of Interest

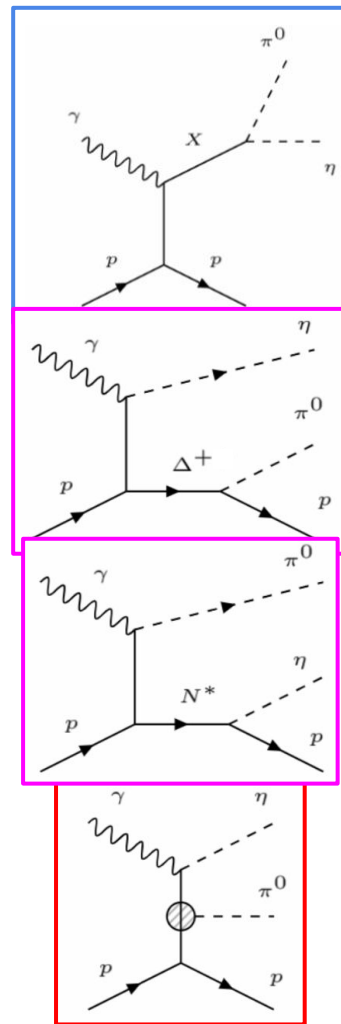
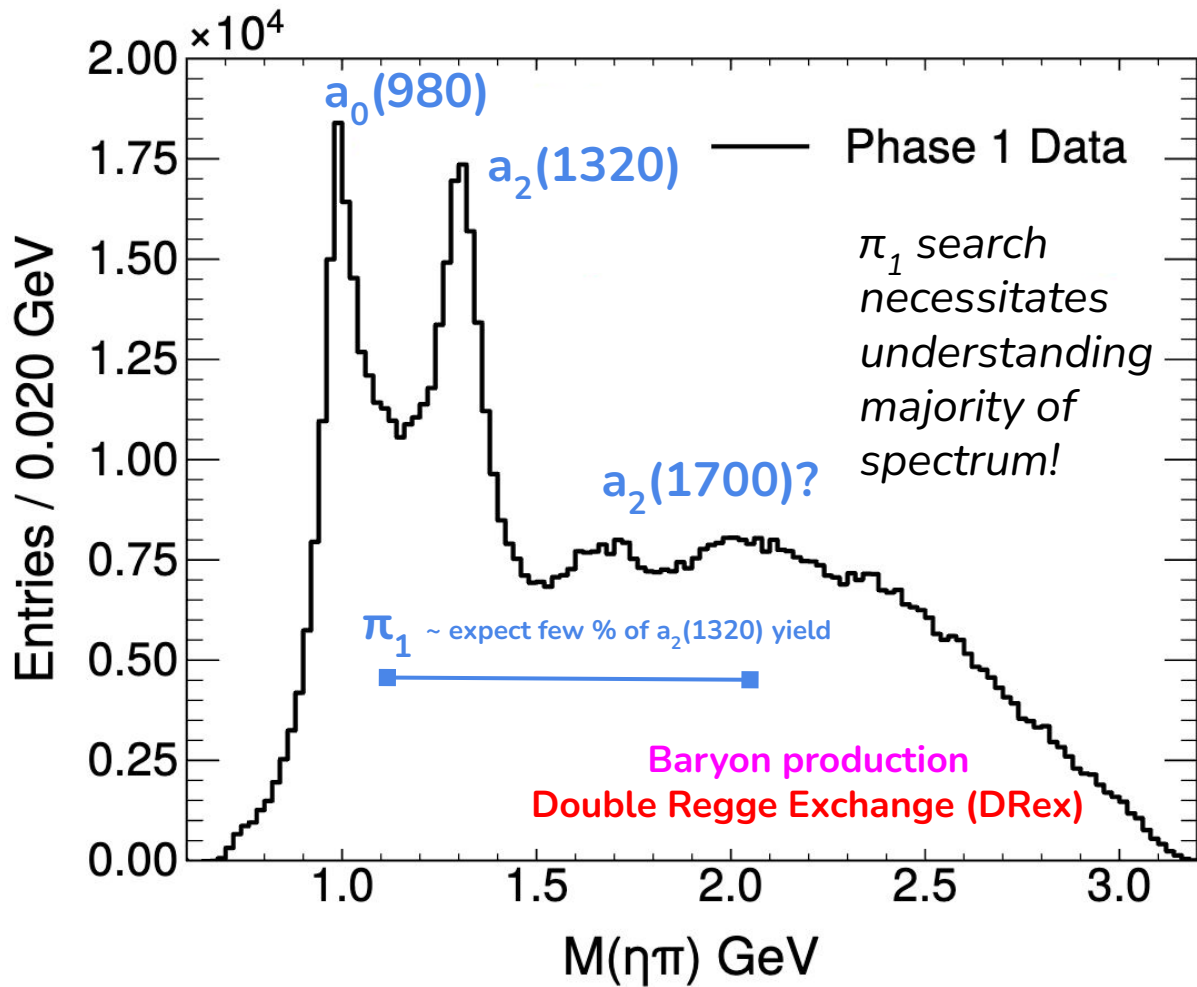
π^0 candidate : $\gamma_1\gamma_2$
 η candidate : $\gamma_3\gamma_4$

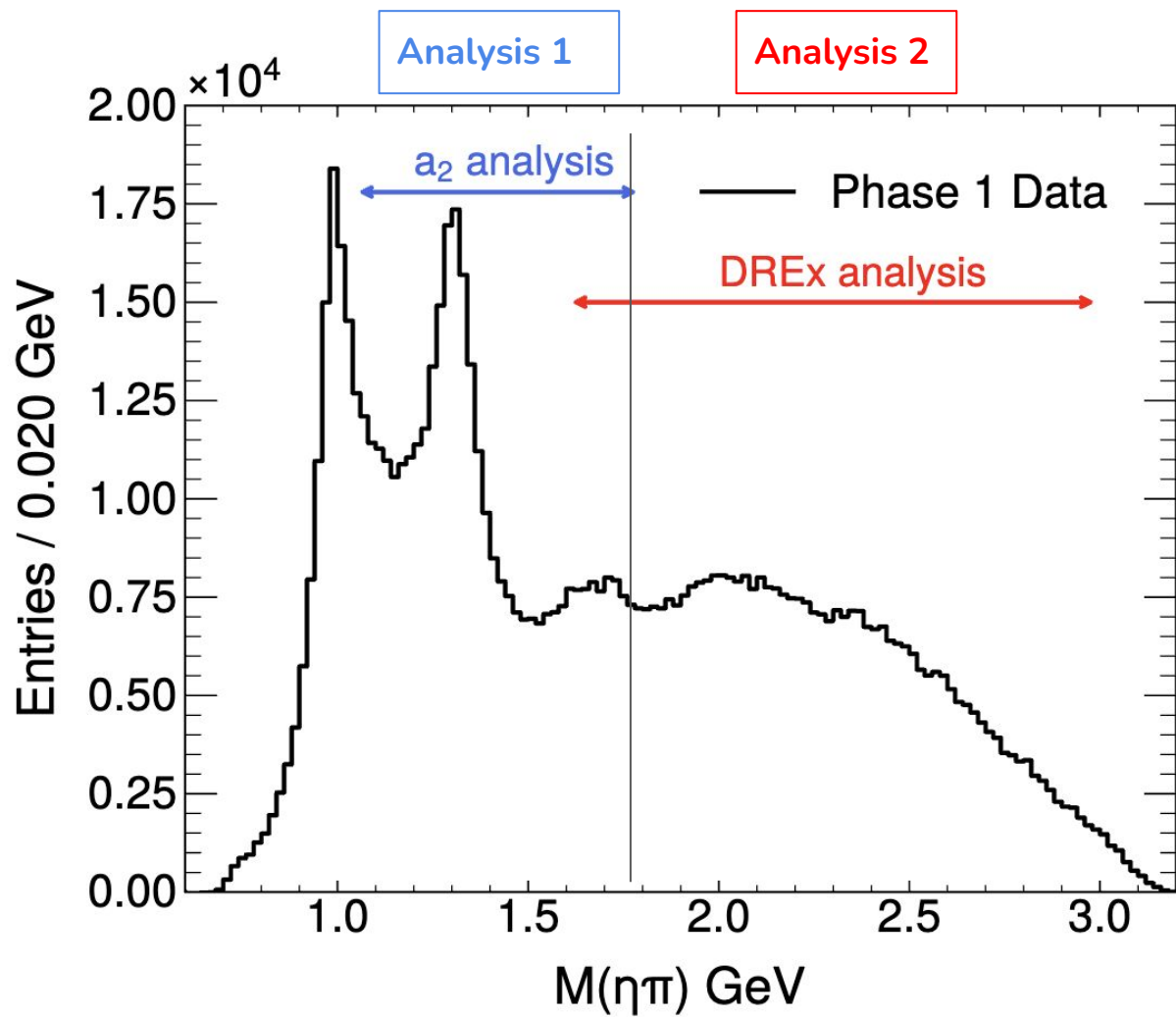


SIGNAL REACTION



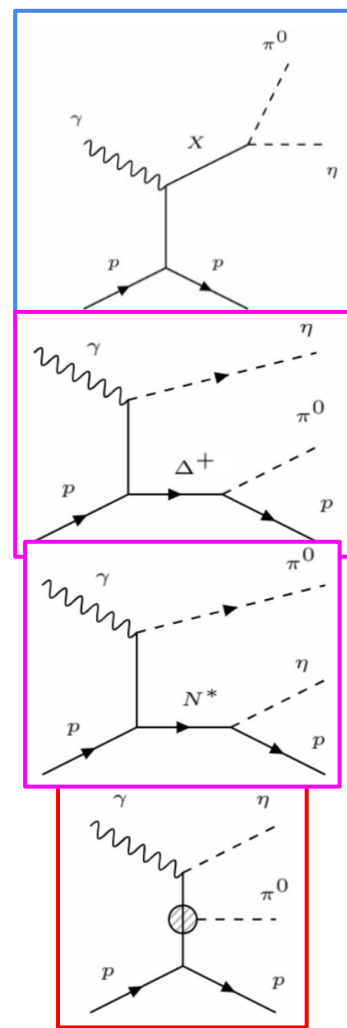
~900k events
with 80% purity

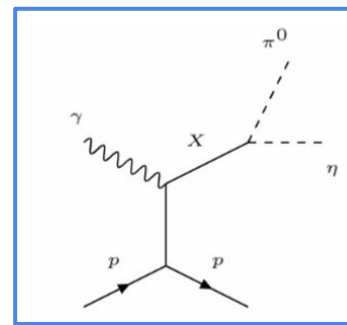
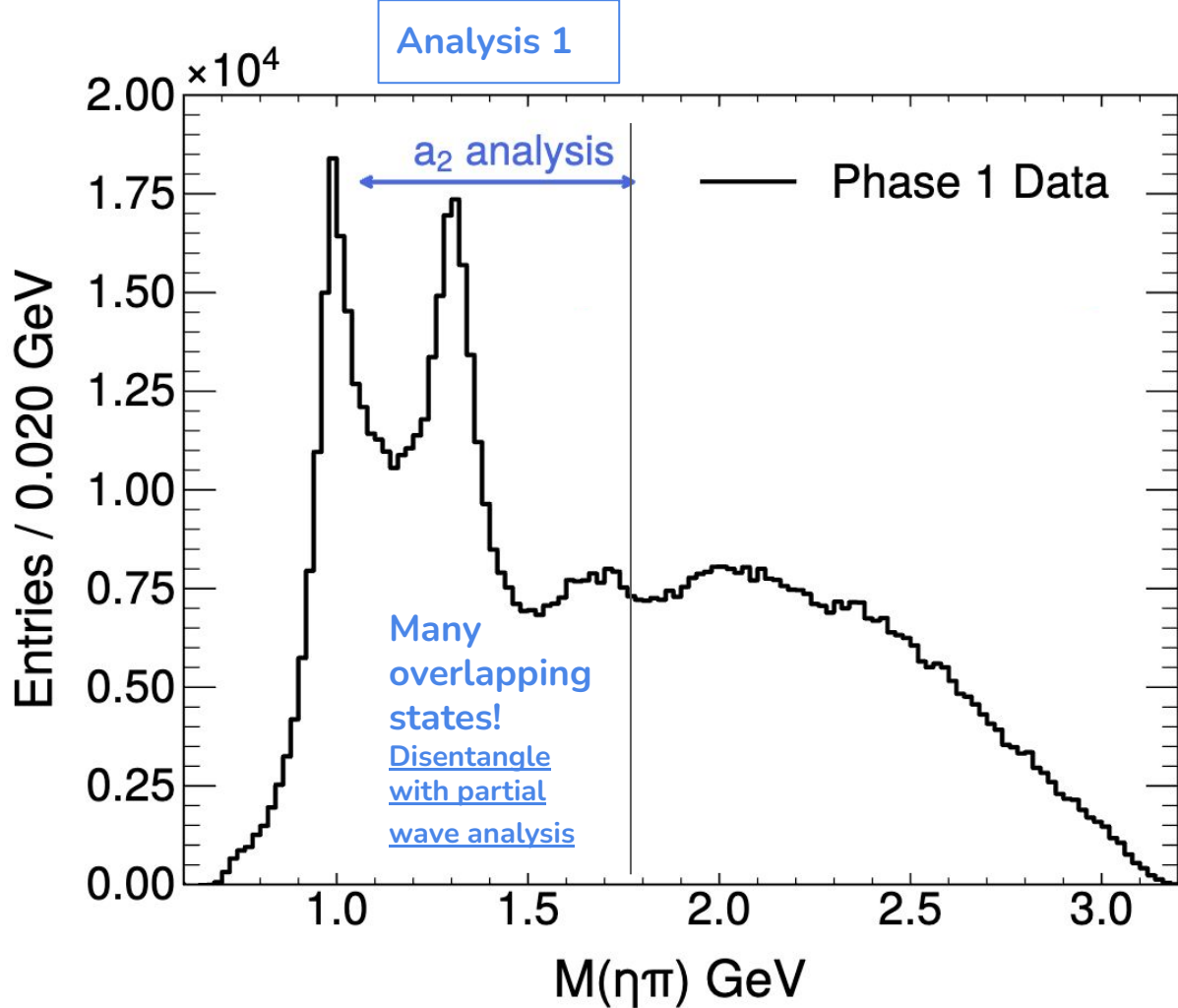




Analysis 1

Analysis 2

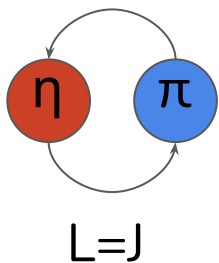




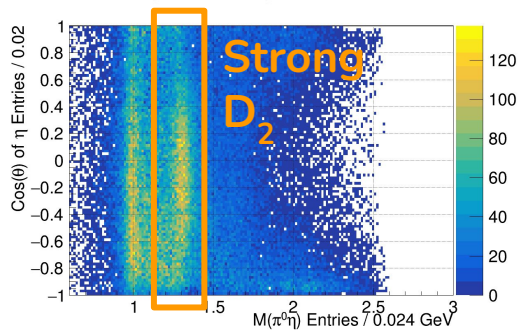
Why the $a_2(1320)$?

- Very prominent
- Unique angular distribution - hard for backgrounds to mimic
- Well known resonance properties: i.e. mass and width
- Need a “phase reference” to determine if π_1 is resonant
- **Measure the $a_2(1320)$ differential cross section**

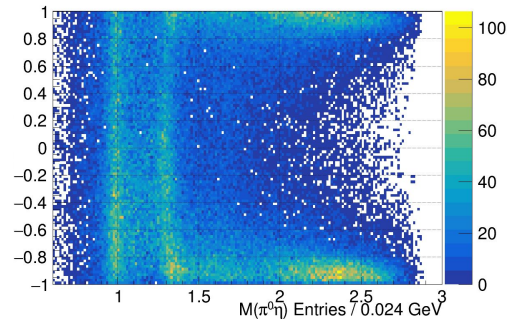
Angular Distributions



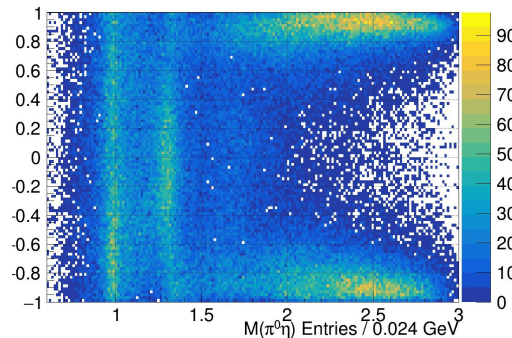
$0.1 < -t < 0.3 \text{ GeV}^2$



$0.3 < -t < 0.6 \text{ GeV}^2$

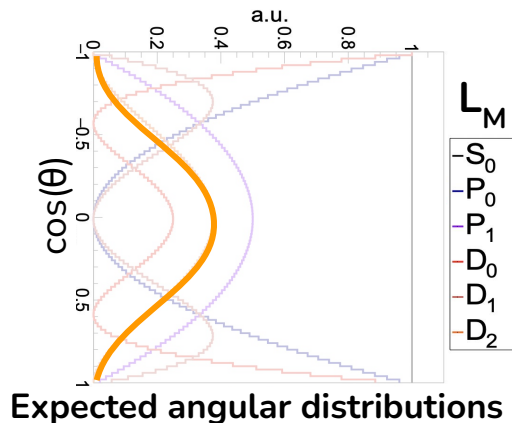


$0.6 < -t < 1.0 \text{ GeV}^2$



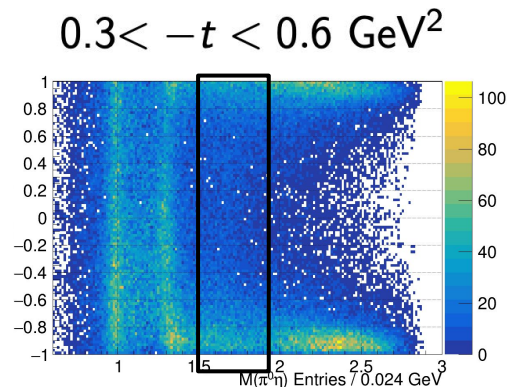
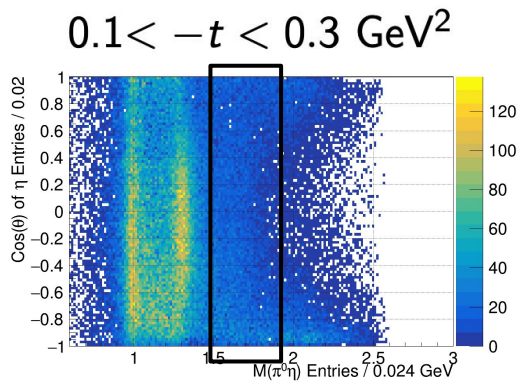
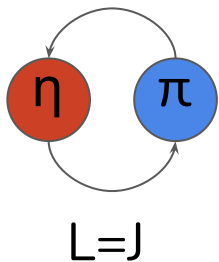
Phase-I data

Can see major features of spectrum



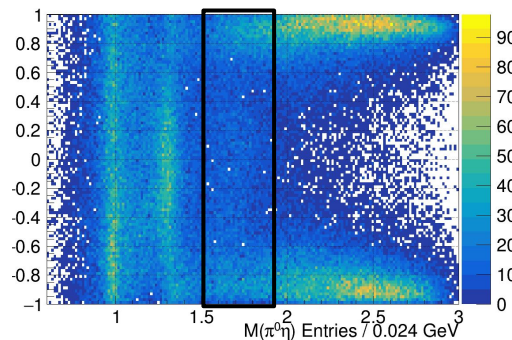
Expected angular distributions

Angular Distributions

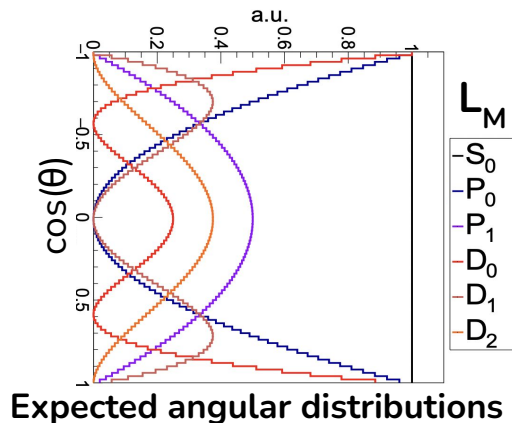


Phase-I data

$0.6 < -t < 1.0 \text{ GeV}^2$



Potential $a_2(1700)$ contribution would interfere with $a_2(1320)$



Partial Wave Analysis

Definition: New polarized amplitudes incorporating beam polarization

$$I(\Omega, \Phi) = 2\kappa \sum_k \left((1 - P_\gamma) \left[\sum_{l,m} [l]_{m;k}^{(-)} \operatorname{Re}[Z_l^m(\Omega, \Phi)] \right]^2 + (1 - P_\gamma) \left[\sum_{l,m} [l]_{m;k}^{(+)} \operatorname{Im}[Z_l^m(\Omega, \Phi)] \right]^2 \right. \\ \left. + (1 + P_\gamma) \left[\sum_{l,m} [l]_{m;k}^{(+)} \operatorname{Re}[Z_l^m(\Omega, \Phi)] \right]^2 + (1 + P_\gamma) \left[\sum_{l,m} [l]_{m;k}^{(-)} \operatorname{Im}[Z_l^m(\Omega, \Phi)] \right]^2 \right)$$

Angular Intensity

Partial Wave Analysis

Definition: New polarized amplitudes incorporating beam polarization

$$I(\Omega, \Phi) = 2\kappa \sum_k \left((1 - P_\gamma) \left[\sum_{l,m} [l]_{m;k}^{(-)} \operatorname{Re}[Z_l^m(\Omega, \Phi)] \right]^2 + (1 - P_\gamma) \left[\sum_{l,m} [l]_{m;k}^{(+)} \operatorname{Im}[Z_l^m(\Omega, \Phi)] \right]^2 \right. \\ \left. + (1 + P_\gamma) \left[\sum_{l,m} [l]_{m;k}^{(+)} \operatorname{Re}[Z_l^m(\Omega, \Phi)] \right]^2 + (1 + P_\gamma) \left[\sum_{l,m} [l]_{m;k}^{(-)} \operatorname{Im}[Z_l^m(\Omega, \Phi)] \right]^2 \right)$$

$$Z_l^m(\Omega, \Phi) = Y_l^m(\Omega) e^{-i\Phi}$$

Φ angle between polarization and production plane

$\Omega = \theta, \varphi$ are angles in the $\eta\pi$ rest frame “Gottfried-Jackson” (or “Helicity Frame”)

Partial Wave Analysis

First time these polarized amplitudes are used!

Definition: New polarized amplitudes incorporating beam polarization

$$I(\Omega, \Phi) = 2\kappa \sum_k \left((1 - P_\gamma) \left[\sum_{l,m} [l]_{m;k}^{(-)} \operatorname{Re}[Z_l^m(\Omega, \Phi)] \right]^2 + (1 - P_\gamma) \left[\sum_{l,m} [l]_{m;k}^{(+)} \operatorname{Im}[Z_l^m(\Omega, \Phi)] \right]^2 \right. \\ \left. + (1 + P_\gamma) \left[\sum_{l,m} [l]_{m;k}^{(+)} \operatorname{Re}[Z_l^m(\Omega, \Phi)] \right]^2 + (1 + P_\gamma) \left[\sum_{l,m} [l]_{m;k}^{(-)} \operatorname{Im}[Z_l^m(\Omega, \Phi)] \right]^2 \right)$$

$$Z_l^m(\Omega, \Phi) = Y_l^m(\Omega) e^{-i\Phi}$$

Φ angle between polarization and production plane

$\Omega = \theta, \varphi$ are angles in the $\eta\pi$ rest frame “Gottfried-Jackson” (or “Helicity Frame”)

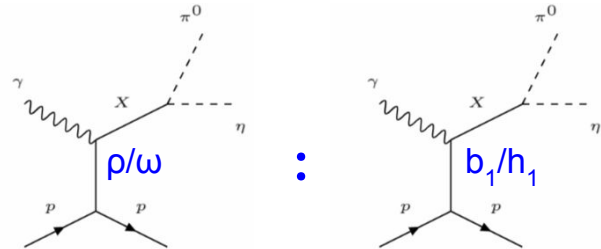
Polarization allows separation of the naturality of the exchange = {+, -}

Leading (+) Natural Parity Exchange: $\mathbf{J}^P = \mathbf{1}^- \dots$ (i.e. ρ, ω)

Leading (-) Unnatural Parity Exchange: $\mathbf{J}^P = \mathbf{1}^+ \dots$ (i.e. b_1, h_1)

Goal: Fit to extract partial wave amplitudes $[l]_m^{(-/+)}$

Different resonances populate different amplitudes

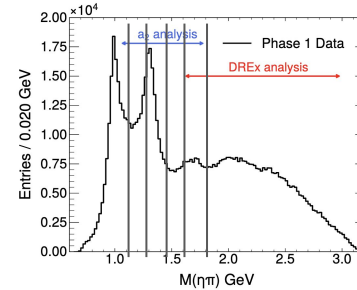


Differential Cross Section of the $a_2(1320)$

Mass independent fits - bin in $M(\eta\pi)$

Pros - greater model independence

Cons - lots of fit parameters
- more leakage and ambiguities



For example

Differential Cross Section of the $a_2(1320)$

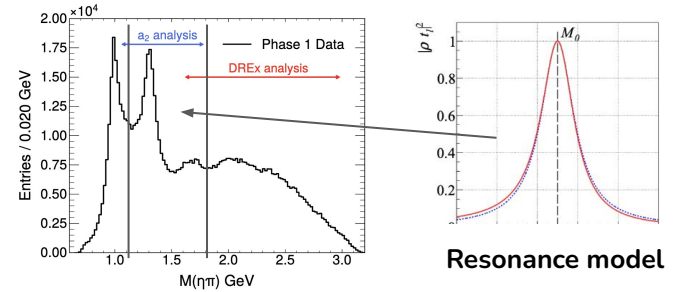
Mass independent fits - bin in $M(\eta\pi)$

Pros - greater model independence

Cons - lots of fit parameters
- more leakage and ambiguities

Mass dependent fits - include a resonance model

Semi-mass indep. = **Breit-Wigner for $a_2(1320)$ and $a_2(1700)$** and **piecewise constant mass dependence for **S-wave**** to model the $a_0(980)$ and pick up backgrounds



Differential Cross Section of the $a_2(1320)$

Mass independent fits - bin in $M(\eta\pi)$

Pros - greater model independence

Cons - lots of fit parameters
- more leakage and ambiguities

Mass dependent fits - include a resonance model

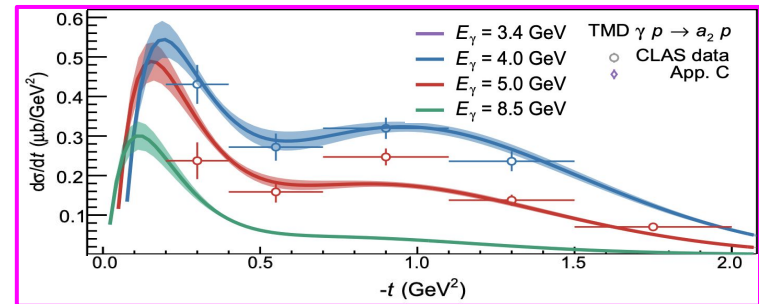
Semi-mass indep. = **Breit-Wigner for $a_2(1320)$ and $a_2(1700)$** and **piecewise** constant mass dependence for **S-wave** to model the $a_0(980)$ and pick up backgrounds

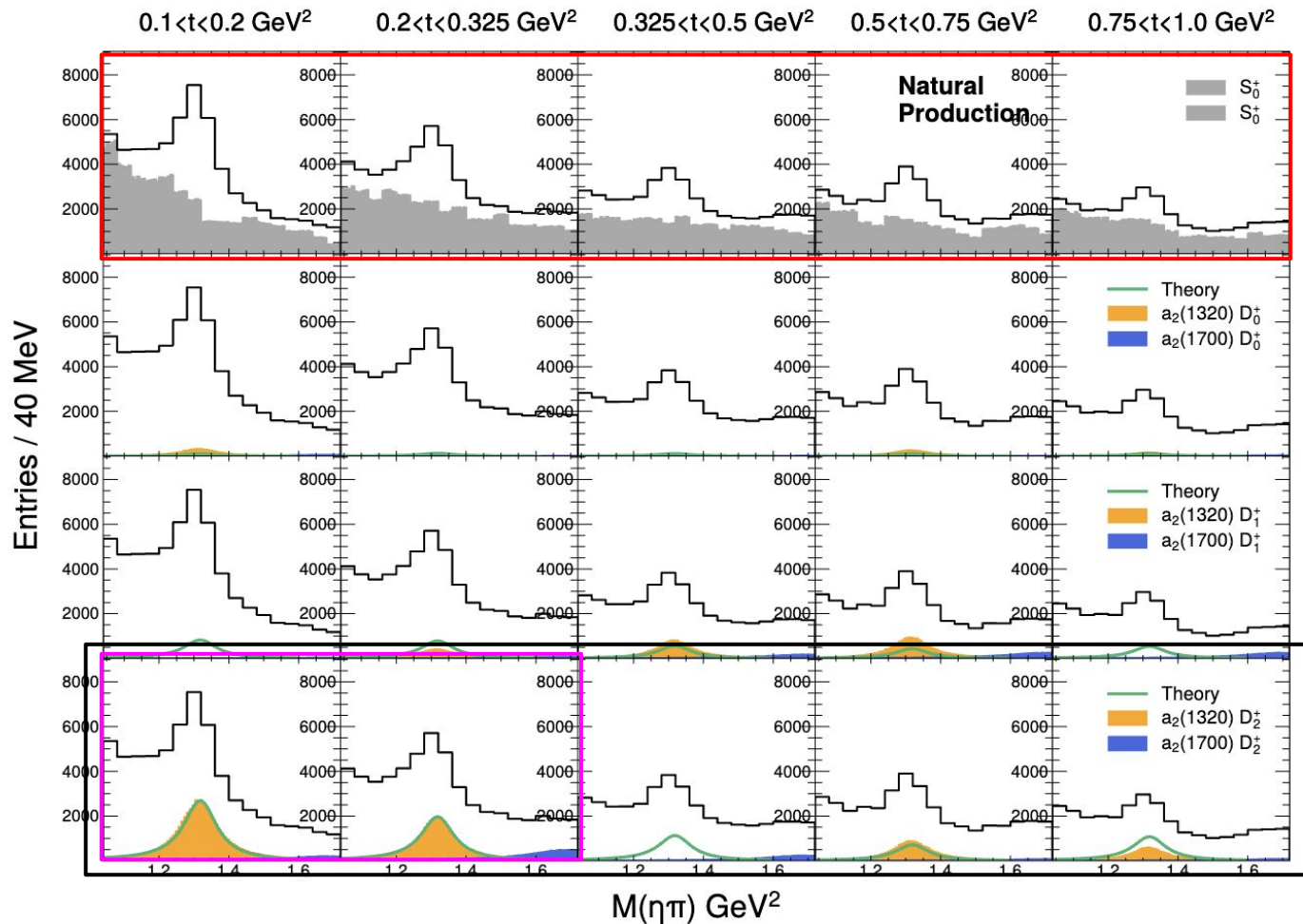
Tensor Meson Dominance Model - **model based on CLAS** photoproduction $d\sigma/dt$ data for a_2 | no partial wave analysis | [3.5, 5.5] GeV

Chosen **waveset**: $S_0^\pm, D_0^\pm, D_1^\pm, D_2^+, D_{-1}^-$

[V.Mathieu et.al. (JPAC) PRD 102, 014003 (2020)]

Measure $d\sigma/dt$ in 5 bins on $-t \in [0.1, 1.0]$
 GeV^2





Production via natural exchanges

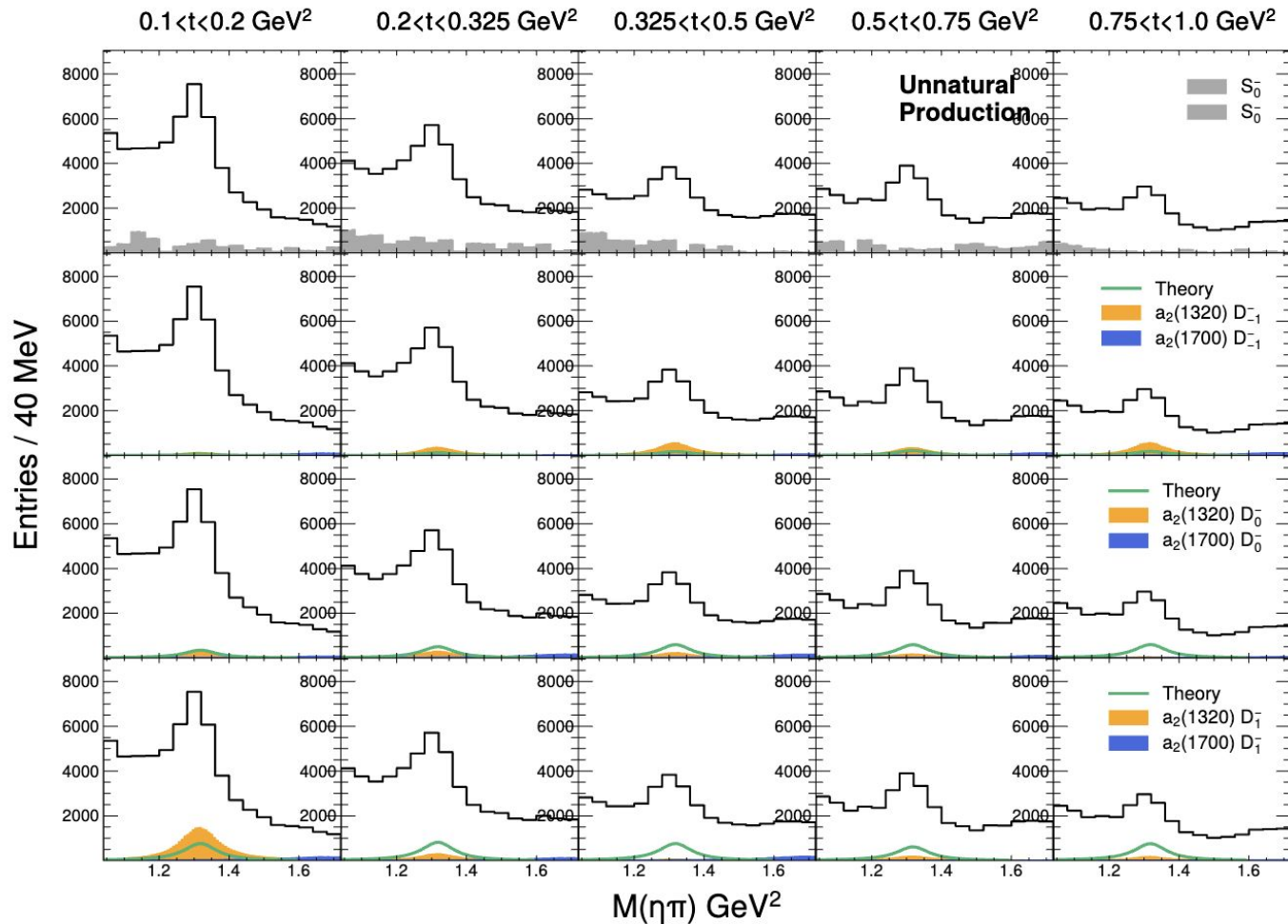
Theory predictions for $a_2(1320)$

Smooth/Strong S-wave intensity

Dominant D_2 in lowest t-bins as we had eyeballed

Strong t-dependence of m-projections!

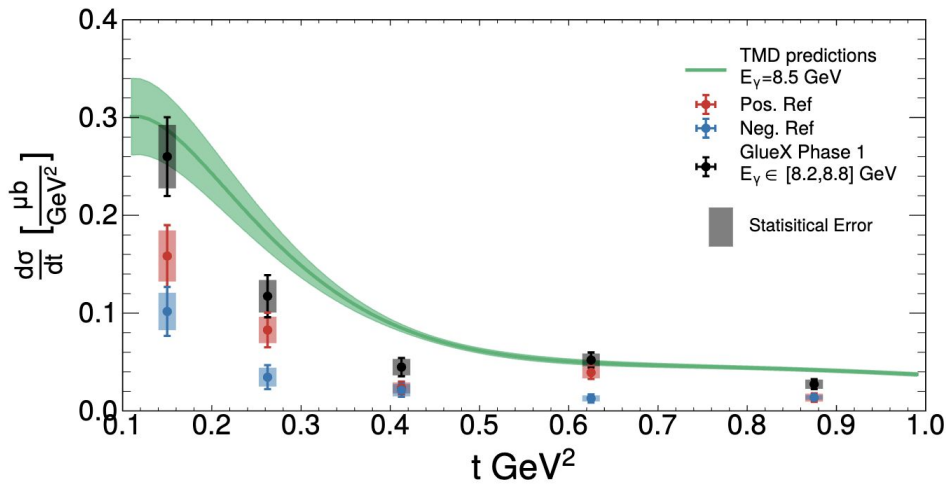
Results agree with mass independent fit results!



Production via unnatural exchanges

Smaller contributions overall

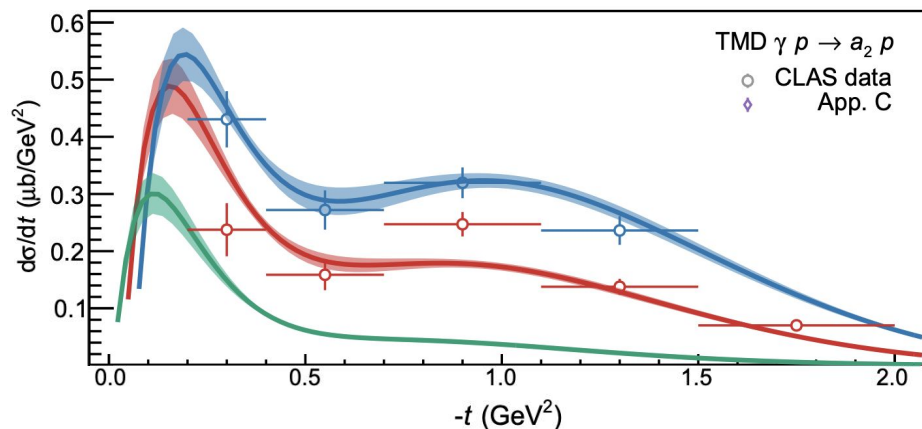
TMD model based on CLAS data with no PWA nor Polarization!

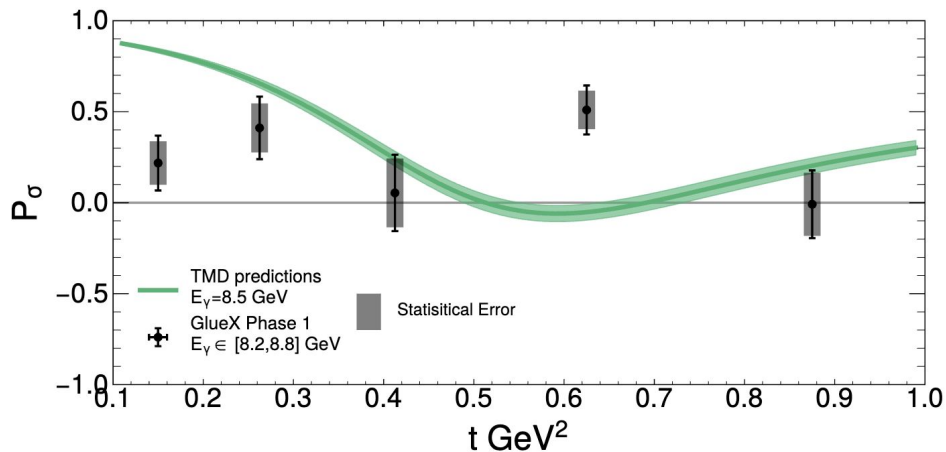
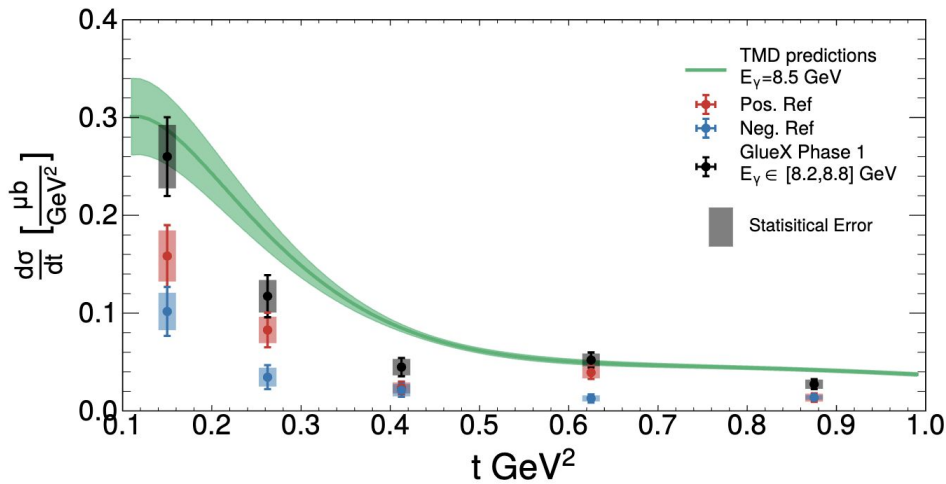


Comparison with theory

Theory predicts the dip in the cross section $\sim 0.5 \text{ GeV}^2$ gets “filled in” at out energies

- Does not appear to be the case
- Dip is consistent with previous experimental data including CLAS



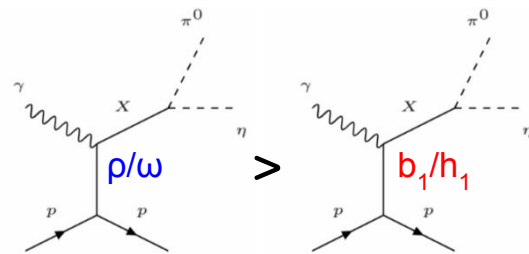


Comparison with theory

Theory predicts the dip in the cross section $\sim 0.5 \text{ GeV}^2$ gets “filled in” at out energies

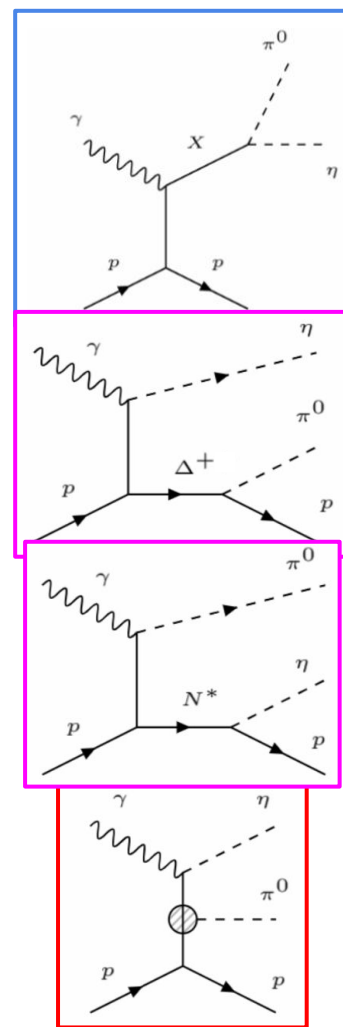
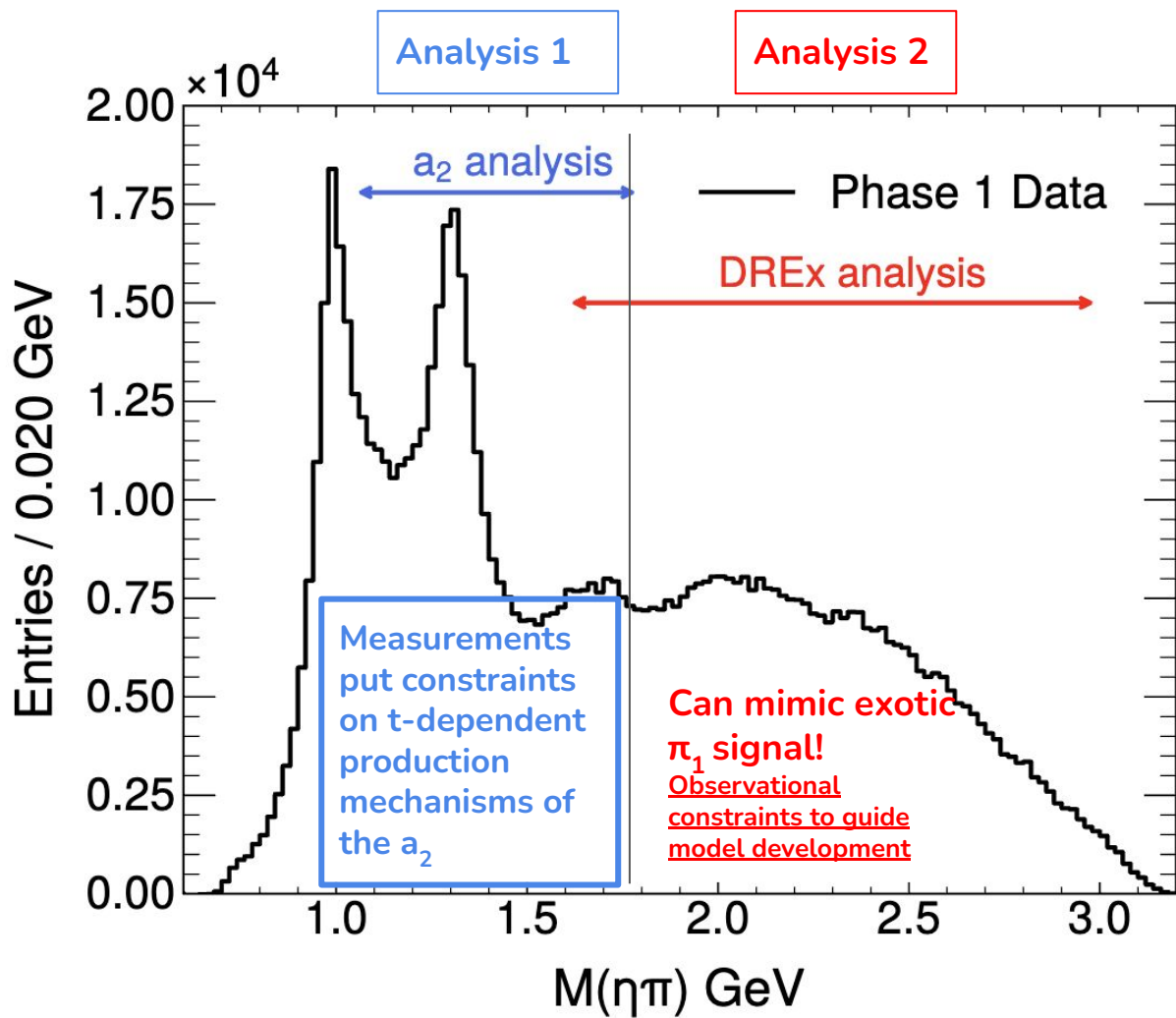
- Does not appear to be the case
- Dip is consistent with previous experimental data including CLAS

$$P_\sigma = \frac{\frac{d\sigma^+}{dt} - \frac{d\sigma^-}{dt}}{\frac{d\sigma^+}{dt} + \frac{d\sigma^-}{dt}}$$

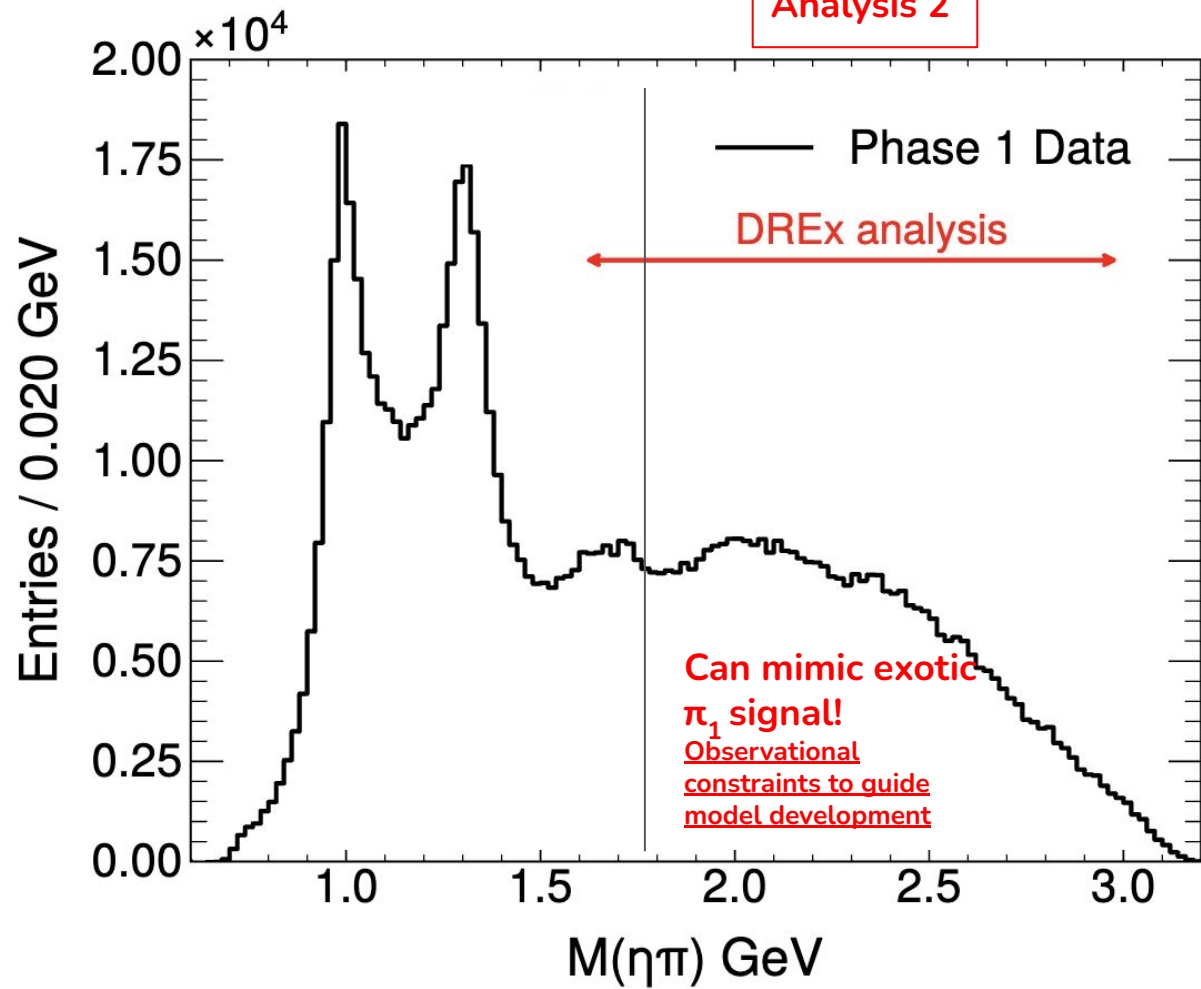


For leading exchanges we roughly get asymmetry between these two diagrams

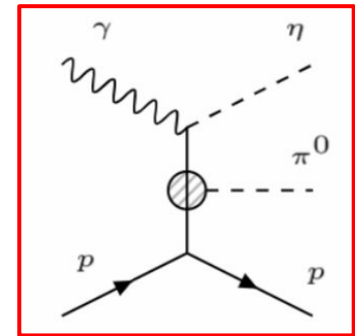
First measurement using the new polarized amplitudes



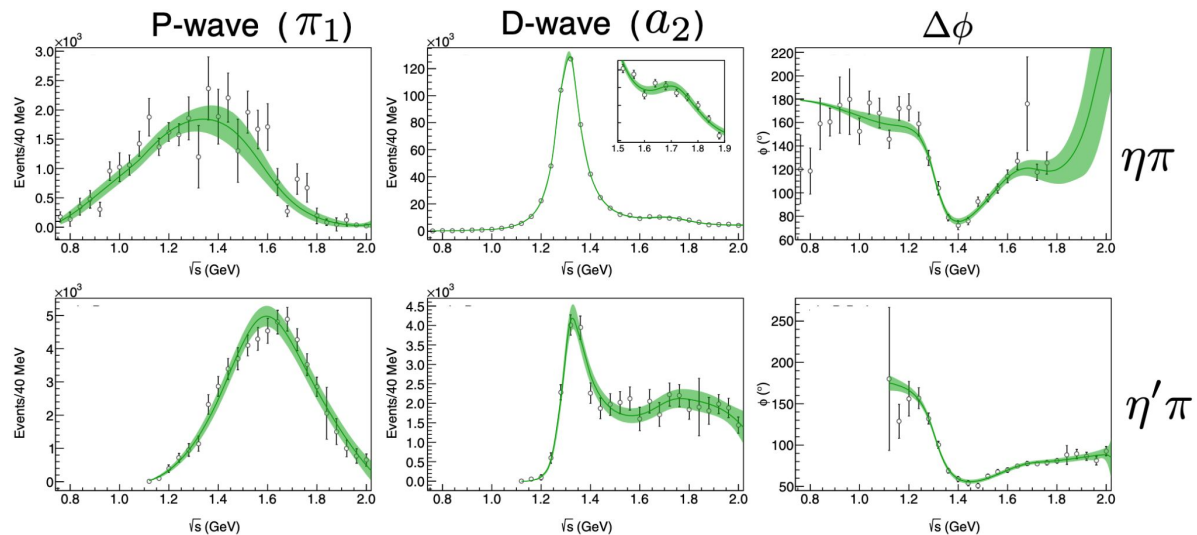
Analysis 2



Double Regge Exchange



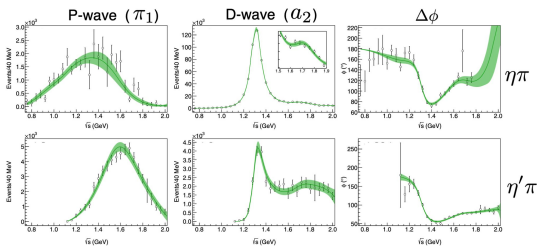
Importance of DREx



Partial wave analysis results

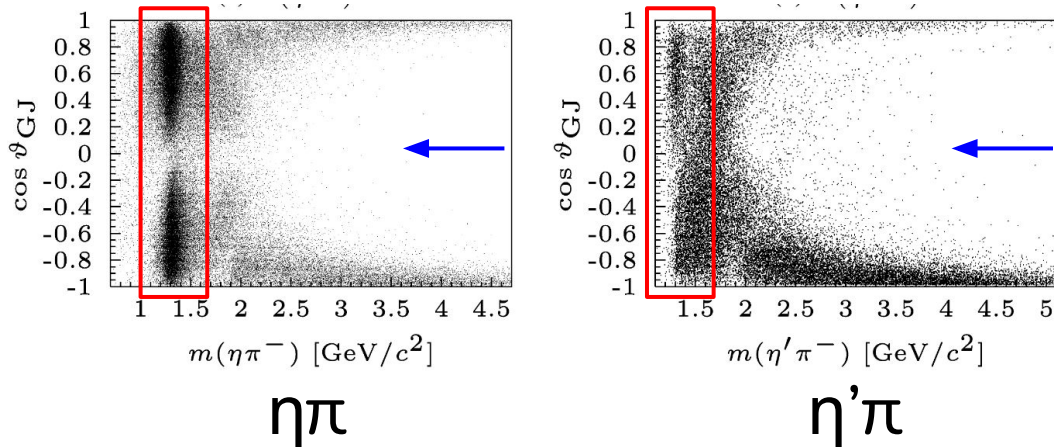
Look at
COMPASS
results
again!

Importance of DREx



Look at COMPASS results again!

Underlying fitted angular distributions



1) Recall all odd-L waves are exotic in $\eta^{(\prime)}\pi$

Familiar strong a_2 in $\eta\pi$ and $\eta'\pi$ (interfered)

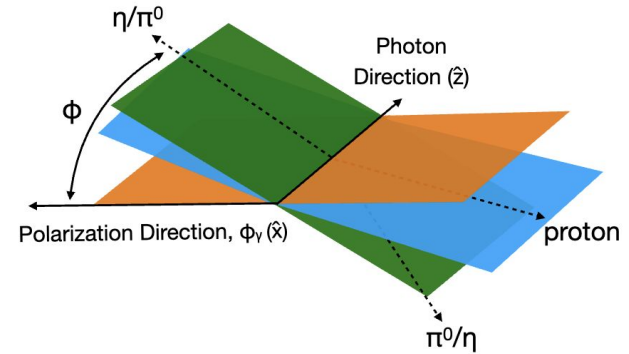
2) Interference between odd-L (i.e. π_1) and even-L (i.e. a_2) waves \Rightarrow asymmetric angular distributions!

asymmetric angular distributions ~~✗~~
 unique signature of an exotic

3) Signature of DREx is these “wings” that dominate at high mass also produce asymmetric angular distributions

How to constrain DREx contribution in π_1 region?

Beam Asymmetry



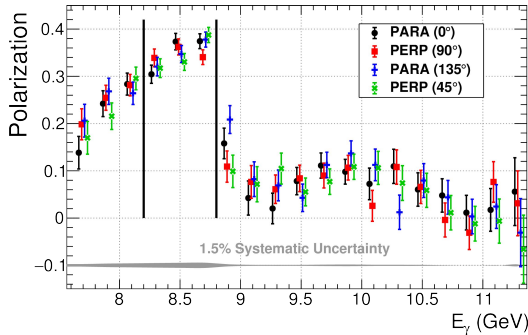
Stichel's Theorem = For linear polarized beam, cross section can be split into two components: one component parallel to **reaction plane** another perpendicular

$$\frac{d\sigma}{dt} = \frac{d\sigma_{\perp}}{dt} + \frac{d\sigma_{\parallel}}{dt}$$

σ_{\perp} : Unnatural exchanges only
 σ_{\parallel} : Natural exchanges only

Define **Beam Asymmetry**

$$\Sigma = \frac{\frac{d\sigma_{\perp}}{dt} - \frac{d\sigma_{\parallel}}{dt}}{\frac{d\sigma_{\perp}}{dt} + \frac{d\sigma_{\parallel}}{dt}}$$



Recall data taken in 2 pairs of orthogonal orientations

Construct **Yield Asymmetry** to extract Σ

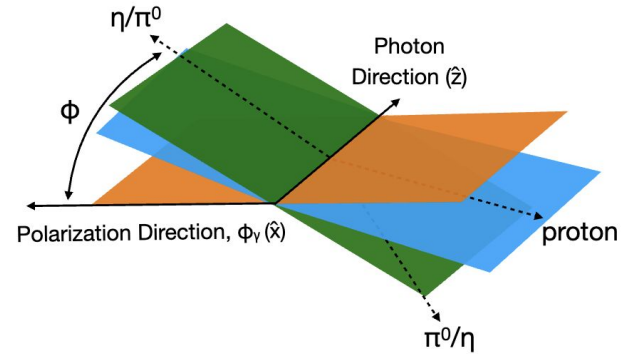
$$Y_A = \frac{Y_{\perp} - F_R Y_{\parallel}}{Y_{\perp} + F_R Y_{\parallel}} = \frac{(P_{\perp} + P_{\parallel})\Sigma \cos 2\phi}{2 + (P_{\perp} - P_{\parallel})\Sigma \cos 2\phi}$$

We measure Yields Y

F_R = flux ratio ~ 1

P = polarization magnitude $\sim 35\%$

Beam Asymmetry



Stichel's Theorem = For linear polarized beam, cross section can be split into two components: one component parallel to **reaction plane** another perpendicular

$$\frac{d\sigma}{dt} = \frac{d\sigma_{\perp}}{dt} + \frac{d\sigma_{\parallel}}{dt} \quad \begin{array}{l} \sigma_{\perp} : \text{Unnatural exchanges only} \\ \sigma_{\parallel} : \text{Natural exchanges only} \end{array}$$

Define **Beam Asymmetry**

$$\Sigma = \frac{\frac{d\sigma_{\perp}}{dt} - \frac{d\sigma_{\parallel}}{dt}}{\frac{d\sigma_{\perp}}{dt} + \frac{d\sigma_{\parallel}}{dt}}$$

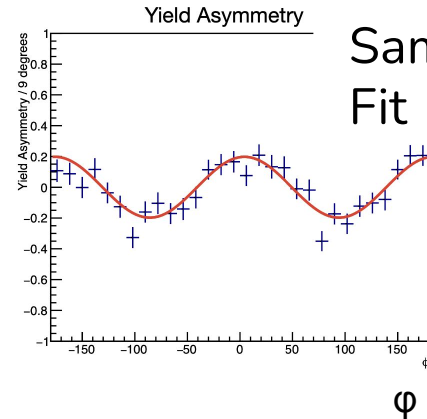
Construct **Yield Asymmetry** to extract Σ

$$Y_A = \frac{Y_{\perp} - F_R Y_{\parallel}}{Y_{\perp} + F_R Y_{\parallel}} = \frac{(P_{\perp} + P_{\parallel})\Sigma \cos 2\phi}{2 + (P_{\perp} - P_{\parallel})\Sigma \cos 2\phi}$$

We measure Yields Y

F_R = flux ratio ~ 1

P = polarization magnitude $\sim 35\%$

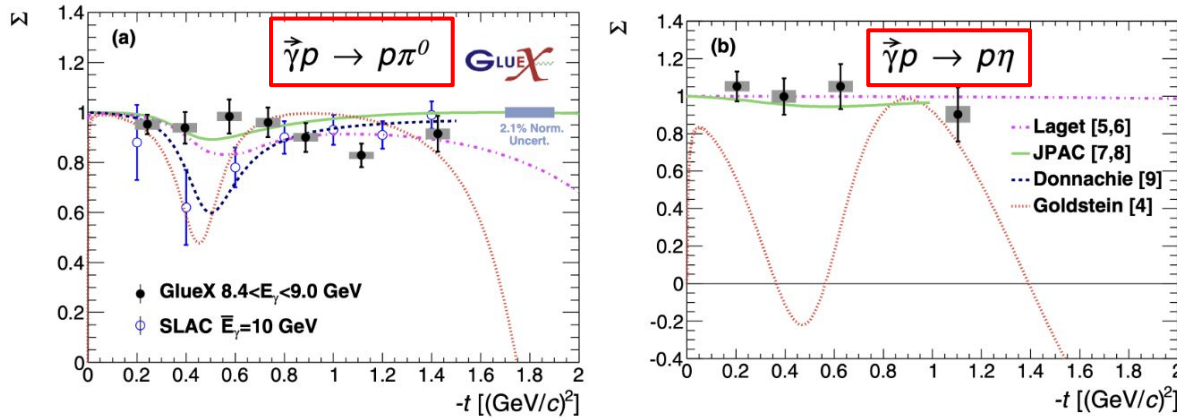


Sample Fit

$\Sigma \sim 0.57$

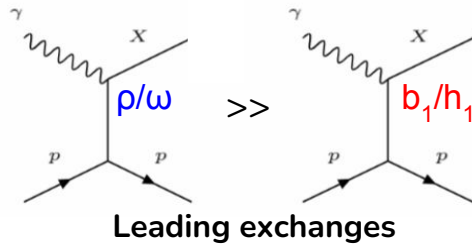
Natural exchange dominant

Previous GlueX Σ Measurements



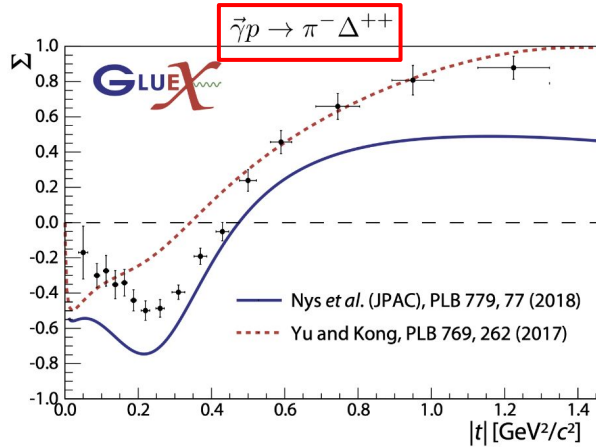
Photoproduction of single pseudoscalars: π^0 and η

- $\Sigma \sim 1$ = Almost all natural exchanges



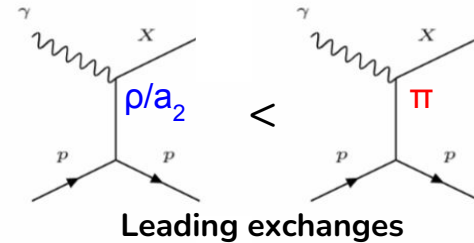
Natural exchanges
Unnatural exchanges

Previous GlueX Σ Measurements

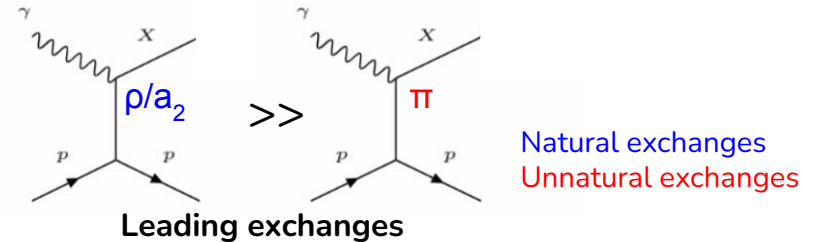


Photoproduction of π^- shows significant t -dependence

Low t

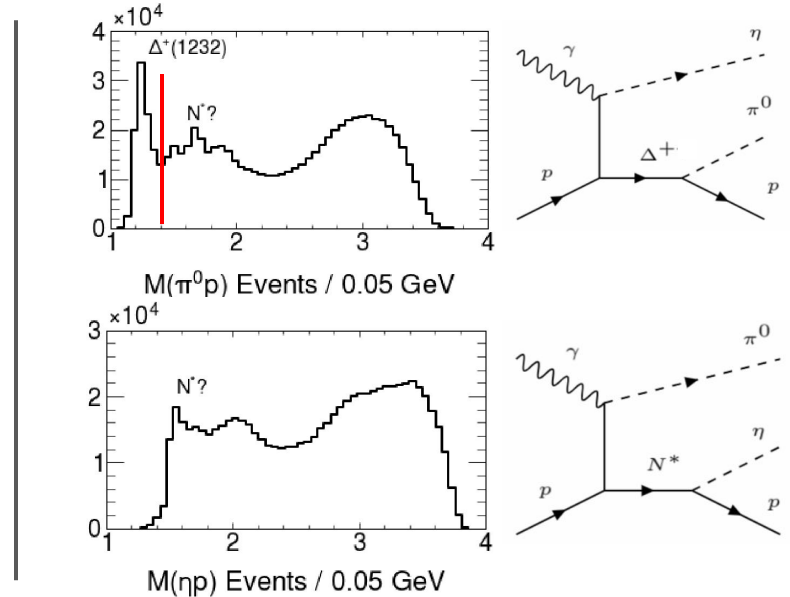
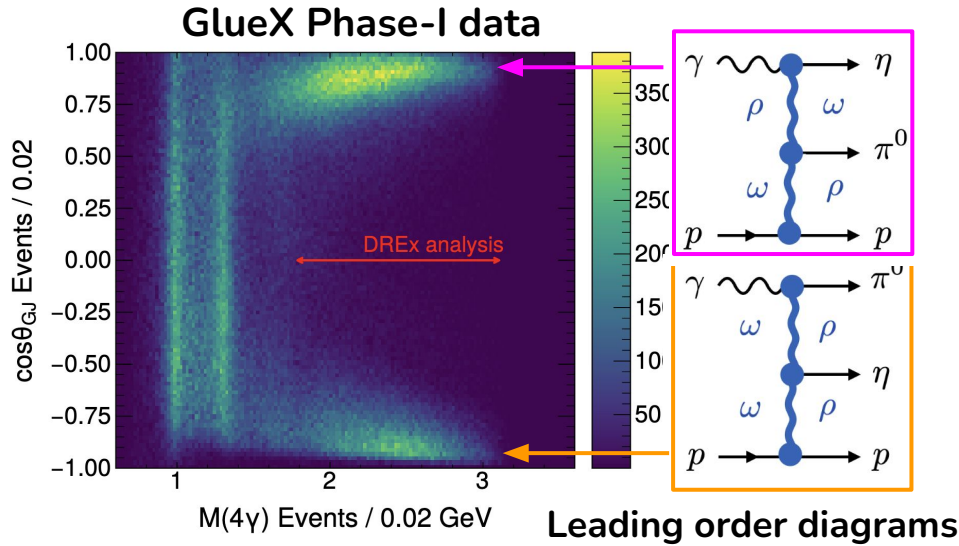


High t



Measuring Σ constrains production mechanism

Double Regge Σ Measurement

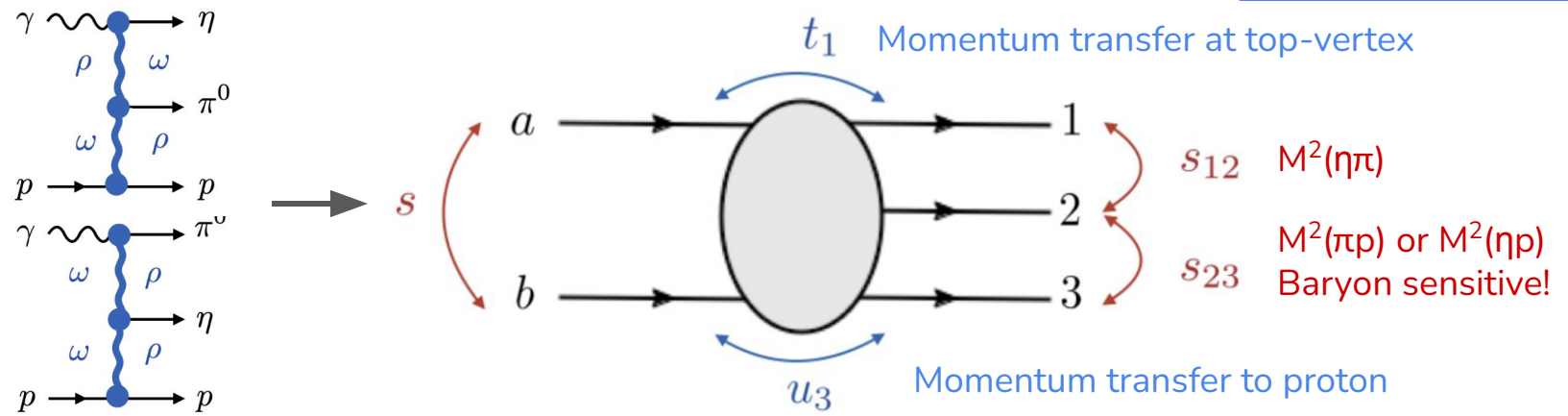


Asymmetric production of processes can produce angular asymmetry just as a signal for a π_1 exotic would!

Baryon production very similar diagrams \Rightarrow very similar parts of phase space!

Double Regge Σ Measurement

$$t_1: \begin{aligned} t_\eta &= (p_\gamma - p_\eta)^2 \\ t_\pi &= (p_\gamma - p_\pi)^2 \end{aligned}$$



Measure beam asymmetry at the top vertex Σ_{t_1} as a function of $s_{12} / s_{23} / u_3$

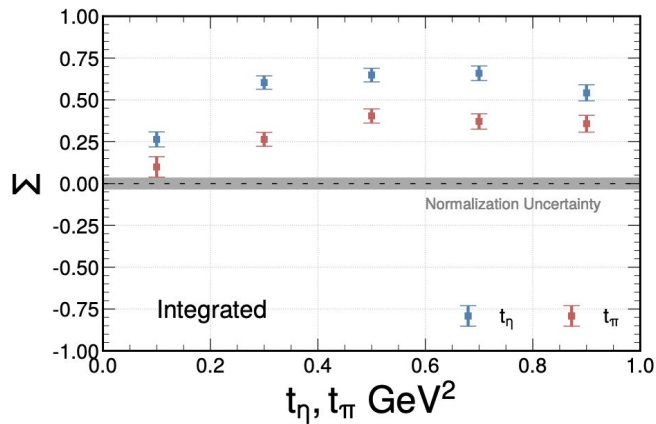
Additional bins should help separate baryon production

Compare results from $\gamma p \rightarrow \eta \pi^0 p$ (this talk)

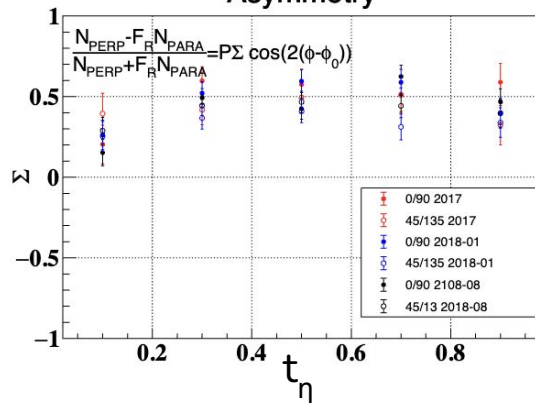
$\gamma p \rightarrow \eta \pi^- \Delta^{++}$ (Complementary channel, Courtesy of Colin Gleason)

Select Σ Results

$\eta\pi^0$

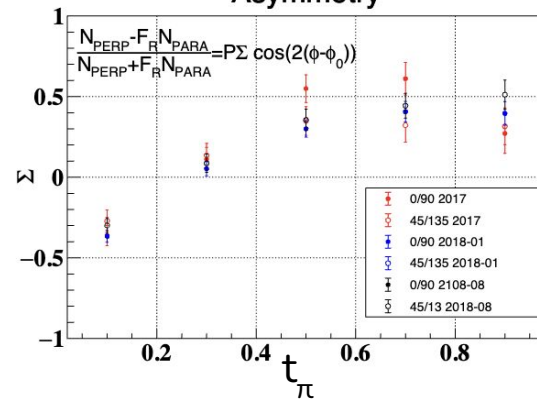


Asymmetry

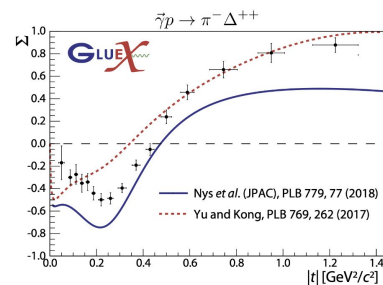


$\eta\pi^-$

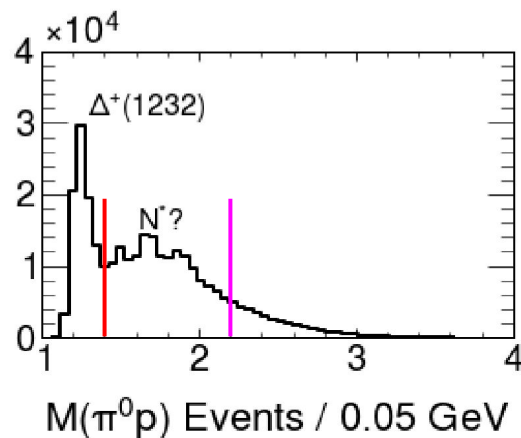
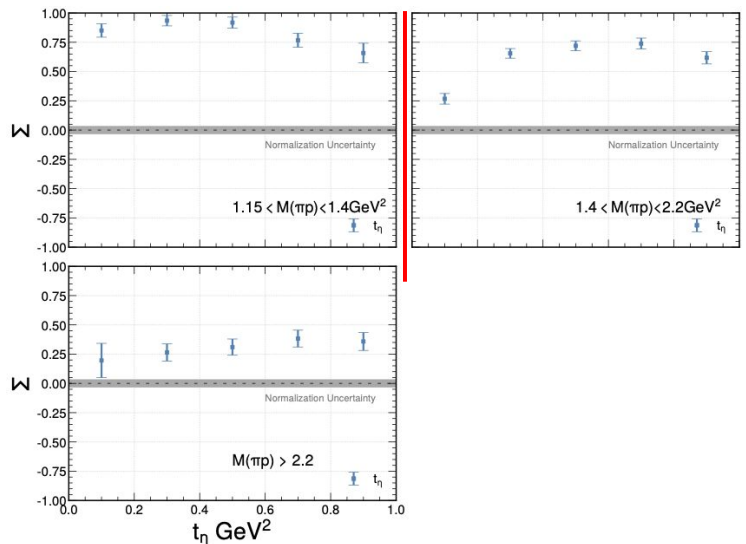
Asymmetry



- No additional bins in $s_{12} / s_{23} / u_3$
- t_η very similar between channels, cross section dominated by natural exchanges, $\Sigma \sim 0.4$
- t_π for $t_1 < 0.5$ much more like $\gamma p \rightarrow \pi^- \Delta^{++}$ but saturates to become similar to the $\eta\pi^0$ channel



Select Σ Results: Σ_η binned in $M(\pi\rho)$



$\eta\pi^0$

Δ^+ removed for all measurements in the $\eta\pi^0$ channel but interesting to probe here

$\Sigma \sim 1$ in the Δ^+ dominated region

$\Sigma \sim 0.6$ where N^* resonances populate

$\Sigma \sim 0.3$ at large $M(\pi\rho)$

$\pi\rho$ baryons produced mostly through natural exchanges

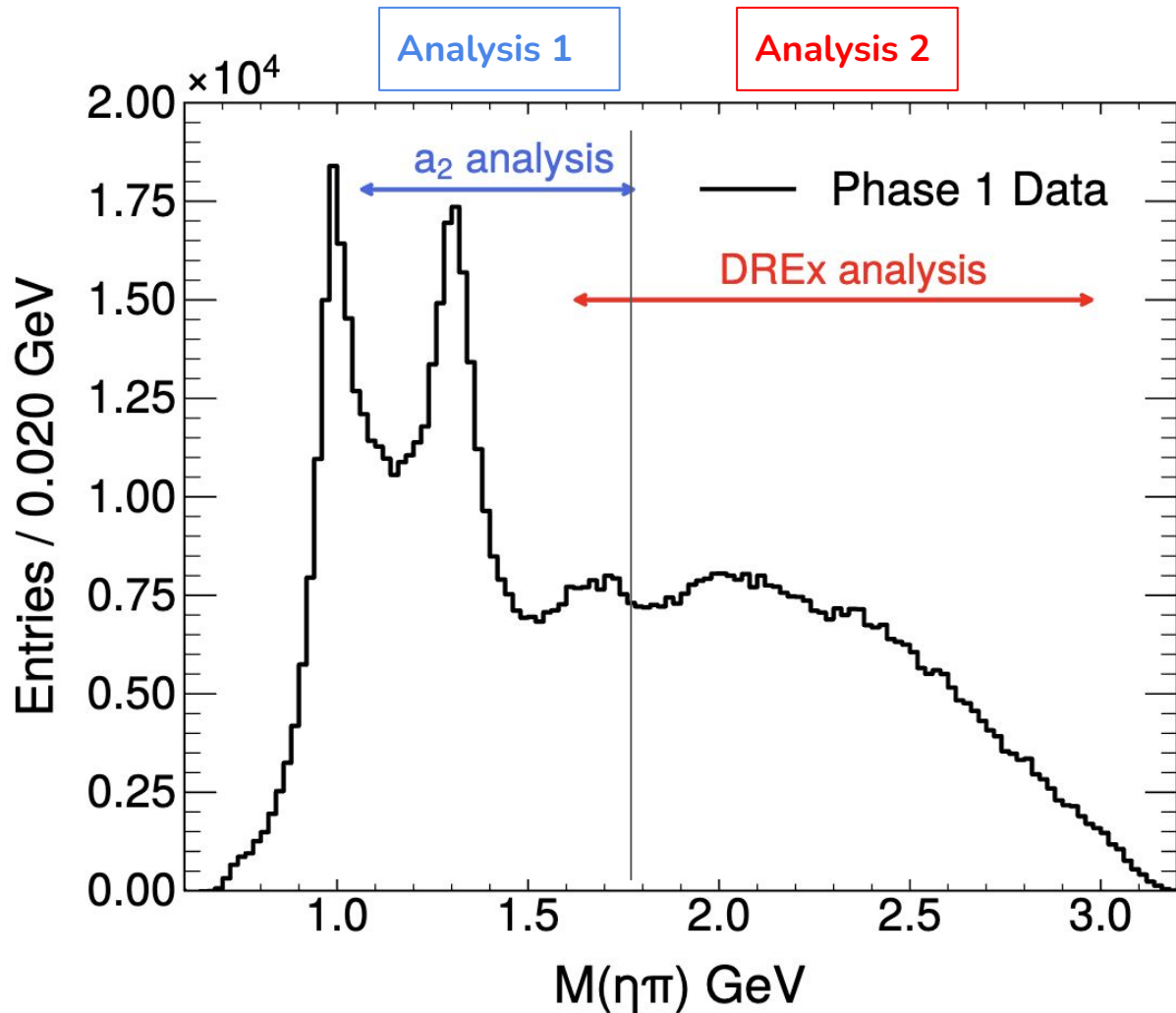
*First observational constraints
on double Regge process in
photoproduction*

Summary

π_1 contribution expected to be small, requires characterization of the majority of the $M(\eta\pi)$ spectrum

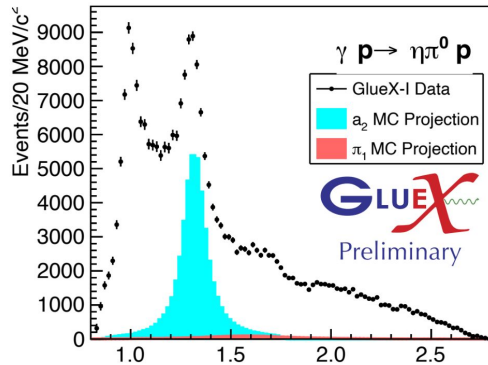
Presented first analysis using new polarized amplitudes to measure a_2 differential cross section

Presented first measurement to set observational constraints on double Regge production mechanisms in photoproduction

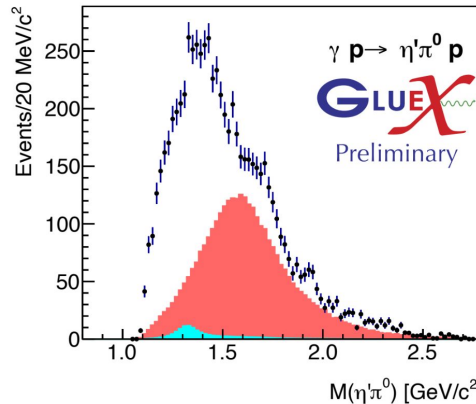


Pathway to the π_1

- Currently, GlueX is setting π_1 cross section upper limit based on $\gamma p \rightarrow \omega \pi \pi p$ and lattice QCD results
 - Project cross section upper limits into $\eta \pi$ and $\eta' \pi$ yield upper limits



Courtesy of Will Imoehl $M(\eta\pi^0)$ [GeV/c²]



a_2 cross sections measured for this dissertation used as an input

Yield(a_2) \gg Yield(π_1) in $\eta \pi$
Yield(a_2) \ll Yield(π_1) in $\eta' \pi$

Next (few) Steps: Perform coupled channel analysis to constrain the a_2 and π_1 contributions across $\eta \pi$ and $\eta' \pi$

*Thank you!
Almost...*

Additional Studies (Machine Learning)



PHYSICAL REVIEW D **105**, L091501 (2022)

Letter

Deep learning exotic hadrons

L. Ng,^{1,†} Ł. Bibrzycki,^{2,†} J. Nys,^{3,‡} C. Fernández-Ramírez,^{4,5,§} A. Pilloni,^{6,7,8,||}
V. Mathieu,^{9,10} A. J. Rasmusson,¹¹ and A. P. Szczepaniak^{11,12,13}

(Joint Physics Analysis Center)

*Study pentaquarks
using neural
networks*



Carnegie Supernova Project-II: Near-infrared spectral diversity and template of Type Ia Supernovae

JING LU (陆晶),¹ ERIC Y. HSIAO (蕭亦麟),¹ MARK M. PHILLIPS,² CHRISTOPHER R. BURNS,³ CHRIS ASHALL,⁴
NIDIA MORRELL,² LAWRENCE NG,² SAHANA KUMAR,¹ MELISSA SHAHBANDEH,^{5,6} PETER HOEFlich,¹ E. BARON,^{7,8}
SYED UDDIN,⁹ MAXIMILIAN D. STRITZINGER,¹⁰ NICHOLAS B. SUNTZEFF,⁹ CHARLES BALTAY,¹¹ SCOTT DAVIS,¹
TIARA R. DIAMOND,¹² GASTON FOLATELLI,^{13,14} FRANCISCO FÖRSTER,^{15,16} JONATHAN GAGNÉ,^{17,2} LLUÍS GALBANY,^{18,19}
CHRISTA GALL,²⁰ SANTIAGO GONZÁLEZ-GAITÁN,²¹ SIMON HOLMBO,¹⁰ ROBERT P. KIRSHNER,^{22,23} KEVIN KRISCIUNAS,⁹
G. H. MARION,²⁴ SAUL PERLMUTTER,^{25,26} PRISCILA J. PESSI,²⁷ ANTHONY L. PIRO,³ DAVID RABINOWITZ,¹¹
STUART D. RYDER,^{28,29} AND DAVID J. SAND³⁰

*Alternative approach
to template generation
Conditional variational
autoencoders*

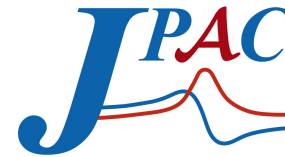


*Give thanks!
Eat a pie*

Thank You!



*Gave thanks!
ηπ*



Backup

Beam Energy Selections	$8.2 < E_\gamma < 8.8 \text{ GeV}$
Charged Track Selections	$ \vec{P} \geq 0.3 \text{ GeV} \cdot c^{-1}$
	$52 \text{ cm} \leq d_z \leq 78 \text{ cm}$
	$\frac{dE}{dx} _{\text{CDC}} \geq 10^{-6} \left(0.9 + e^{3.0 - \frac{3.5[\vec{P} +0.05]}{0.93827}} \right)$
Neutral Shower Selections	$E \geq 0.1 \text{ GeV}$
	$2.5^\circ \leq \theta \leq 10.3^\circ \quad \theta > 11.9^\circ$
Exclusivity Selections	Unused Energy = 0.0 GeV
	Missing Mass Squared $\leq 0.05 \text{ GeV}^2$
	$\chi^2 \leq 13.277 \quad \textit{with 4 DOF}$
Event Counting	Accidental Subtraction: see Equation 2.7
	Sideband Subtraction: see Table 2.3

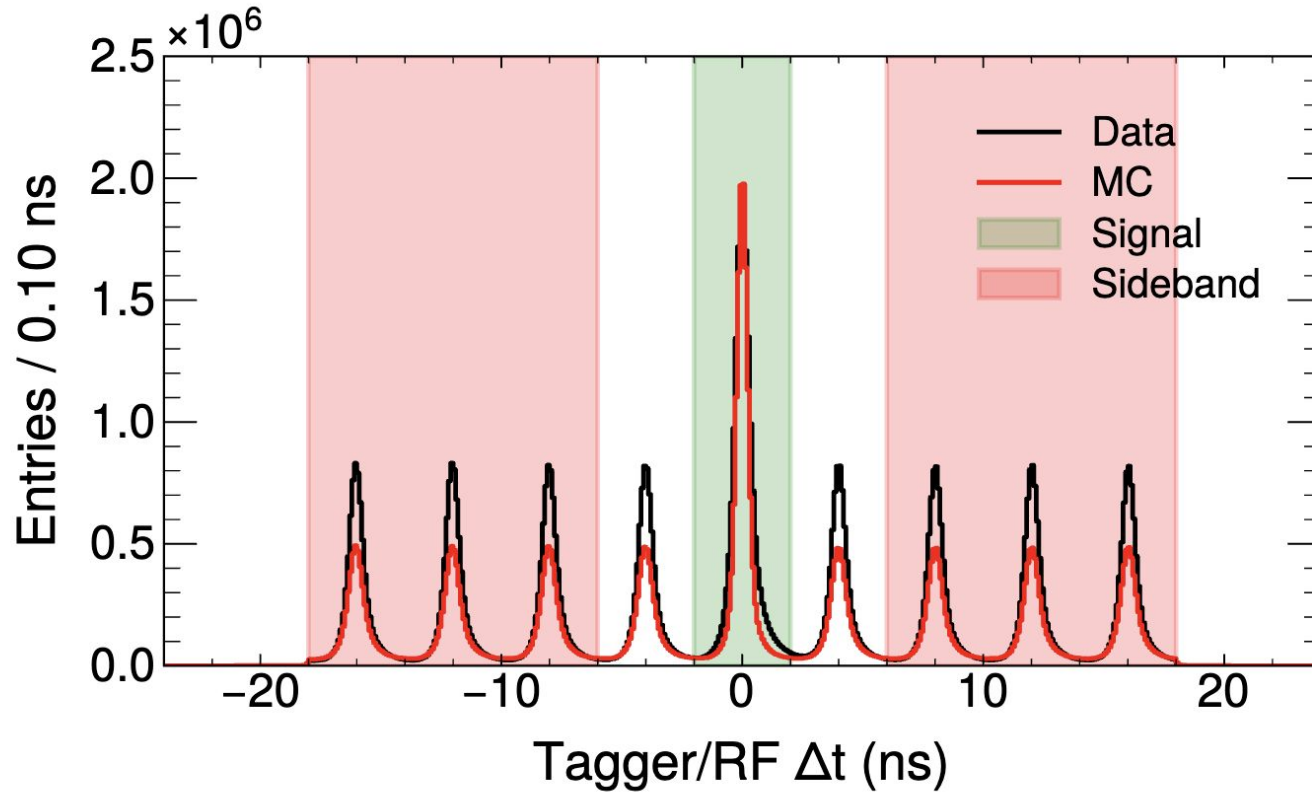
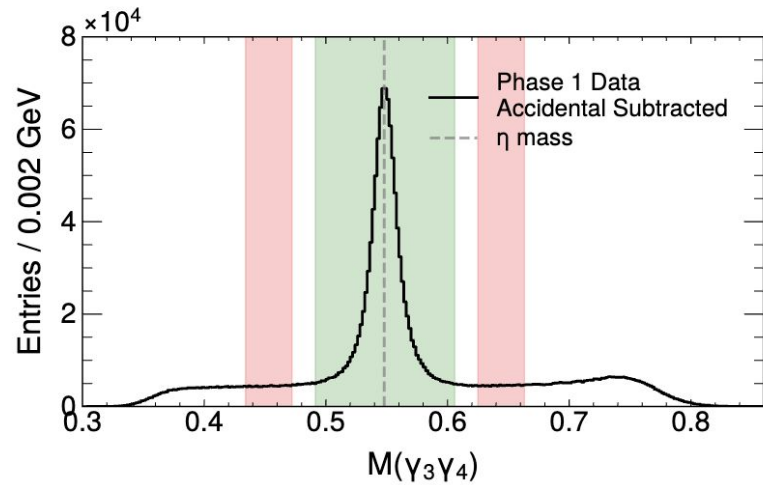
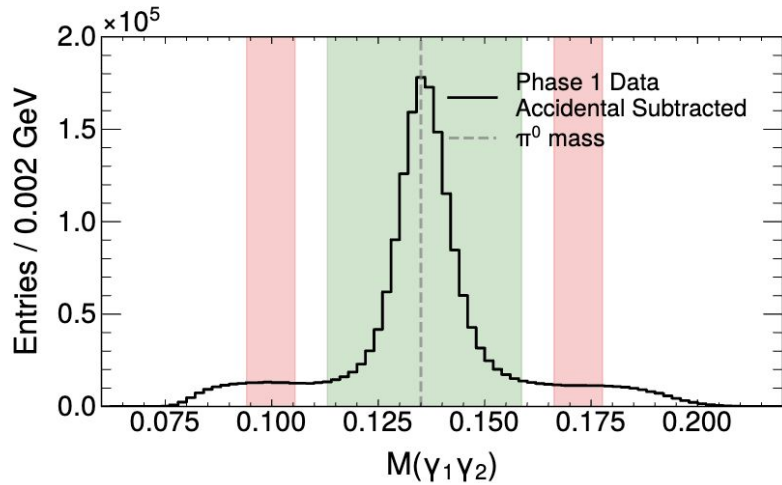
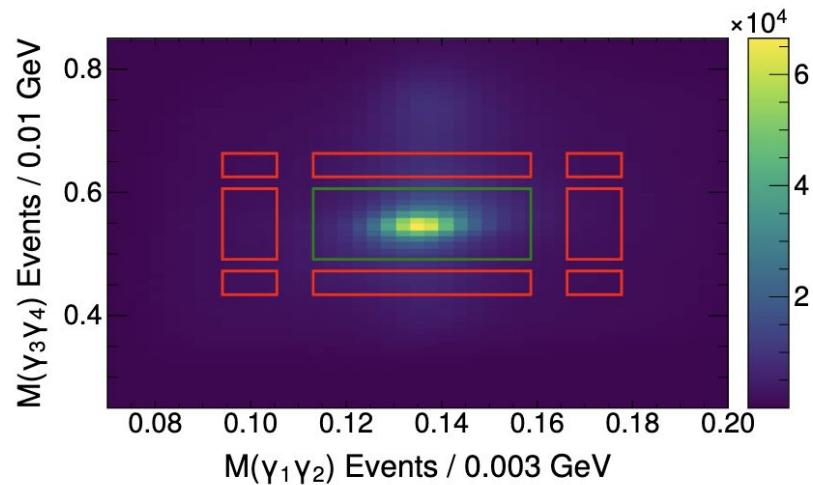
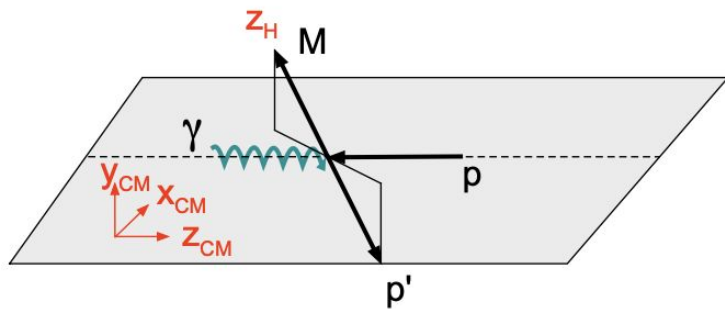
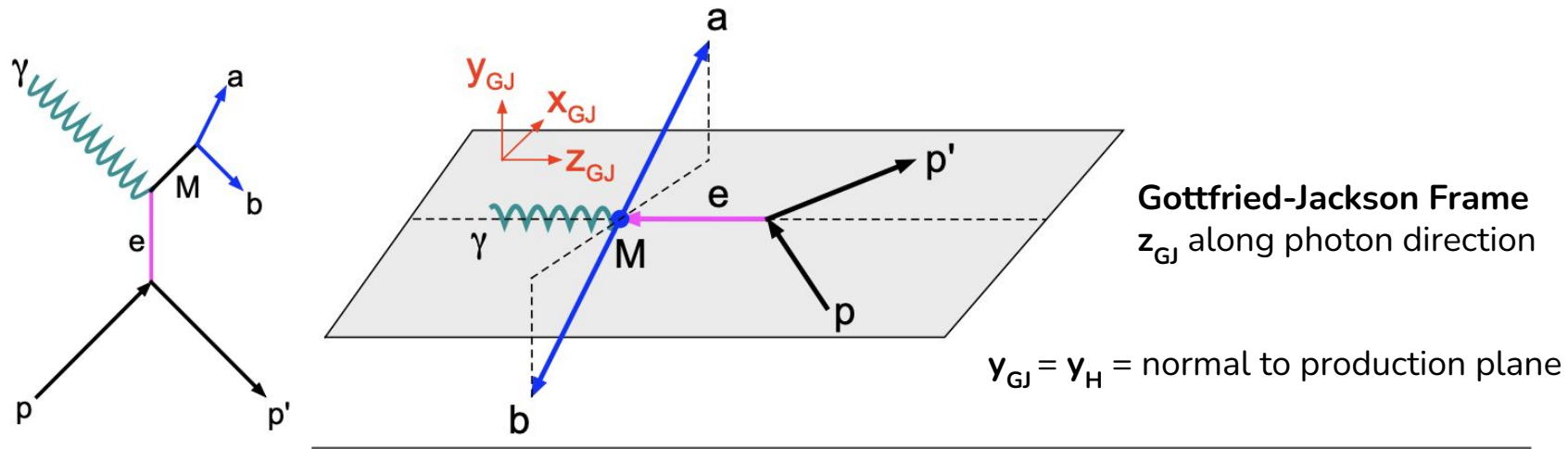


Figure 2.3: Distribution of the tagger time with respect to the RF time. Events in the coherent peak have been selected.

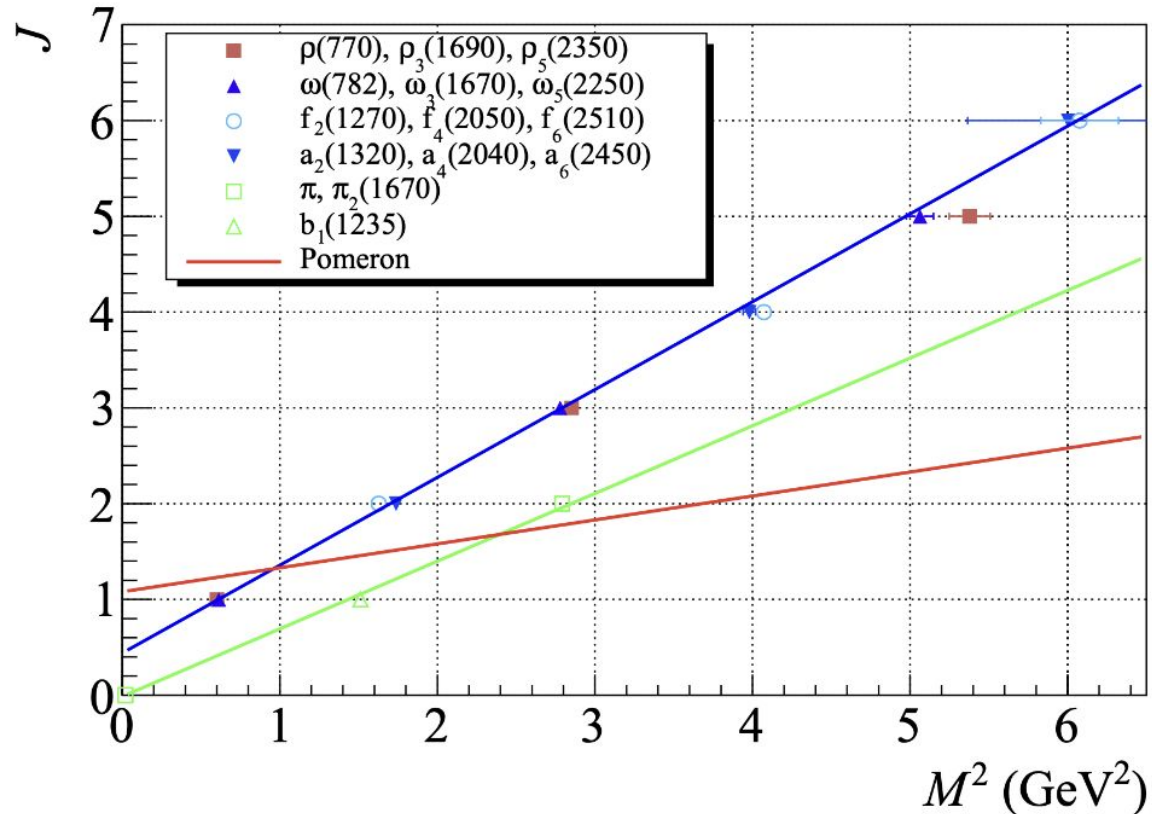


Sideband Subtraction





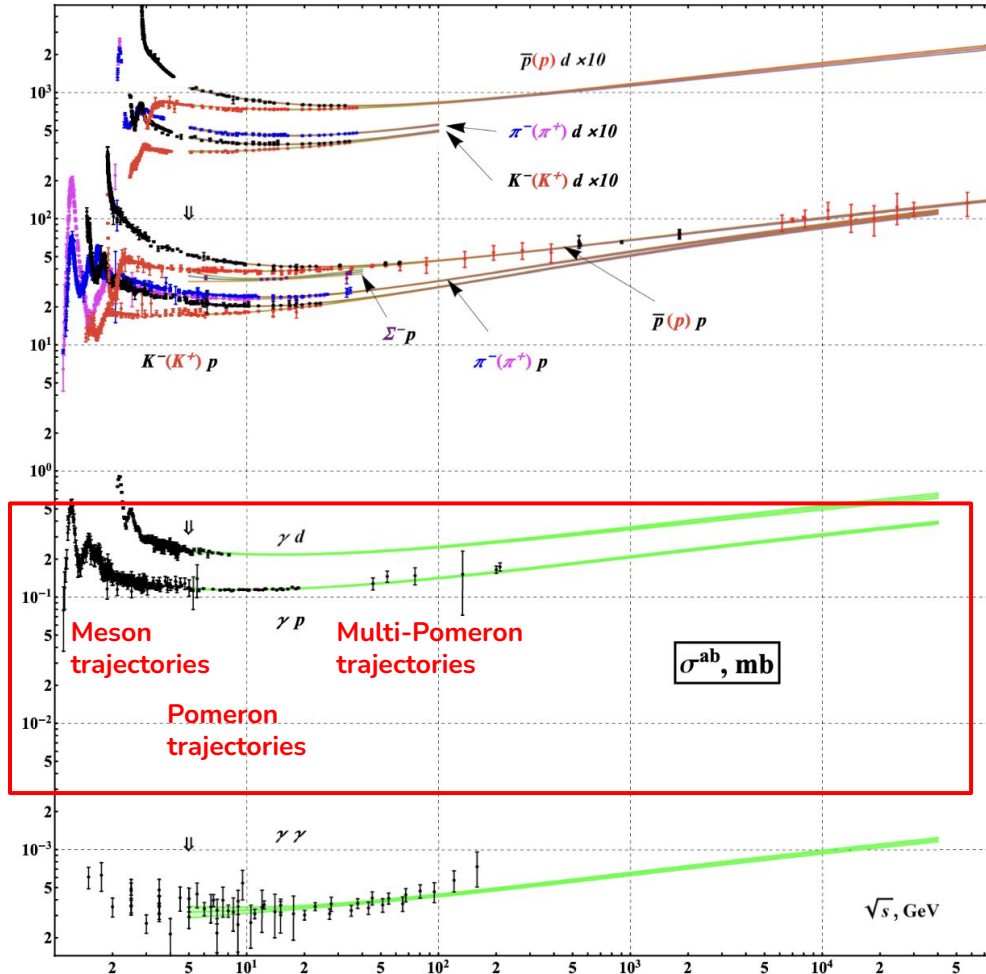
Regge Trajectory



Total hadronic cross section

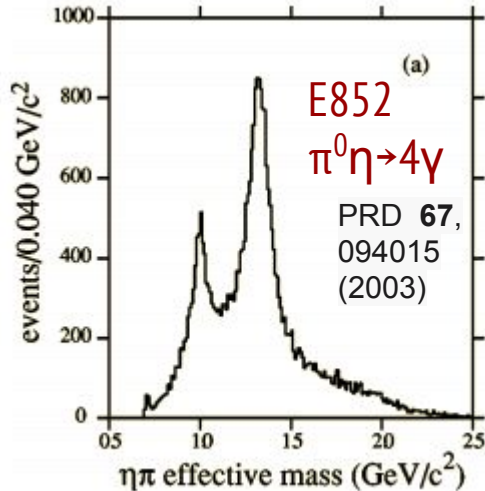
$$\sigma \sim s^{\alpha(0)-1}$$

- Meson trajectories: $\alpha(0) < 0.5$
- Pomeron trajectory: $\alpha(0) \sim 1$
- Multi-Pomeron exchange



$\pi_1(1400)$

Mode	Mass (GeV)	Width (GeV)	Experiment	Reference
$\eta\pi^-$	1.405 ± 0.020	0.18 ± 0.02	GAMS	[121]
$\eta\pi^-$	1.343 ± 0.0046	0.1432 ± 0.0125	KEK	[123]
$\eta\pi^-$	1.37 ± 0.016	0.385 ± 0.040	E852	[127]
$\eta\pi^0$	1.257 ± 0.020	0.354 ± 0.064	E852	[129]
$\eta\pi$	1.40 ± 0.020	0.310 ± 0.050	CBAR	[130]
$\eta\pi^0$	1.36 ± 0.025	0.220 ± 0.090	CBAR	[131]
$\rho\pi$	1.384 ± 0.028	0.378 ± 0.058	Obelix	[132]
$\rho\pi$	~ 1.4	~ 0.4	CBAR	[133]
$\eta\pi$	1.354 ± 0.025	0.330 ± 0.035	PDG	[118]



$\pi_1(1600)$

Mode	Mass (GeV)	Width (GeV)	Experiment	Reference
$b_1\pi$	1.58 ± 0.03	0.30 ± 0.03	VES	[171]
$b_1\pi$	1.61 ± 0.02	0.290 ± 0.03	VES	[141]
$b_1\pi$	~ 1.6	~ 0.33	VES	[125]
$b_1\pi$	1.56 ± 0.06	0.34 ± 0.06	VES	[126]
$f_1\pi$	1.64 ± 0.03	0.24 ± 0.06	VES	[126]
$\eta'\pi$	1.58 ± 0.03	0.30 ± 0.03	VES	[171]
$\eta'\pi$	1.61 ± 0.02	0.290 ± 0.03	VES	[141]
$\eta'\pi$	1.56 ± 0.06	0.34 ± 0.06	VES	[126]
$\rho\pi$	1.593 ± 0.08	0.168 ± 0.020	E852	[143]
$\eta'\pi$	1.597 ± 0.010	0.340 ± 0.040	E852	[145]
$f_1\pi$	1.709 ± 0.024	0.403 ± 0.080	E852	[146]
$b_1\pi$	1.664 ± 0.008	0.185 ± 0.025	E852	[147]
$b_1\pi$	~ 1.6	~ 0.23	CBAR	[149]
$\rho\pi$	1.660 ± 0.010	0.269 ± 0.021	COMPASS	[153]
$\eta'\pi$	1.670 ± 0.030	0.240 ± 0.050	CLEO-c	[150]
all	$1.662^{+0.008}_{-0.009}$	0.241 ± 0.040	PDG	[118]

PPNP **82**, pg. 21-58 (2015)

- ❖ Many experimental observations of 1^{--} aka the π_1
- ❖ Models suggest 1.4 GeV is too low
- ❖ $\pi_1(1600)$ has much richer set of observations and statistics
- ❖ JPAC provided a resolution by performing a coupled channel analysis on COMPASS $\eta\pi$ data

Crystal Barrel (2020)

Crystal Barrel (proton-antiproton collider)

- Coupled channel analysis of: $p\bar{p} \rightarrow K^+K^-\pi^0, \pi^0\pi^0\eta, \pi^0\eta\eta$
 - π_1 wave coupling to $\pi^0\eta$ in $p\bar{p} \rightarrow \pi^0\eta\eta$

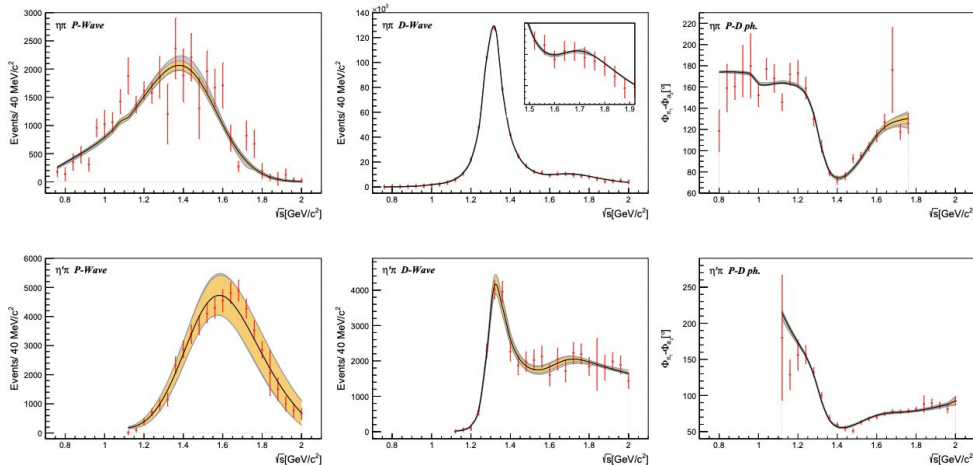
Then... they did another analysis

- Including 11 different $\pi\pi$ scattering datasets
- Including $\pi\eta'$ and $\pi\eta$ results from COMPASS

~120k Events in
total (~90k in $\pi^0\eta\eta$)

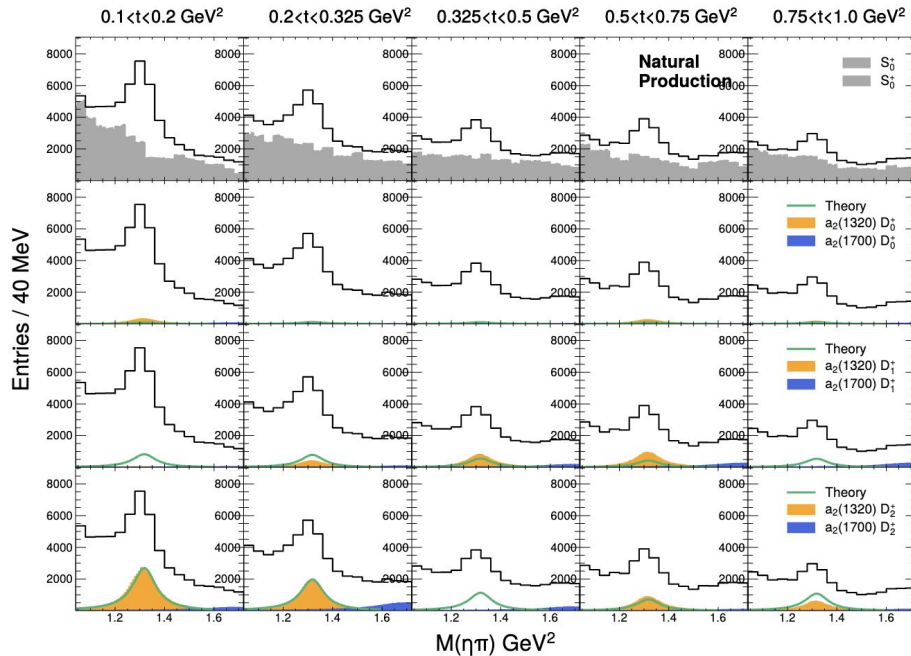
Eur. Phys. J. C (2020) 80:453

Eur. Phys. J. C (2020) 81:1056



N

$$\sigma = \frac{N}{\epsilon * \text{Flux} * \text{Target} * \Gamma(a_2(1320) \rightarrow \eta\pi^0)\Gamma(\eta \rightarrow 2\gamma)\Gamma(\pi^0 \rightarrow 2\gamma)}$$



ϵ = efficiency can be estimated from simulations

Flux measured by pair spectrometer

Target = target thickness = known property of our LH_2 target

Γ = Branching fractions taken from Particle Data Group (PDG)

We have all the ingredients!

Example Plot

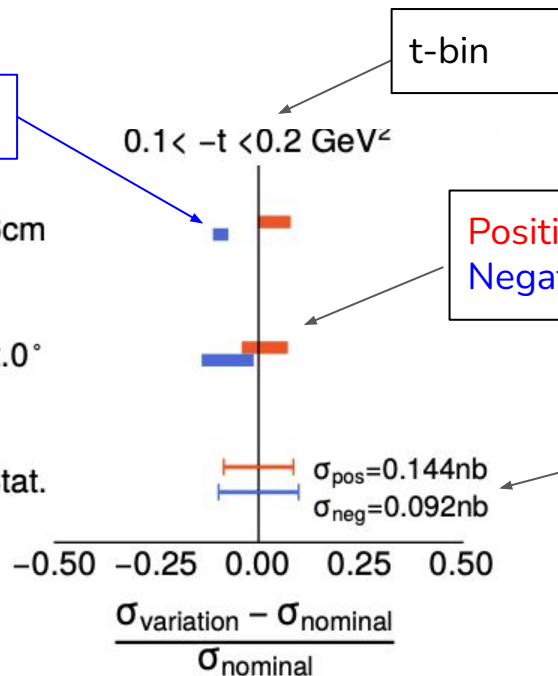
$N_{\text{barlow}} \sim 5 = \text{Significant}$

Variations

$54 < z_{\text{proton}} < 76\text{cm}$

$\theta_{\gamma, \text{beam}} > 2.0^\circ$

Nominal Stat.



Positive Reflectivity
Negative Reflectivity

Nominal values and statistical uncertainty

Cross Section Percent Deviation

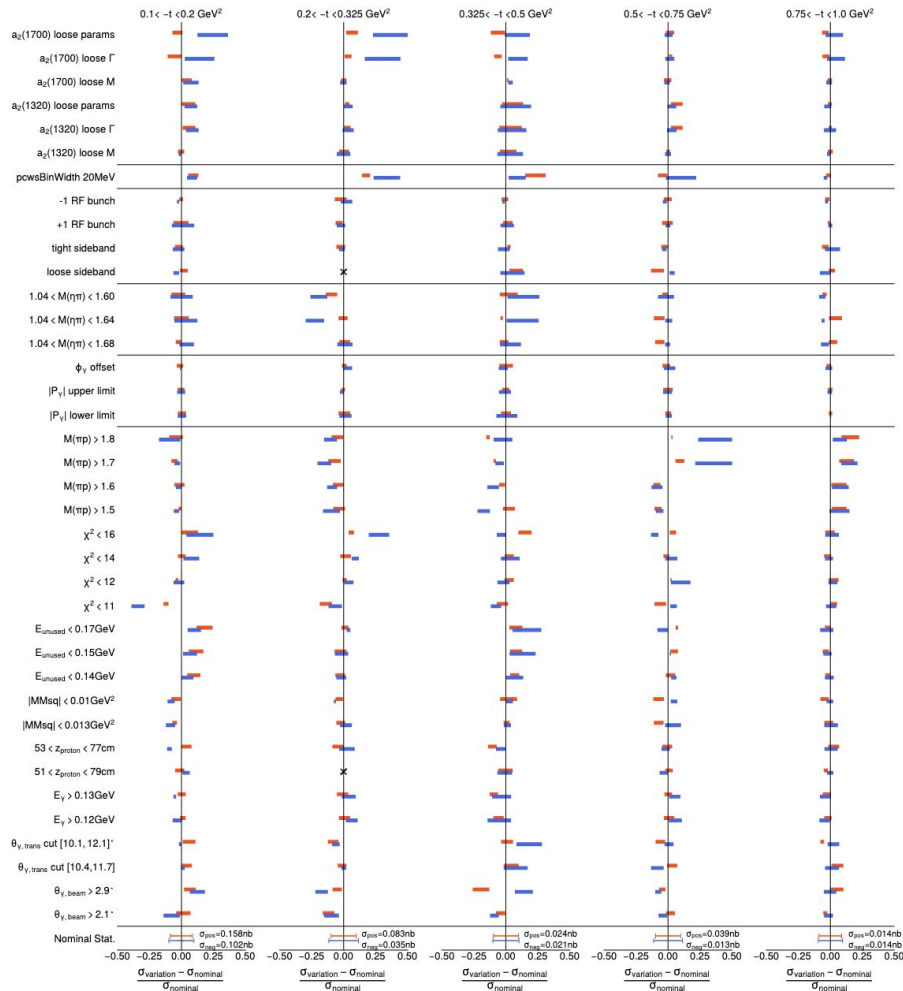
Bar Center

$$N_{\text{barlow}} = \frac{|x_{\text{nom}} - x_{\text{vary}}| / x_{\text{nom}}}{\text{sqrt}(|\sigma(x)_{\text{nom}}|^2 - \sigma(x)_{\text{vary}}|^2)} / x_{\text{nom}}$$

Bar Width

Significant if $N_{\text{barlow}} > A$ where A set to 4

<https://arxiv.org/pdf/hep-ex/0207026.pdf>



D-wave parameterization

S-wave parameterization

Event counting

Fit Range

Polarization

General event selections

Breit-Wigner Resonances

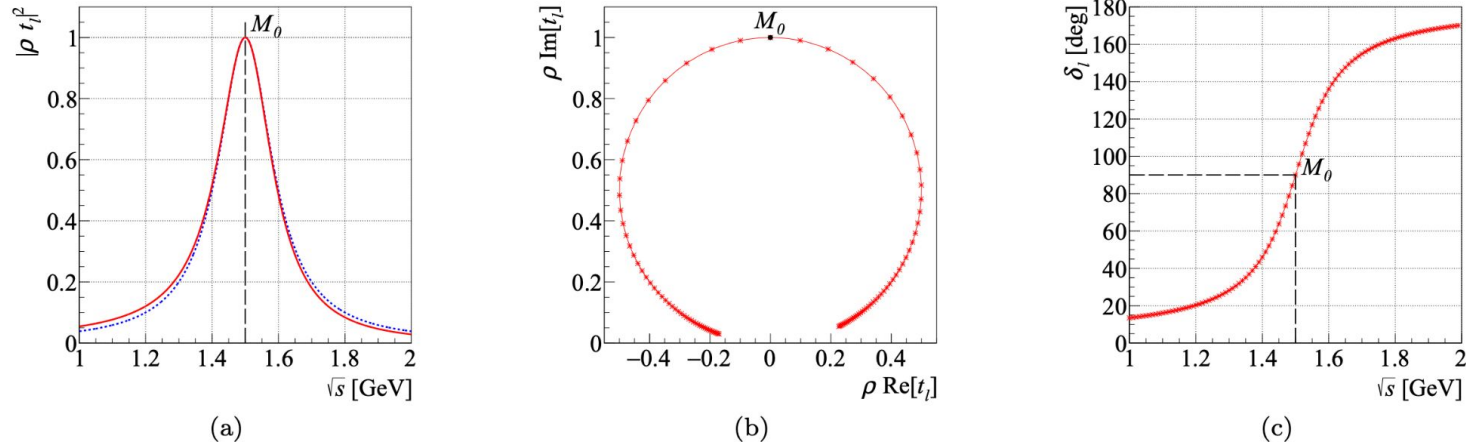


Figure 10: Breit-Wigner amplitude for elastic scattering through a fictitious resonance in the two-body partial wave with orbital angular momentum ℓ with mass $M_0 = 1500$ MeV and constant width $\Gamma_0 = 200$ MeV. (a) Modulus squared of (red) the relativistic, Eq. (87), and (blue) the non-relativistic Breit-Wigner, Eq. (85). (b) Imaginary versus real part (Argand diagram), (c) phase δ_ℓ as a function of \sqrt{s} for the relativistic Breit-Wigner amplitude. The points in (b) and (c) are spaced equidistantly in 10 MeV bins of \sqrt{s} with s increasing in counter-clockwise direction from 1 to 2 GeV.

TMD predictions overestimating GlueX measurements

- TMD scaled by 50% to agree with CLAS

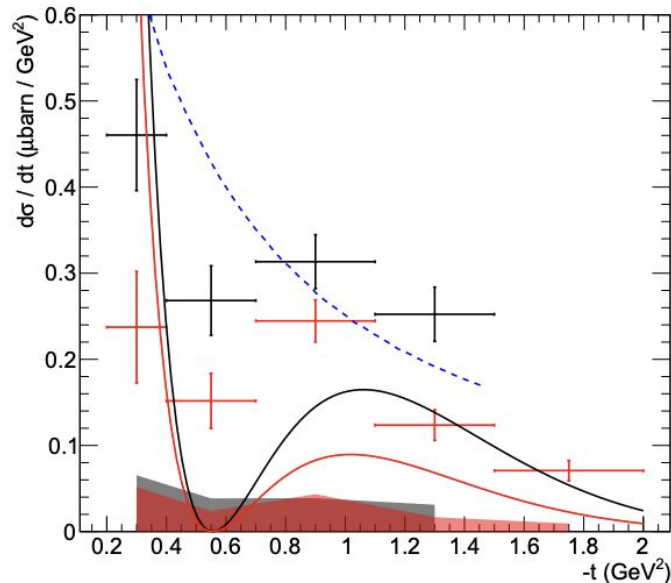


FIG. 3. Differential cross section $d\sigma/dt$ for the reaction $\gamma p \rightarrow a_2(1320)p$, for $E_{\text{beam}} = 3.5\text{--}4.5$ GeV (black) and $E_{\text{beam}} = 4.5\text{--}5.5$ GeV (red). The vertical error bars show the statistical uncertainty, whereas horizontal error bars correspond to the $-t$ bins width. The bottom bands show the systematic uncertainty. The continuous lines are predictions from the JPAC model [27], computed respectively for a beam energy of 4 GeV (black) and 5 GeV (red). The blue dashed line is the prediction from the model by Xie *et al.* [28], for beam energy 3.4 GeV. For better readability, this was scaled vertically by a factor $\times 0.5$.

Q-Factors

3 main items

- ❖ Multivariate combo-based weighting technique
 - **Multivariate side-band subtraction using probabilistic event weights** - M. Williams , M. Bellis and C. A. Meyer --- Journal of Instrumentation 4 10003(2009)
- ❖ Knowledge of **signal + background distribution** of at least one variable (reference)
- ❖ Procedure for all combos
 - Under some **phase space** find k nearest neighbors to combo i
 - Fit the reference variable for the k neighbors
 - Calculate signal fraction/probability = *Q-Factor*
- ❖ Used in many other papers

PRL **122** 162301 (2019)

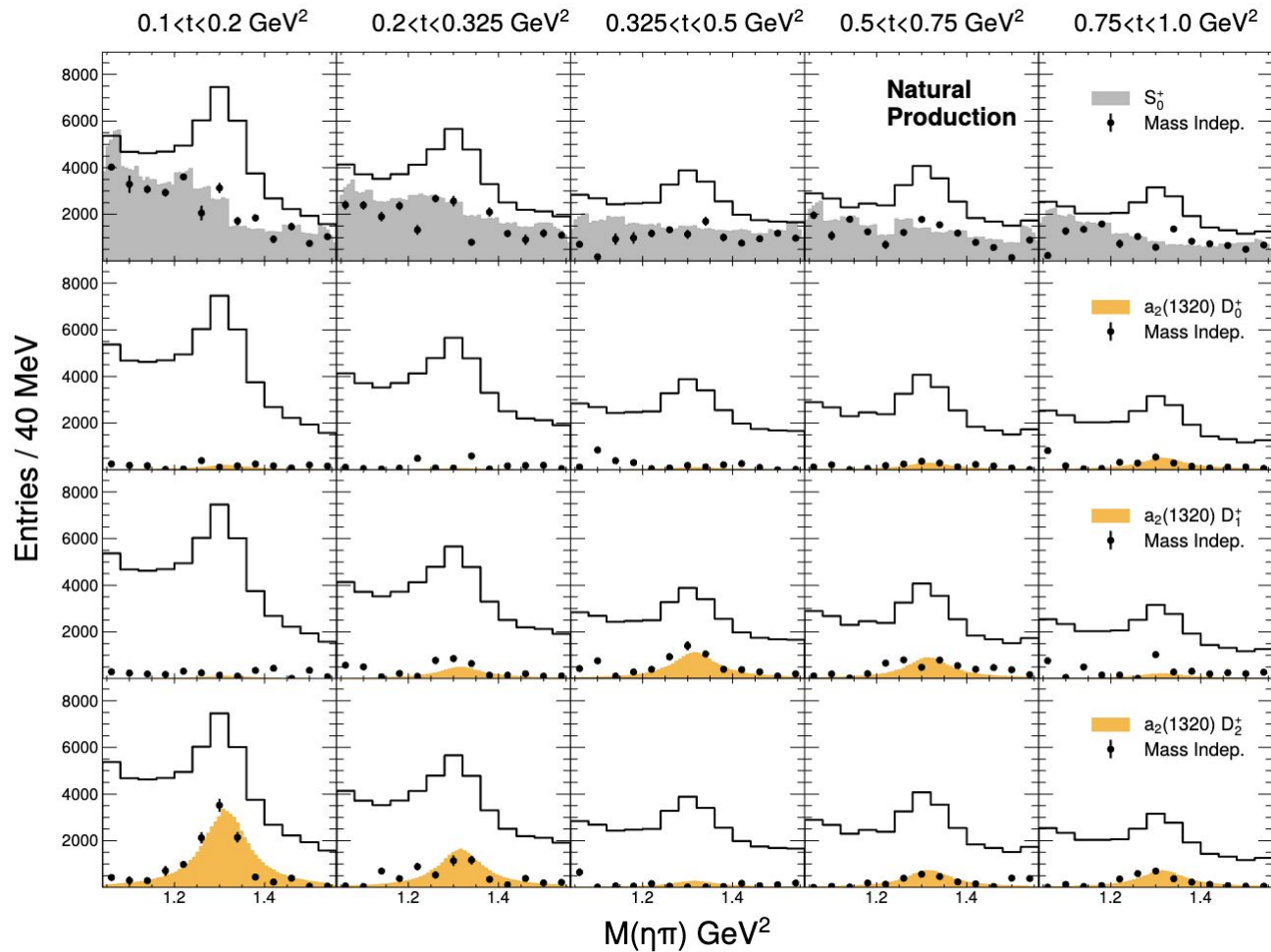
First Measurements of the Double-Polarization Observables F , P , and H in ω Photoproduction off Transversely Polarized Protons in the N^* Resonance Region
CLAS Collaboration (P. Roy (Florida State U., Tallahassee (main)) *et al.*). Dec 5, 2018. 7 pp.
Published in **Phys.Rev.Lett.** **122** (2019) no.16, 162301

Coupled Channel Analysis of $\bar{p}p \rightarrow \pi^0\pi^0\eta, \pi^0\eta\eta$ and $K^+K^-\pi^0$ at 900 MeV/c and of $\pi\pi$ -Scattering Data
M. Albrecht (Ruhr U., Bochum) *et al.*. Sep 16, 2019.

Eur. Phys. J. C (2020) 80:453

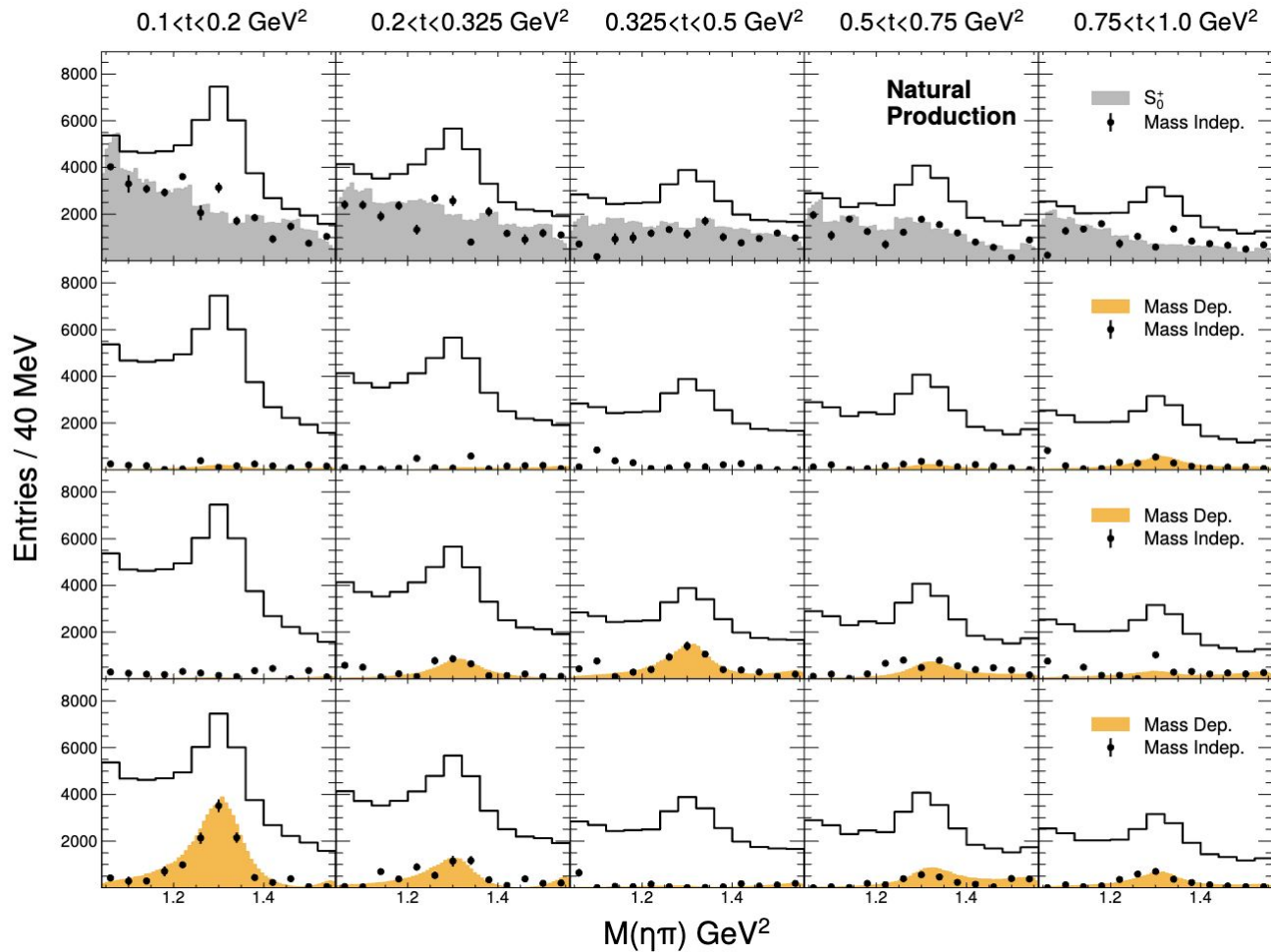
Spin Density Matrix of the ω in the Reaction $\bar{p}p \rightarrow \omega\pi^0$
Crystal Barrel Collaboration (C. Amsler (Zurich U.) *et al.*). Oct 14, 2014. 12 pp.
Published in **Eur.Phys.J.** **C75** (2015) no.3, 124

Eur. Phys. J. C (2015) 75:124



Comparing Mass Independent and Mass Dependent fits

Breit-Wigner for a₂(1320)



Comparing Mass Independent and Mass Dependent fits

Breit-Wigner for $a_2(1320)$ AND $a_2(1700)$

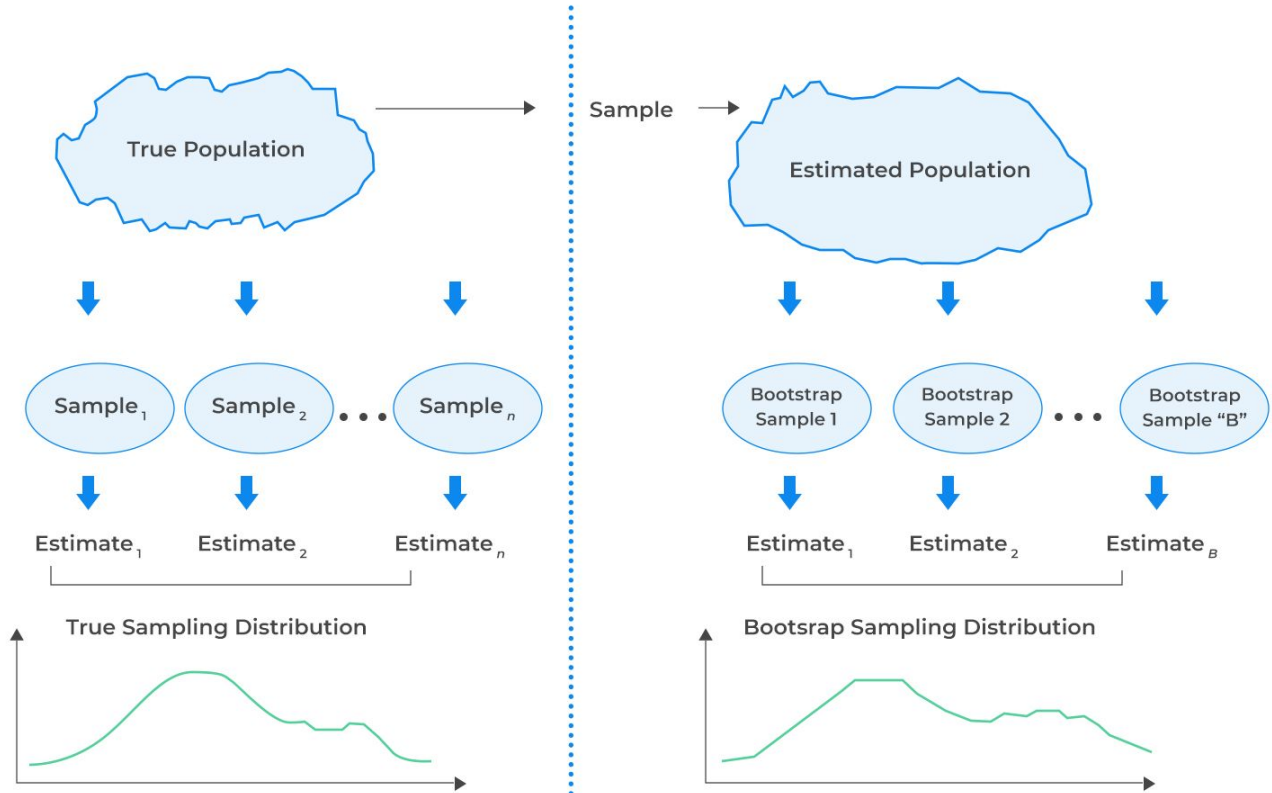
Bootstrap resampling

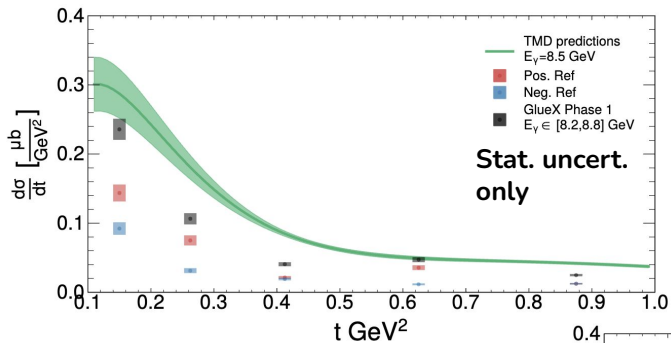
Draw bootstrapped samples with **replacement** from the sample

Calculate some statistic

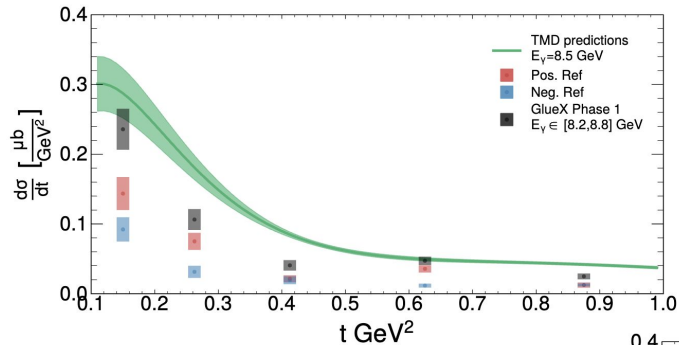
Repeat N times

Distribution formed by the N statistic estimates is the bootstrap sampling distribution

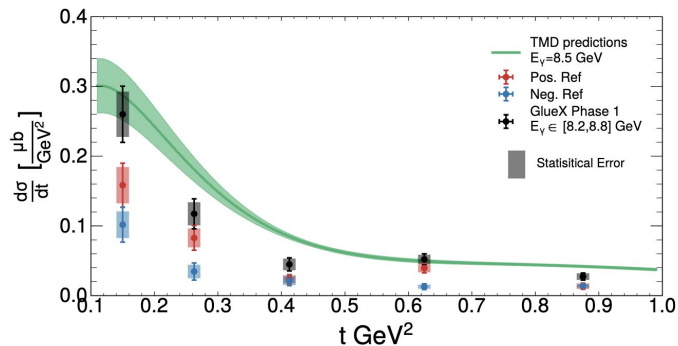




Obtain better **statistical uncertainty** estimates via bootstrap resampling



Include **systematic uncertainty** estimates
 i.e. model dependence, event selections, reconstruction efficiencies



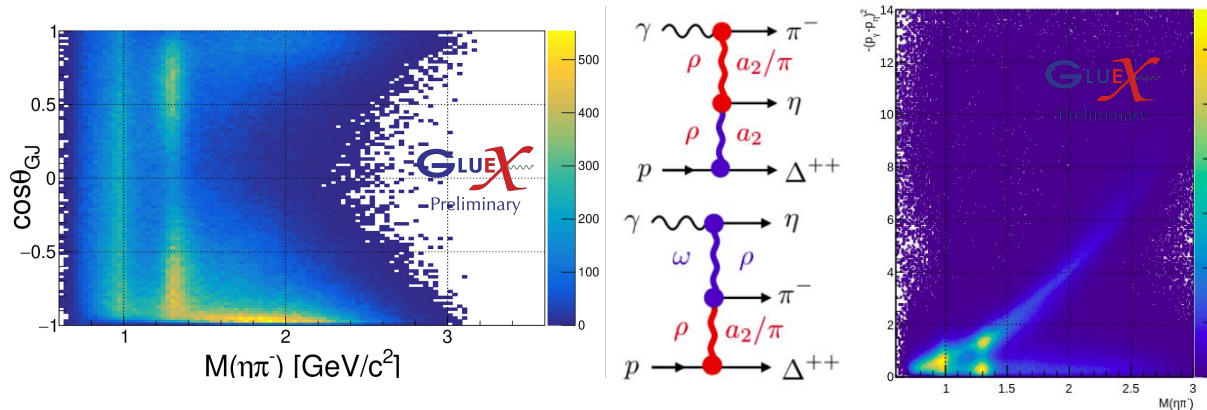
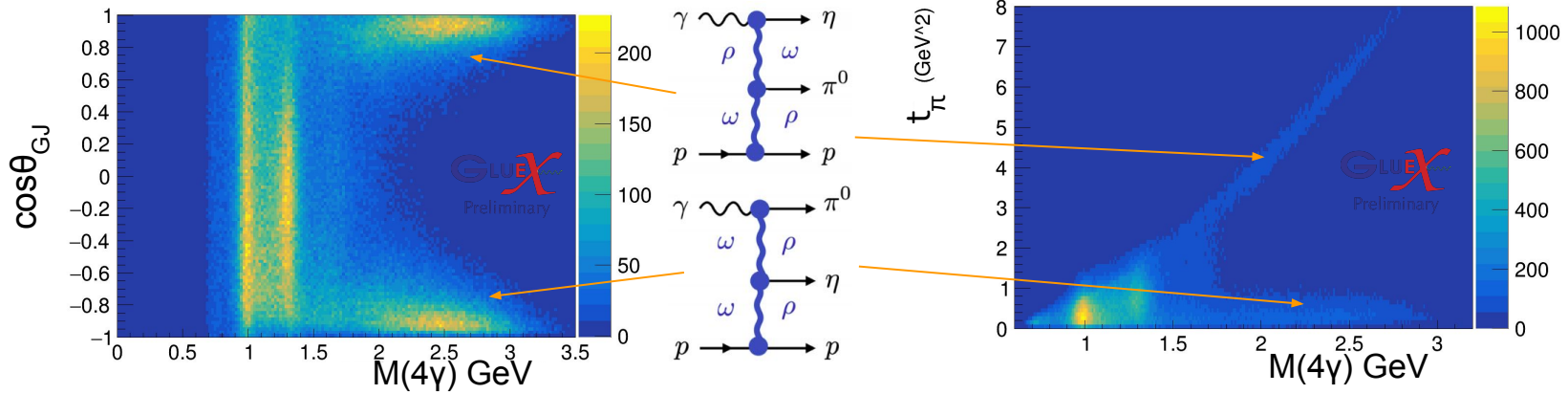
Differential cross section

Pos. Ref. = Natural Exchange component

Neg. Ref. = Unnatural Exchange component

TMD predictions

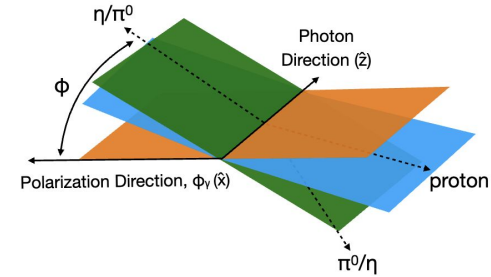
Double Regge Exchange



Clear separation of processes at high mass

π exchange has **unnatural** parity
 ρ , ω , a_2 exchanges have **natural** parity

Beam Asymmetry



Stichel's Theorem = Cross section can be split into two components: one component parallel to **reaction plane** another perpendicular

$$\frac{d\sigma}{dt} = \frac{d\sigma_{\perp}}{dt} + \frac{d\sigma_{\parallel}}{dt}$$

σ_{\perp} : Unnatural exchanges only
 σ_{\parallel} : Natural exchanges only



Define **Beam Asymmetry**

$$\Sigma = \frac{\frac{d\sigma_{\perp}}{dt} - \frac{d\sigma_{\parallel}}{dt}}{\frac{d\sigma_{\perp}}{dt} + \frac{d\sigma_{\parallel}}{dt}}$$

Cross section given by:

$$\sigma(\phi) = \sigma_0(1 - P_{\gamma}\Sigma\cos2(\phi_p - \phi_{\gamma}))$$

ϕ_{γ} polarization angle = {0, 45, 90, -45}

P_{γ} polarization magnitude ~ 0.35

Observed yields given by:

$$Y_{\perp} \propto N_{\perp}(1 + P_{\gamma}\Sigma\cos2\phi)$$

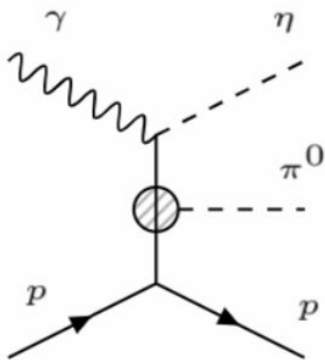
$$Y_{\parallel} \propto N_{\parallel}(1 - P_{\gamma}\Sigma\cos2\phi)$$

Construct **Yield Asymmetry** to extract Σ

$$Y_A = \frac{Y_{\perp} - F_R Y_{\parallel}}{Y_{\perp} + F_R Y_{\parallel}} = \frac{(P_{\perp} + P_{\parallel})\Sigma \cos2\phi}{2 + (P_{\perp} - P_{\parallel})\Sigma \cos2\phi}$$

F_R = flux ratio, known quantity

Non-Resonant Deck Production



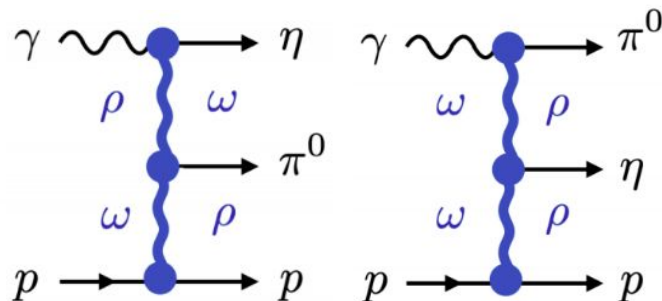
Define:

$$t_\eta = (p_\gamma - p_\eta)^2$$

$$t_\pi = (p_\gamma - p_\pi)^2$$

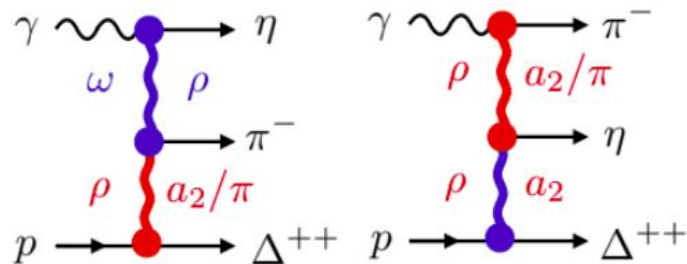


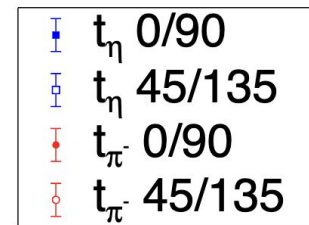
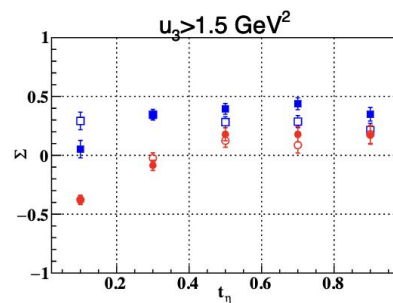
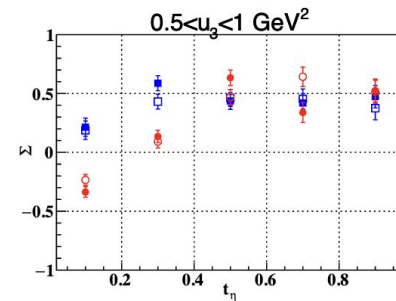
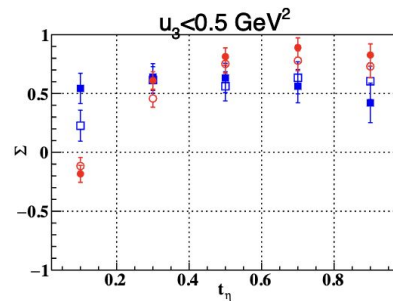
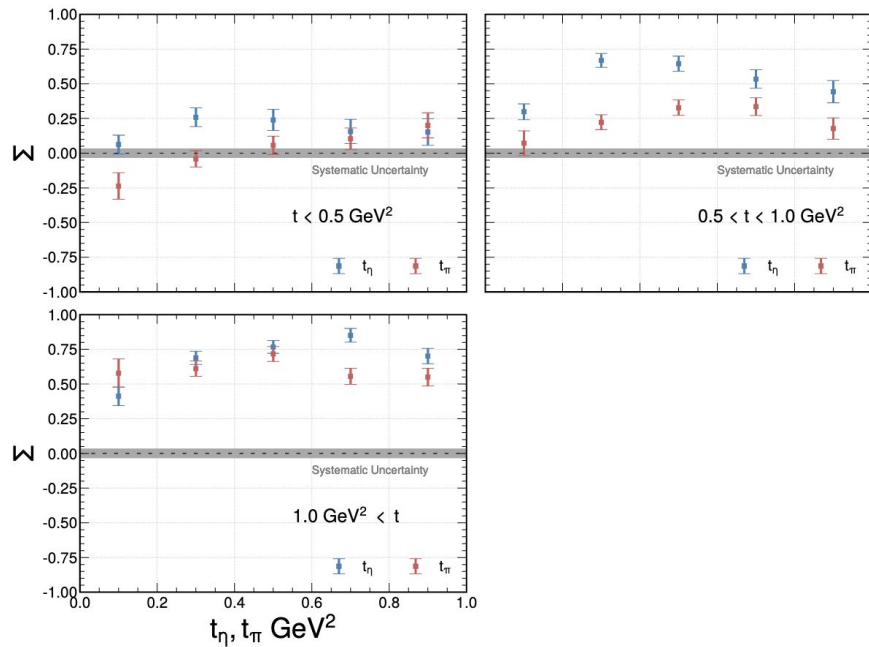
$\gamma p \rightarrow \pi^0 \eta$ $p \rightarrow 4\gamma p$



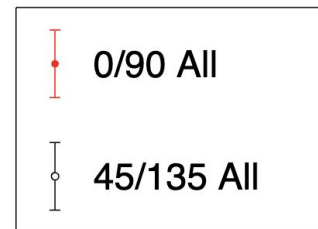
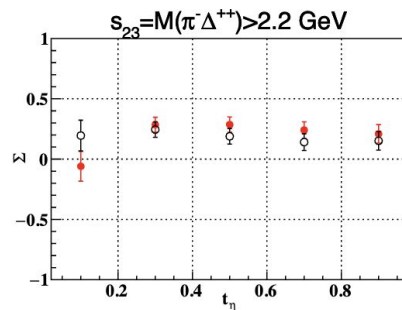
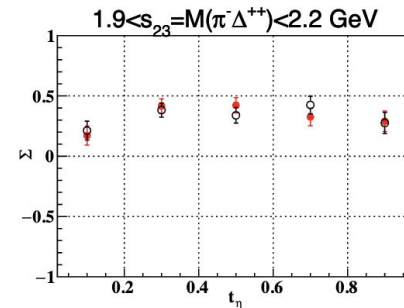
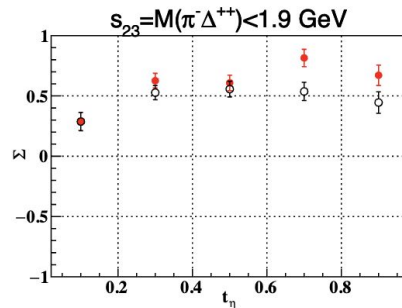
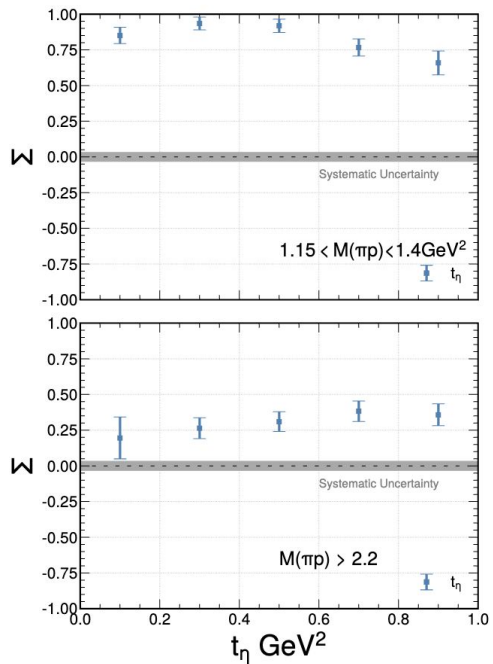
$\gamma p \rightarrow \pi^- \eta$ $\Delta^{++} \rightarrow 2\gamma \pi^- \Delta^{++}$

Charged plots courtesy of Colin Gleason

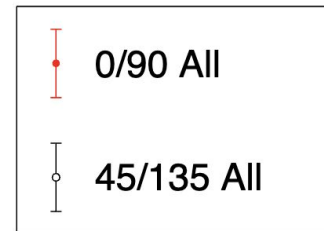
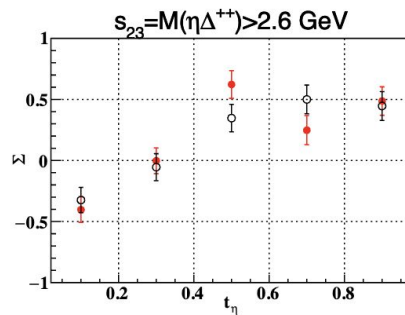
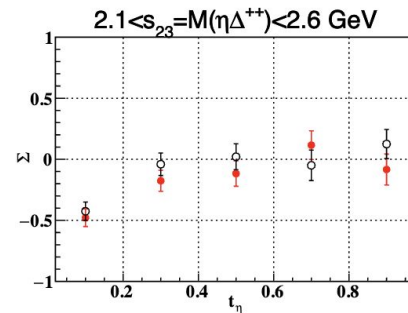
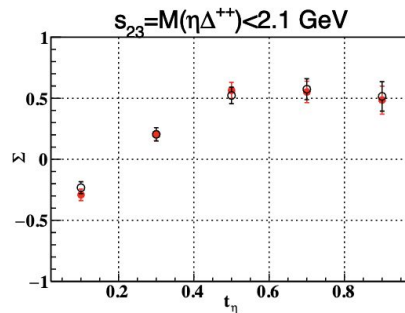
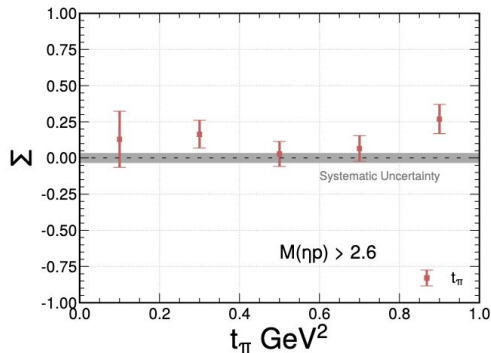
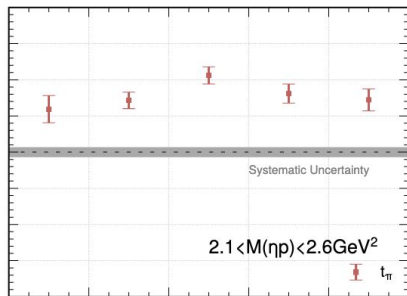
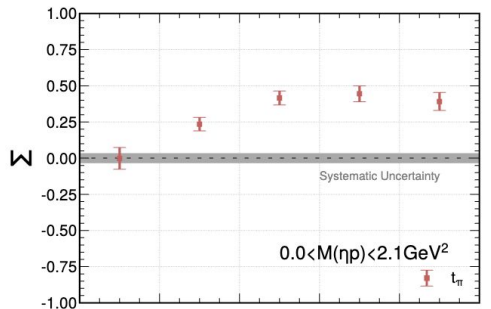




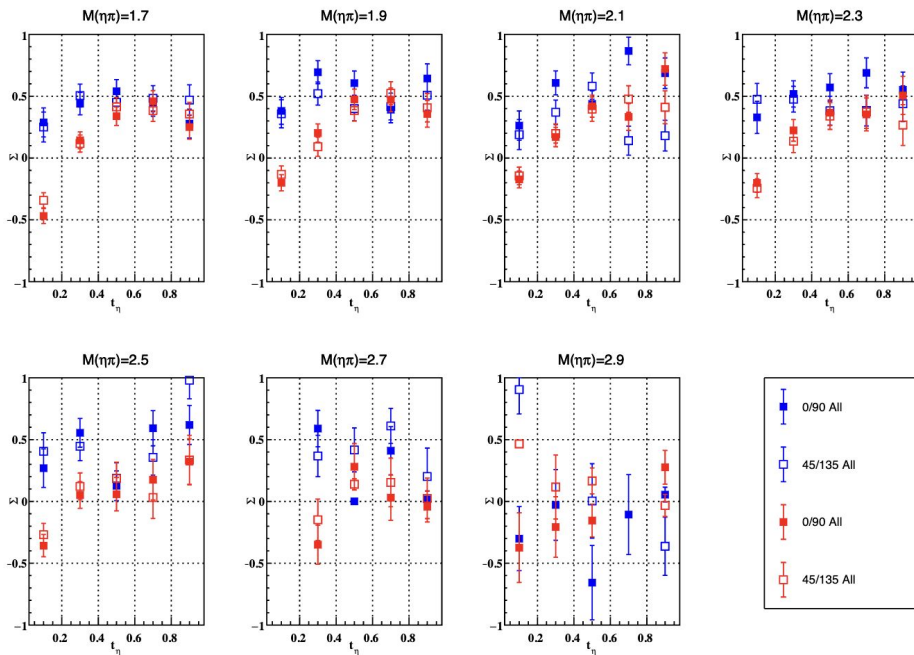
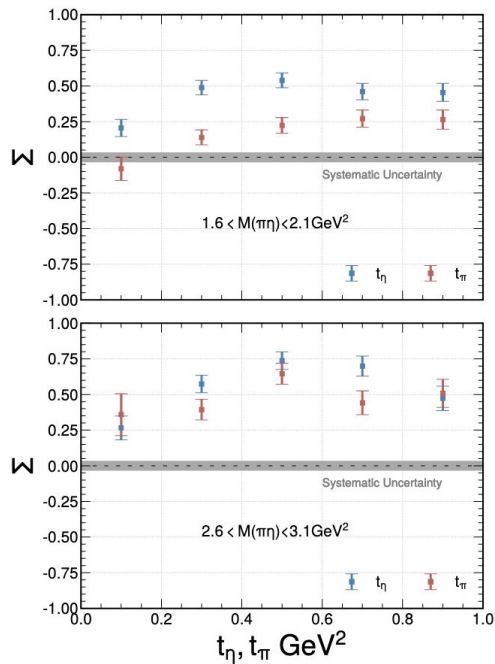
Σ_{t_1} binned in u_3



Σ_η binned in $M(\pi\rho)$



\sum_π binned in $M(\eta p)$



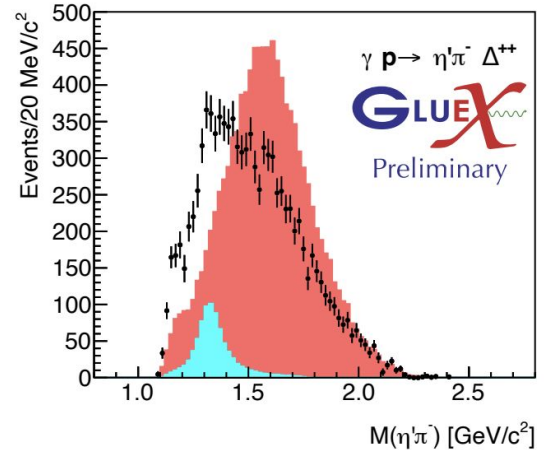
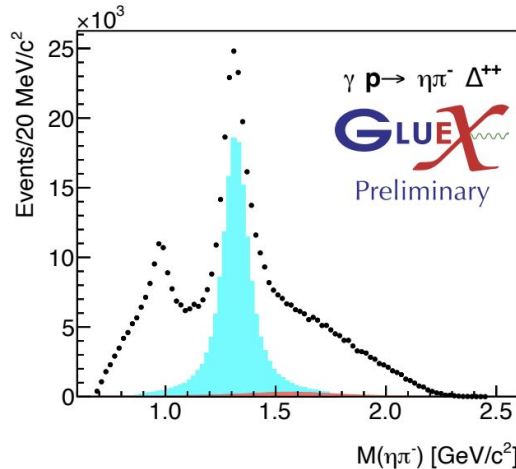
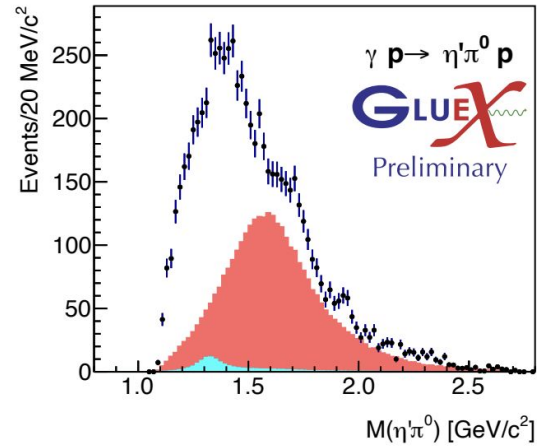
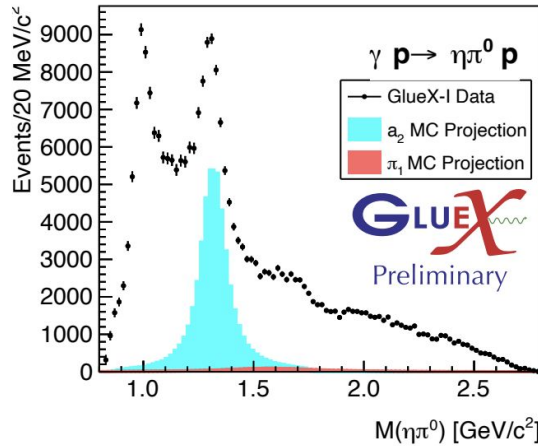
Σ_{t_1} binned in s_{12}

π_1 upper limit at GlueX

- 1) Measure cross sections in several $\gamma p \rightarrow \omega \pi \pi p$ reactions
- 2) Use isospin relations to isolate $l=1$ component
- 3) Fit cross section assuming only $a_2(1320)$ and π_1 contributions

Projections of the $a_2(1320)$ MC and π_1 upper limits onto the GlueX data

π_1 is the vast majority of the spectrum in $\eta'\pi$



Deep Learning Exotic Hadrons

PHYSICAL REVIEW D **105**, L091501 (2022)

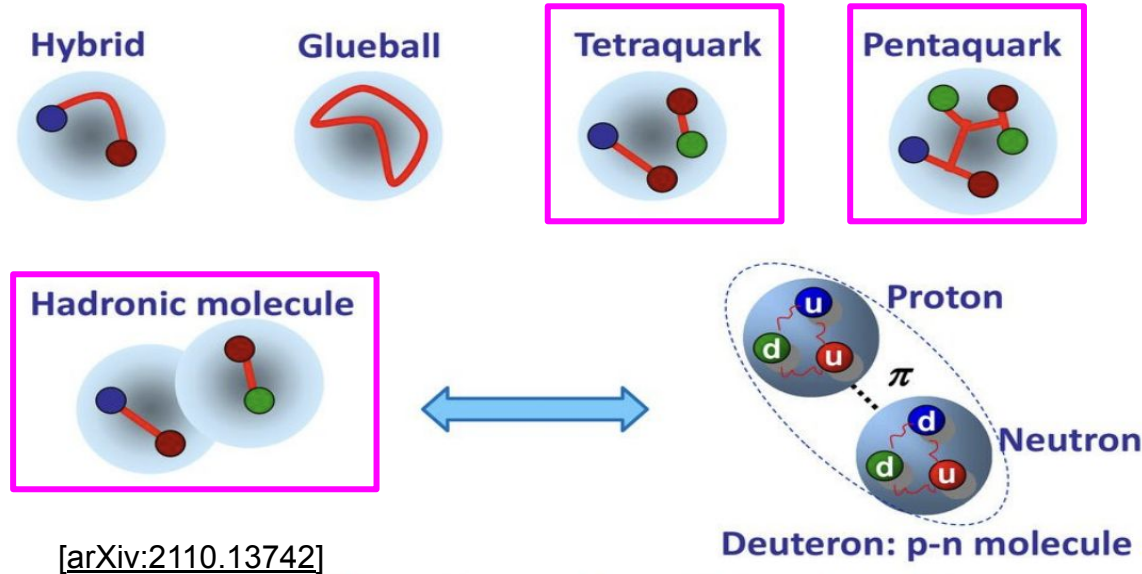
Letter

Deep learning exotic hadrons

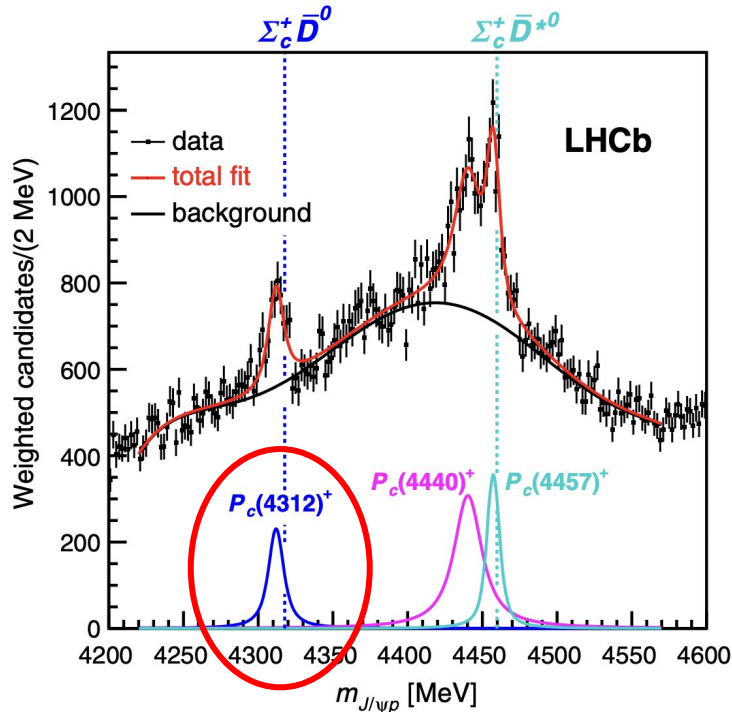
L. Ng,^{1,*} Ł. Bibrzycki,^{2,†} J. Nys,^{3,‡} C. Fernández-Ramírez^{4,5,§}, A. Pilloni,^{6,7,8,||}
V. Mathieu,^{9,10} A. J. Rasmusson,¹¹ and A. P. Szczepaniak^{11,12,13}

(Joint Physics Analysis Center)

Part 2: Neural Networks and Hadron spectroscopy



Lineshape \rightarrow Microscopic origins



Phys. Rev. Lett. 122, 222001 June 2019

Top down:

Develop a microscopic model and fit to data

1. Assigns physical interpretation
2. Biased to assumed dynamics

Bottom up:

Develop minimally biased amplitudes based on basic principles

1. Harder to deduce the nature but possible
2. Less bias

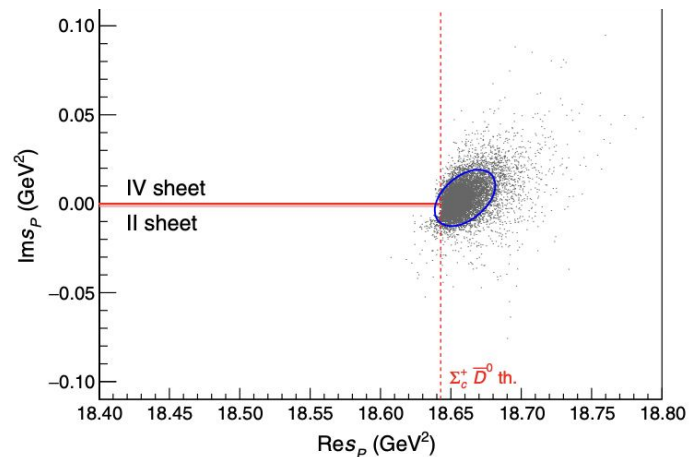
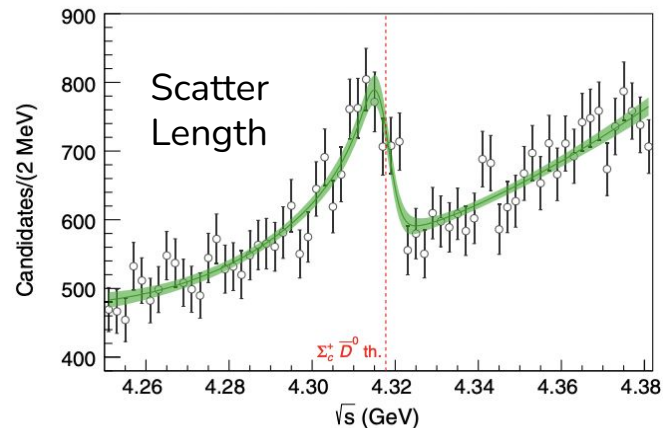
Results

Minimally biased: Reaction amplitudes respecting S-matrix principles

Two channels: $J/\psi p$ (channel 1) and $\Sigma_c^+ \bar{D}^0$ (channel 2)

Location of the poles of amplitude when channels decouple determine the nature

Suggest $P_c(4312)^+$ is virtual (unbound) state - not strong enough to bind Σ_c^+ and \bar{D}^0 to form a molecule



Phys. Rev. Lett. 123, 092001 August 2019

Neural Networks

Use those minimally biased amplitudes to develop a training set

Alternative tool to analyze and interpret data as opposed to a standard χ^2 fit for a single hypothesis

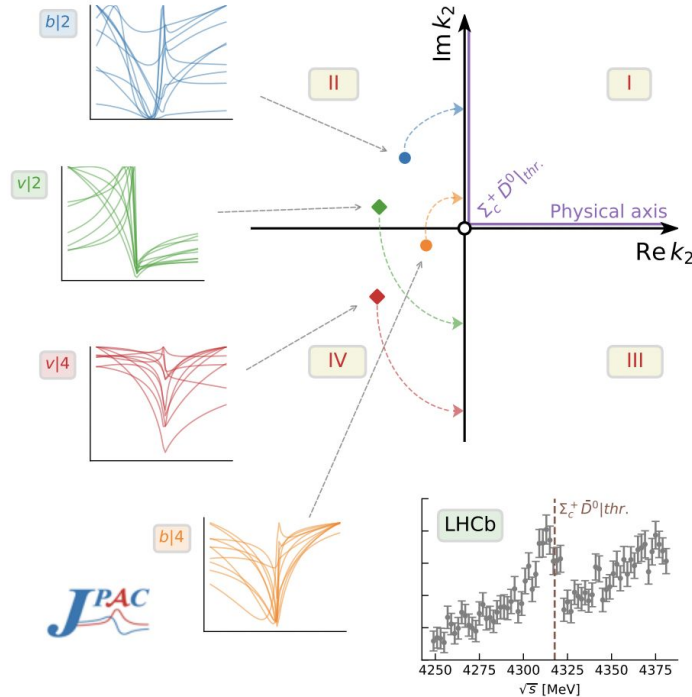
- Multi-class prediction
- Understand the impact of lineshape features to the class assignment

Outline for the rest of the talk

1. Training set
2. Neural Network architecture
3. Feature impact and explainable AI
4. Results

Training set

$$T(s) = \frac{M_{22} - ik_2}{(M_{11} - ik_1)(M_{22} - ik_2) - M_{12}^2}$$



$T(s)$ encodes dynamics of $J/\psi p$ rescattering
Poles = zeros of denominator

Complex momentum plane split into 4 sheets
Poles can only lay on II and IV sheet

Migration of poles when channels decouple ($M_{12} \rightarrow 0$)
 $M_{22} < 0$ = bound state in $\Sigma_c^+ \bar{D}^0$ channel
 $M_{22} > 0$ = virtual (unbound) state

Data generated for wide range of model parameters and over a larger energy range

Classify:

{bound, II}, {bound, IV}, {virtual, II}, {virtual, IV}

Inputs:

Spectrum (incorporating noise and resolution)

Network Architecture

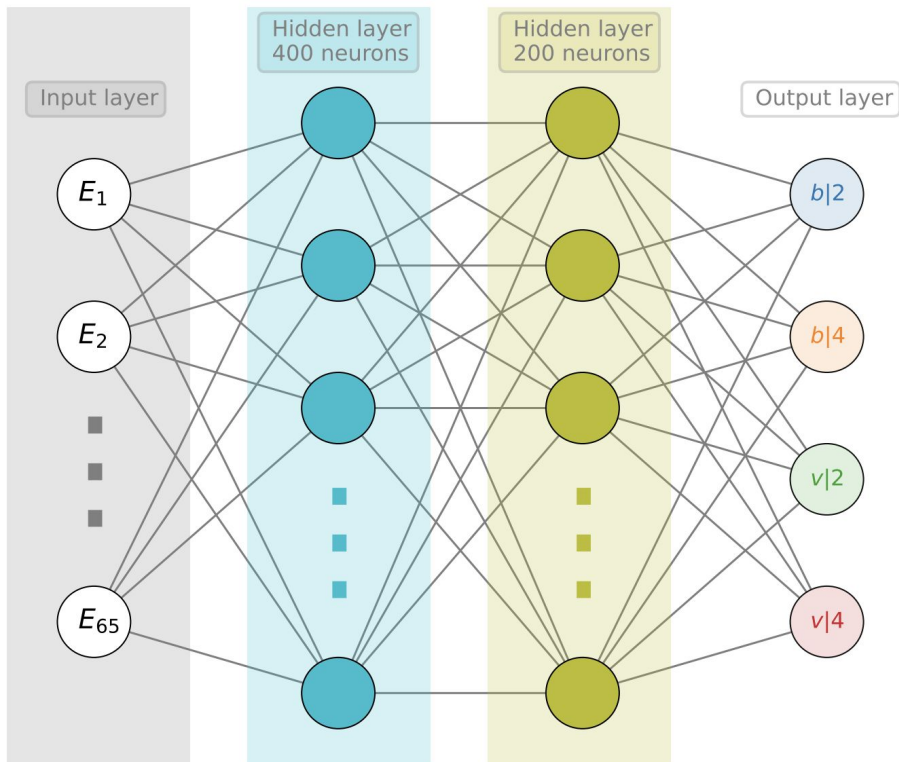
Fixed input size (65) + 2 hidden layers (ReLU activation) +
Output layer size (4, for each class)

Dropout included in between hidden layers

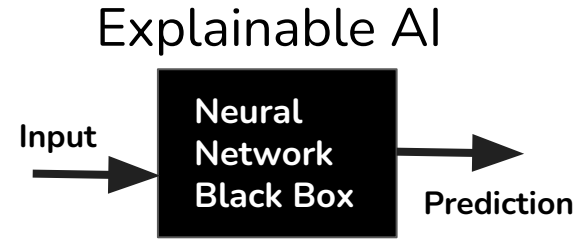
- Randomly zero nodes with some probability [0.2, 0.5]
- Prevents overfitting (regularization)
- Allows determination of classification probability uncertainty

Output / Loss = Softmax output + Multiclass cross-entropy

Optimized stochastically with Adam, batch-size 1024



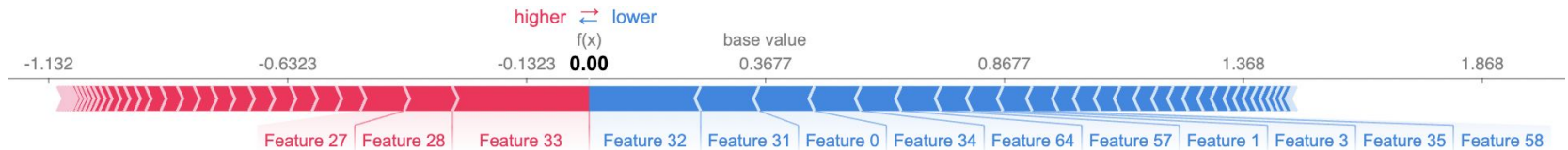
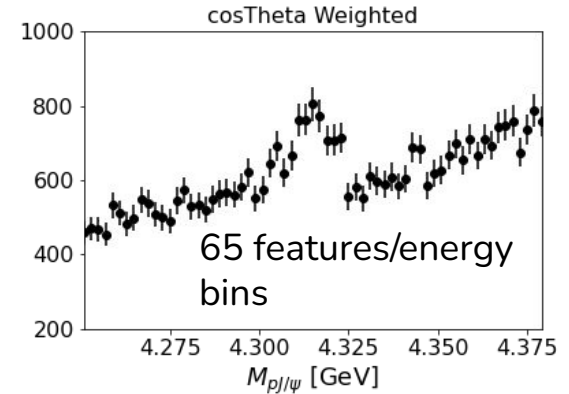
Game Theory: Determining player contribution



- ❖ How to split money among a group of players?
 - Determining contributions of a feature to the loss function
- ❖ Fairness:
 - Additivity - Sum of values = total money
 - Consistency - More contribution = more money
- ❖ Only ONE fair way of doing this - Shapely values
 - Lloyd Shapely won a nobel prize in economics
 - His father, Harlow Shapely - Astronomer - first to determine correct position of the sun in the Milky way
 - Harlow's student, Georges Lemaitre - first derived Hubble's Law and first estimation of hubble constant in 1927 - nominated twice for Nobel Prize

Shapely Values

- ❖ Average marginal contribution across all feature coalitions
- ❖ Coalition - Set of features of any size
- ❖ Marginal Contribution - Changes to prediction with feature included in a coalition
- ❖ Additive local explanations
 - For **each** spectrum we can determine how much each energy bin contributes to the overall response (classification probability)



Determining the energy/input window

Typically the input window depends on some heuristic

Train a network using a wider energy/feature window = [4.1, 4.4] GeV

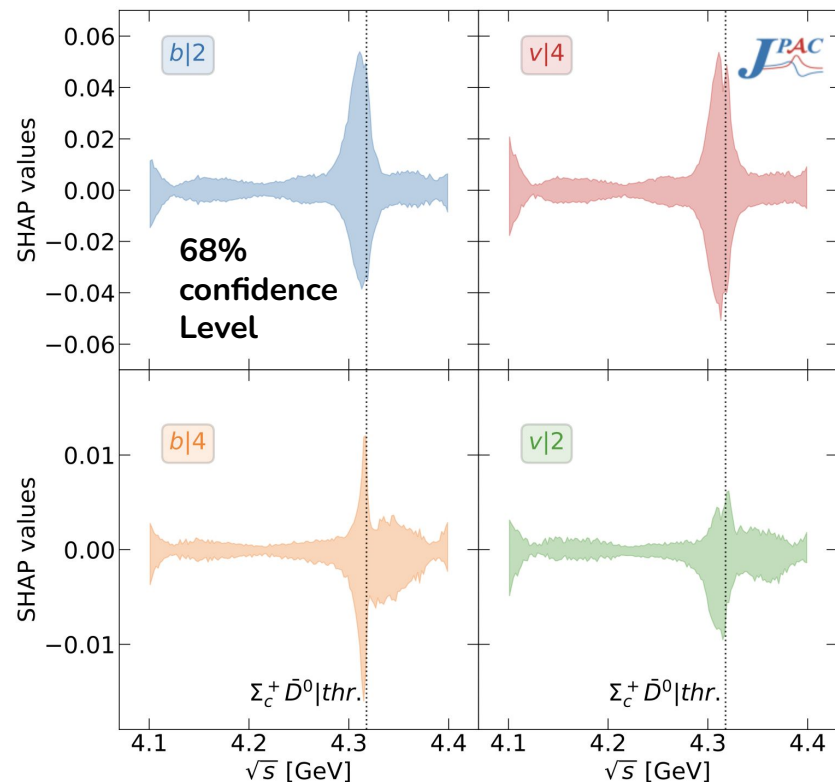
Use **SH**apley **A**dditive **E**xplanations (**SHAP python package**)

Determines feature importance

+(-) SHAP values push a network to predict into(outside) a given class

Large abs(SHAP) = high feature importance

Select energy region → [4.251, 4.379] GeV
+ **Retrain**



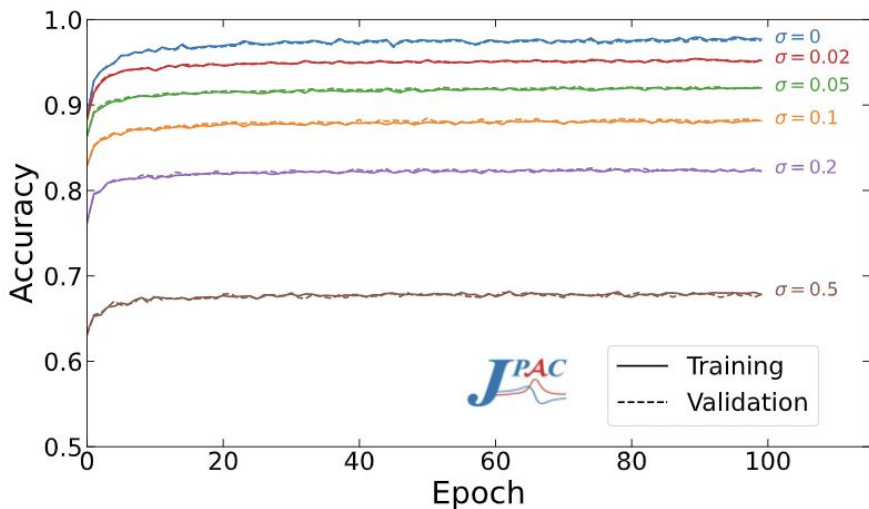
Network Performance

Network trained using various amounts of noise

LHCb data ~ 5% noise

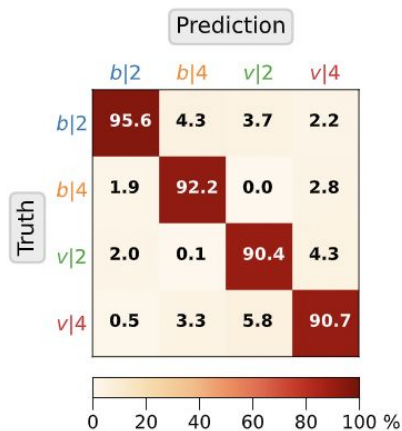
Network saturates > 90% accuracy

Confusion matrix for 5% noise normalized column-wise



Probability point estimates for LHCb data

	$b 2$	$b 4$	$v 2$	$v 4$
$\cos \theta_{P_c}$ -weighted	0.6%	< 0.01%	1.1%	98.3%
$m_{Kp} > 1.9$ GeV	1.4%	< 0.1%	1.6%	97.0%
m_{Kp} all	5.4%	< 0.1%	21.0%	73.6%



Exploring Uncertainties

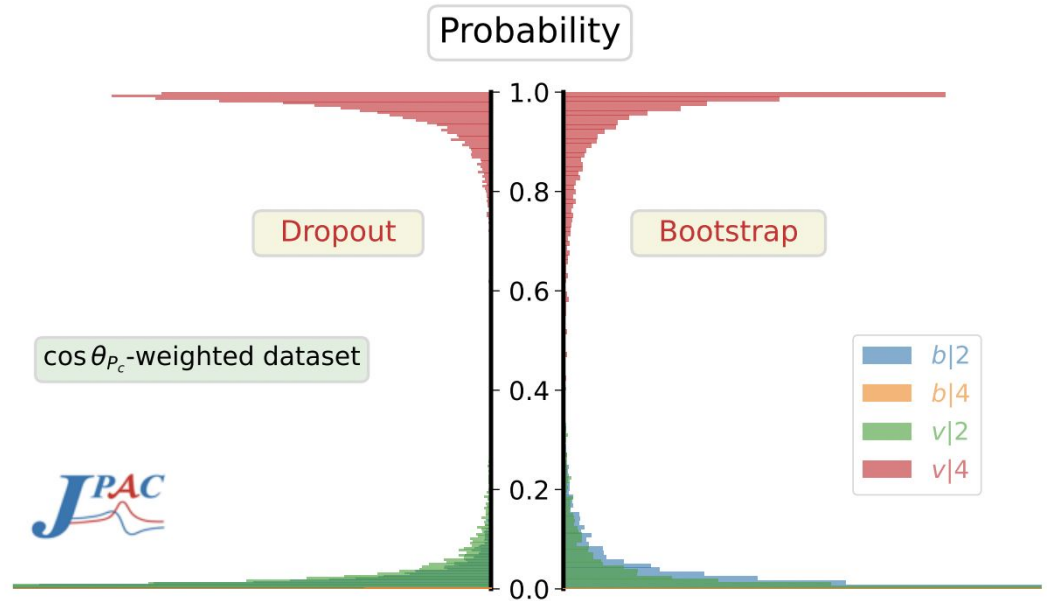
Dropout

Approximate deep Gaussian process a Bayesian probabilistic model
arXiv:1506.02142

Bootstrap

Resample LHCb data around its uncertainties, pass through network with dropout off

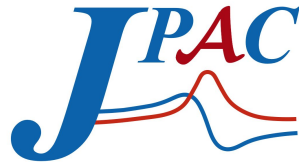
Good agreement between approaches



Uncertainties on the softmax probabilities strongly favor $v|4$ class

Conclusion

- ❖ Prescription to develop a neural network to investigate exotic lineshapes
- ❖ Incorporates noise and resolution
- ❖ Shapley values to determine regions importance
- ❖ Prediction uncertainty quantification through dropout and bootstrapping
- ❖ Pentaquark case study favors virtual state interpretation of $P_c(4312)^+$
- ❖ Numerous future prospects



Carnegie Supernova Project-II: Near-infrared spectral diversity of Type Ia supernova

Carnegie Supernova Project-II: Near-infrared spectral diversity and template of Type Ia Supernovae

JING LU (陆晶),¹ ERIC Y. HSIAO (萧亦麒),¹ MARK M. PHILLIPS,² CHRISTOPHER R. BURNS,³ CHRIS ASHALL,⁴
NIDIA MORRELL,² LAWRENCE NG,¹ SAHANA KUMAR,¹ MELISSA SHAHBANDEH,^{5,6} PETER HOEFELICH,¹ E. BARON,^{7,8}
SYED UDDIN,⁹ MAXIMILIAN D. STRITZINGER,¹⁰ NICHOLAS B. SUNTZEFF,⁹ CHARLES BALTAY,¹¹ SCOTT DAVIS,¹
TIARA R. DIAMOND,¹² GASTON FOLATELLI,^{13,14} FRANCISCO FÖRSTER,^{15,16} JONATHAN GAGNÉ,^{17,2} LLUÍS GALBANY,^{18,19}
CHRISTA GALL,²⁰ SANTIAGO GONZÁLEZ-GAITÁN,²¹ SIMON HOLMBO,¹⁰ ROBERT P. KIRSHNER,^{22,23} KEVIN KRISCIUNAS,⁹
G. H. MARION,²⁴ SAUL PERLMUTTER,^{25,26} PRISCILA J. PESSI,²⁷ ANTHONY L. PIRO,³ DAVID RABINOWITZ,¹¹
STUART D. RYDER,^{28,29} AND DAVID J. SAND³⁰



Credit: JWST



Credit: Yuri Beletsky
Magellan, LCO

- Evolution effect

- Dust Extinction

Selection bias

Systematic Uncertainties !

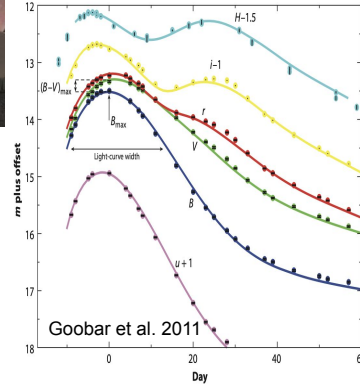
Approach 2: Study the NIR spectral diversity of SNe~Ia and build an improve NIR spectral template

Observations

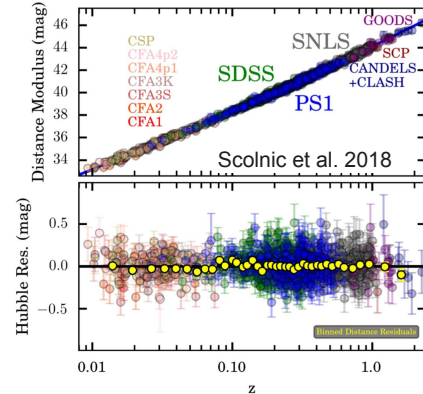
Photometric Calibrations

Light Curves Fitting $\rightarrow \mu$

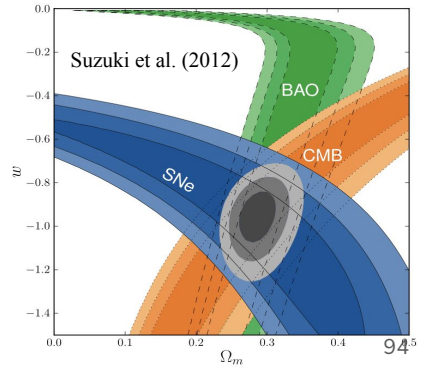
Statistics $\rightarrow H_0, \Omega, w$



Calibration



LC fitting



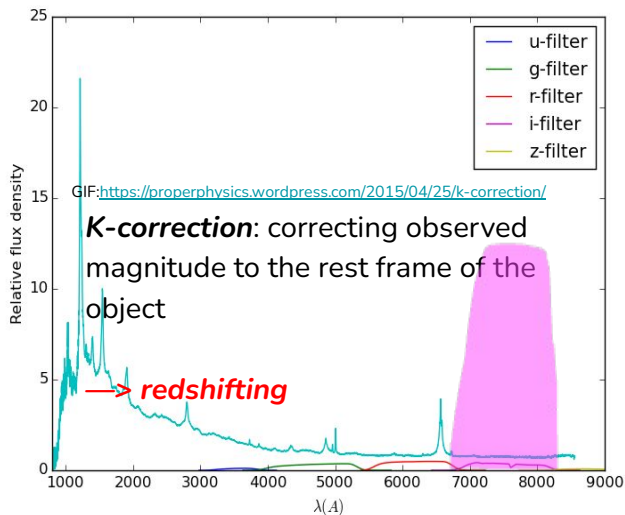
Light Curves fitters covers NIR

→ **Need spectral template!**

SNooPy

Burns et al. 2011

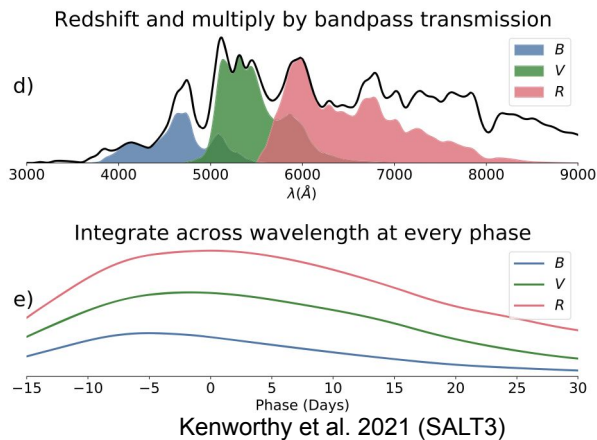
- Use Hsiao template (Hsiao 2009) for K-correction



SALT3-NIR

Pierel et al. 2022

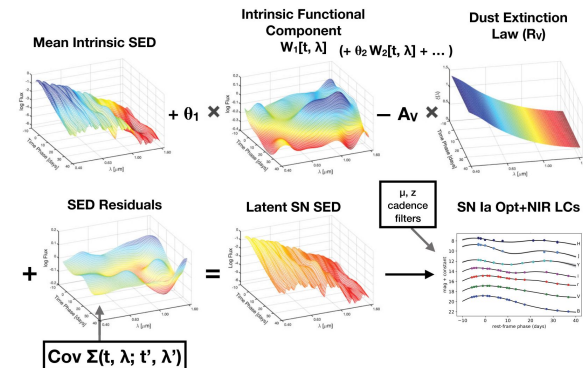
- Spectral model
- “Native” K-correction



BayeSN

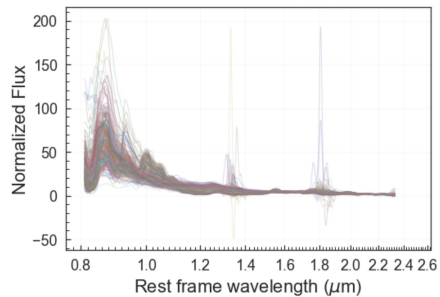
Mandel et al. 2022

- Spectral model (use Hsiao template as the baseline)
- “Native” K-correction

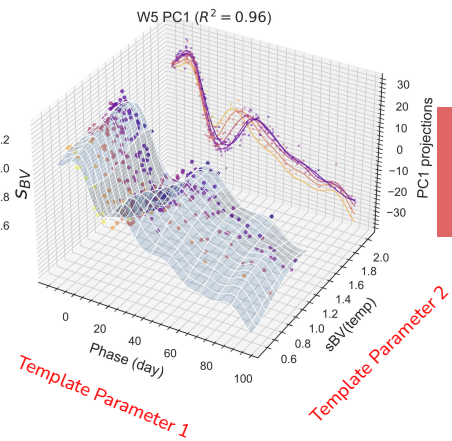


Mandel et al. 2022

Gaussian Process Regression
to include external parameters
+
Select top-N eigenvectors



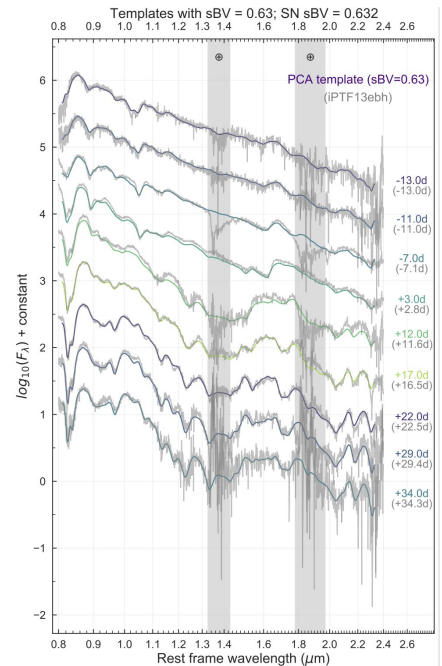
PCA
“encoder”



PCA
“decoder”

Input

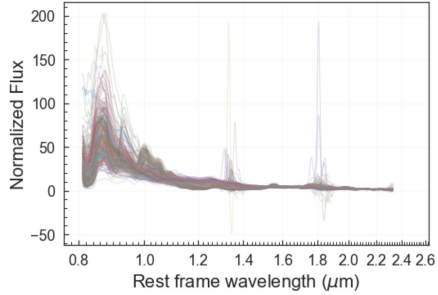
~400 NIR supernovae
spectra



Output

Templates for any
(s_{BV} , epoch) parameters

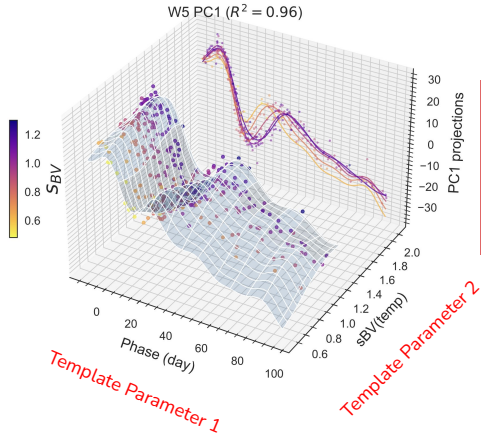
Condition both networks on
template parameters
+
Choice of latent space dimension



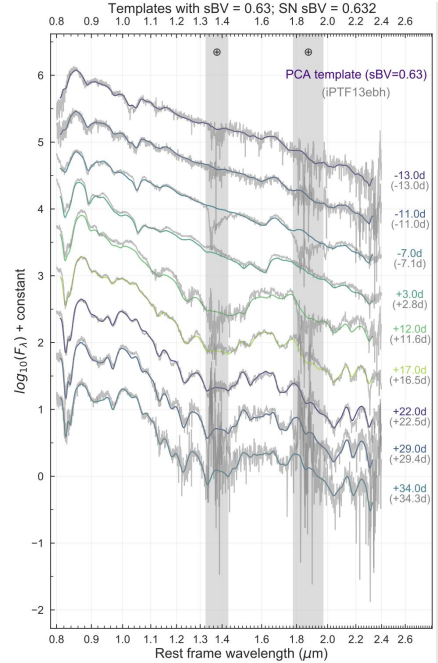
Input

~400 NIR supernovae spectra

Neural Network Encoder



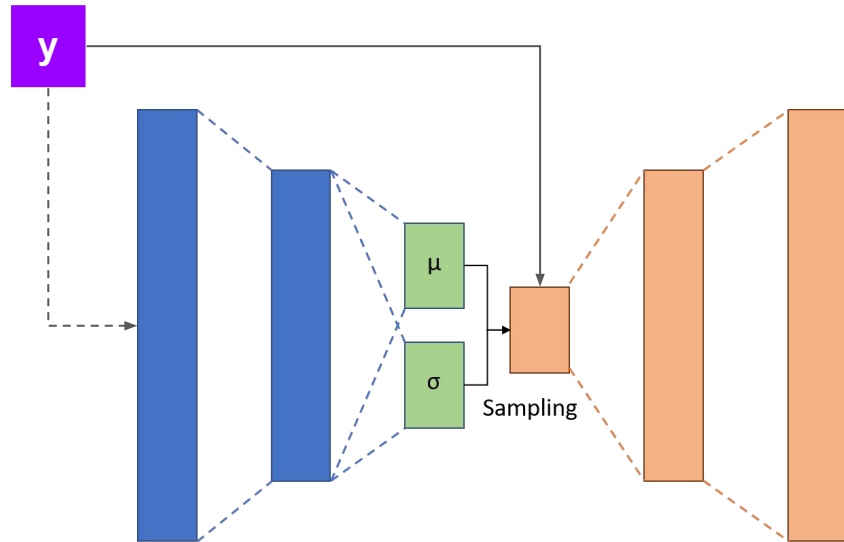
Neural Network Decoder



Output

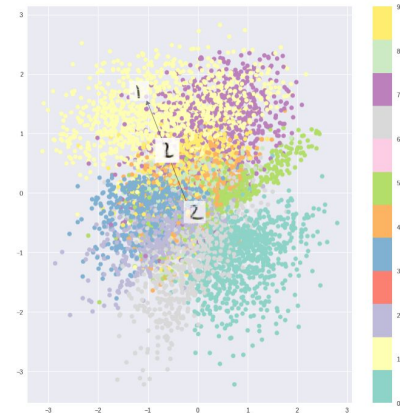
Templates for any (s_{BV}, epoch) parameters

(Conditional) Variational Autoencoder

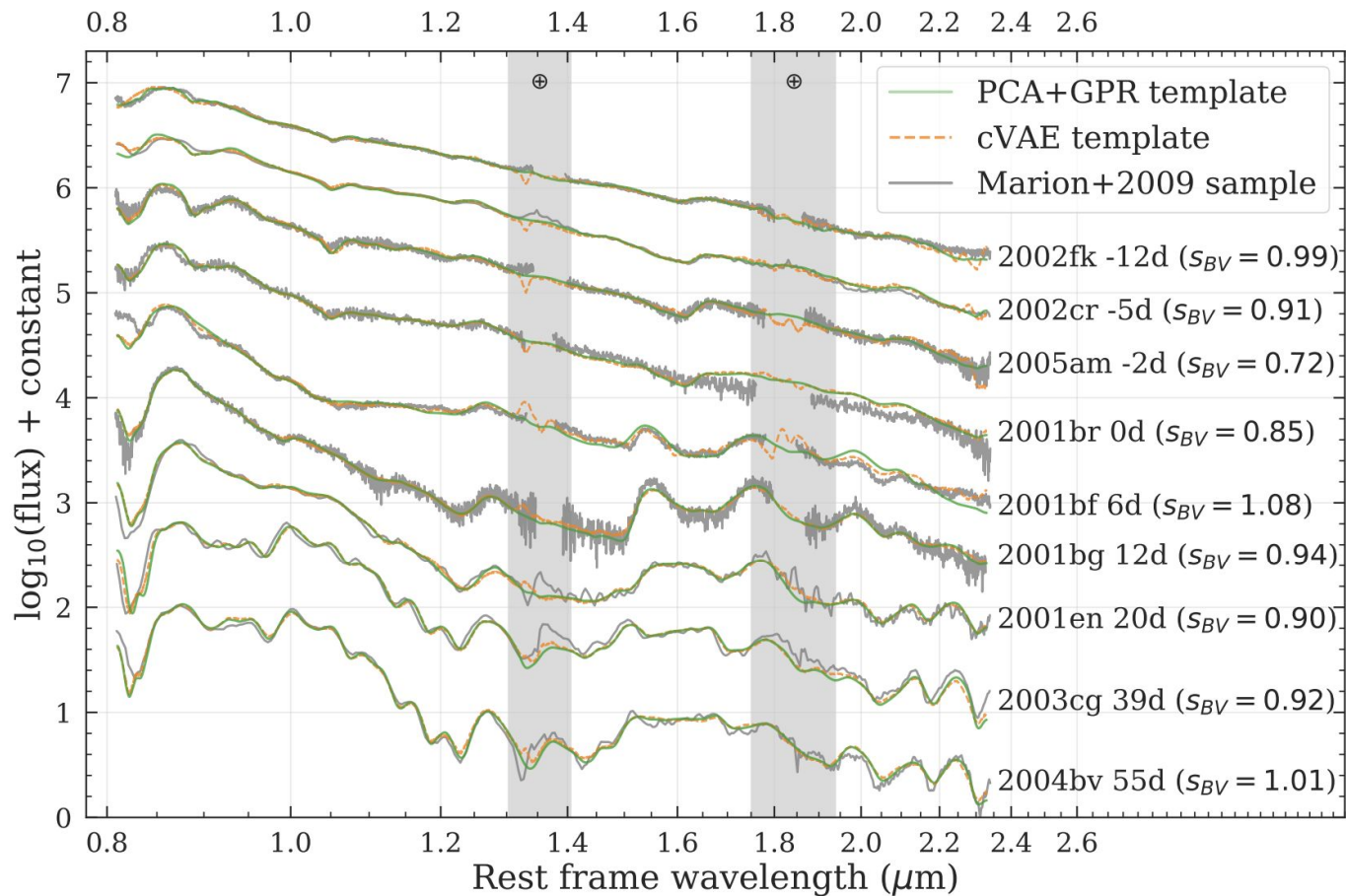


X = input spectra
 y = template parameters

- Input spectra mapped to a probability distribution (Gaussian) vs a single point
- Gives probabilistic outputs
- Optimization/Loss function
 - Regularizing term forces distribution to be closely clustered
 - Reconstruction loss term forces clusters to be distinct



Example of VAE latent space with MNIST numbers dataset



Both techniques perform similarly

cVAE more prone to noise in shaded telluric regions where data is bad

More real data or samples through data augmentation via bootstrap can improve performance

No need for wavelength interpolation nor stitching